Chapter 8
Incompressible Materials and Flow Problems

Although the approximation of incompressible flows by finite element methods has grown quite independently of the main stream of mixed and hybrid methods, it was soon recognised that a precise analysis requires the framework of mixed methods. In many cases, one may directly apply the techniques and results of Chaps. 4 and 5. In particular, the elements used are often standard elements or simple variants of standard elements. The specificity of the Stokes problem has however led to the development of special techniques; we shall present some of them that seem particularly interesting. Throughout this study, the main point will be to make a clever choice of elements leading to the satisfaction of the *inf-sup* condition which is here the important one as coercivity considerations are almost always straightforward.

This chapter, after a quick description of the problem, will present some simple examples of elements and techniques of proof which can be used as an introduction to the subject. This will be followed by a more detailed presentation. It will not be possible to analyse in detail all the elements for which results are known; we shall try to group them by families which can be treated by similar methods. These families will be arbitrary and will overlap in many cases.

Besides this presentation of elements, we shall also consider solution techniques by penalty methods and we will develop the related problem of almost incompressible elastic materials. We shall consider the equivalence of penalty methods and mixed methods and some questions arising from it. Stabilisation techniques will also be considered.

Finally, a section will be devoted to numerical considerations and to the choice of elements.

D. Boffi et al., *Mixed Finite Element Methods and Applications*, Springer Series in Computational Mathematics 44, DOI 10.1007/978-3-642-36519-5_8,

8.1 Introduction

We have already considered, in Example 1.3.1, the Stokes problem or creeping flow problem for an incompressible fluid. We had written it as a system of variational equations: *find* $\underline{u} \in V$ *and* $p \in Q$ *such that*

$$\begin{cases} 2\mu \displaystyle\int_\Omega \underline{\underline{\varepsilon}}(\underline{u}) : \underline{\underline{\varepsilon}}(\underline{v})\, dx - \int_\Omega p \operatorname{div} \underline{v}\, dx = \int_\Omega \underline{f} \cdot \underline{v}\, dx \quad \forall\, \underline{v} \in V, \\ \displaystyle\int_\Omega q \operatorname{div} \underline{u}\, dx = \int_\Omega g\ q\, dx, \quad \forall\, q \in Q, \end{cases} \tag{8.1.1}$$

where $V := (H_0^1(\Omega))^n$ and Q is the subspace of $L^2(\Omega)$ consisting of functions with zero mean value on Ω. In this formulation, $\underline{u}$ is the velocity of the fluid and p is its pressure. A similar problem arises for the displacement of an incompressible elastic material.

Remark 8.1.1. Although incompressibility corresponds to the case $g = 0$, we shall see in Remark 8.2.2 that non zero boundary conditions correspond implicitly to introducing $g \neq 0$. □

Remark 8.1.2 (Almost incompressible materials). For a linear elastic material, following Example 1.2.2, we have to solve the variational equation

$$2\mu \int_\Omega \underline{\underline{\varepsilon}}(\underline{u}) : \underline{\underline{\varepsilon}}(\underline{v})\, dx + \lambda \int_\Omega \operatorname{div} \underline{u}\ \operatorname{div} \underline{v}\, dx = \int_\Omega \underline{f} \cdot \underline{v}\, dx, \quad \forall\, v \in V. \tag{8.1.2}$$

The case where λ is large, or equivalently, when the Poisson ratio $\nu = \lambda/2(\lambda + \mu)$ approaches $1/2$, can be considered as an approximation of (8.1.1) by a penalty method as in Sect. 5.6.3. The limiting case is exactly (8.1.1) up to the fact that $\underline{u}$ is a displacement instead of a velocity. Problems where λ is large are quite common and correspond to almost incompressible materials. Results of Sect. 5.5.2 can be applied and give conditions under which error estimates can be found that do not depend on λ. Problem (8.1.2) will be considered in detail in Sect. 8.12. □

It is also worth recalling that, defining

$$A\underline{u} := \begin{cases} \dfrac{\partial^2 u_1}{\partial x_1^2} + \dfrac{1}{2}\dfrac{\partial}{\partial x_2}\left(\dfrac{\partial u_1}{\partial x_2} + \dfrac{\partial u_2}{\partial x_1}\right) \\ \dfrac{\partial^2 u_2}{\partial x_2^2} + \dfrac{1}{2}\dfrac{\partial}{\partial x_1}\left(\dfrac{\partial u_1}{\partial x_2} + \dfrac{\partial u_2}{\partial x_1}\right), \end{cases} \tag{8.1.3}$$

that is, $A\underline{u} = \operatorname{div} \underline{\underline{\varepsilon}}(\underline{u})$, problems (8.1.1) and (8.1.2) are then respectively equivalent to

$$\begin{cases} -2\mu A\underline{u} + \underline{\text{grad}}\, p = \underline{f}, \\ \text{div}\, \underline{u} = g, \\ \underline{u}|_\Gamma = 0 \end{cases} \tag{8.1.4}$$

and

$$-2\mu A\underline{u} - \lambda\, \underline{\text{grad}}\, \text{div}\, \underline{u} = \underline{f}. \tag{8.1.5}$$

Remark 8.1.3. The above problems are sometimes written in a simplified way. Indeed, we have, for incompressible materials,

$$\mu A\underline{u} = \mu \triangle \underline{u} + \mu\ \underline{\text{grad}}\, \text{div}\, \underline{u} = \mu \triangle \underline{u}. \tag{8.1.6}$$

However, this simplification of the operator is valid only if Dirichlet conditions are considered everywhere. Otherwise, the natural Neumann conditions are different and those associated with the simplified operator are unphysical. □

Remark 8.1.4. The problems described above are, of course, physically unrealistic, as they involve body forces and homogeneous Dirichlet boundary conditions. The aim of doing so is to avoid purely technical difficulties and this implies no loss of generality. The results obtained will be valid, unless otherwise stated, for all acceptable boundary conditions. □

To approximate the Stokes problem, two approaches follow quite naturally from the preceding considerations. *The first* one is to use system (8.1.1) and to discretise $\underline{u}$ and p by standard (or less standard) finite element spaces. *The second* one is to use formulation (8.1.2) with λ large as a penalty approximation to system (8.1.1).

It rapidly became clear that both these approaches could yield strange results. In particular, the first one often led to non convergence of the pressure (see Sect. 8.3.1) and the second one to a *locking mechanism*, the numerical solution being uniformly zero, or unnaturally small for λ large. For velocity-pressure approximations, empirical cures were found by Hughes and Allik [255], Hood and Taylor [249] and others. At about the same time, some elements using discontinuous pressure fields were shown to work properly [165,200] from the mathematical point of view.

For the penalty method, the cure was found in selective or reduced integration procedures. This consisted in evaluating terms like $\int_\Omega \text{div}\, \underline{u}\ \text{div}\, \underline{v}\, dx$ by quadrature formulae of low order. This *sometimes* led to good results.

It was finally stated [287], even if the result was implicit in earlier works [59], that the analysis underlying the two approaches is the same. Penalty methods are often equivalent to some mixed methods. In such cases, the penalty method works if and only if the associated mixed method works [60]. This will be developed in Sect. 8.12.

First, we must give a more precise framework to our problem.

8.2 The Stokes Problem as a Mixed Problem

8.2.1 Mixed Formulation

We shall describe in this section how the Stokes problem (8.1.1) can be analysed in the general framework of Chaps. 4 and 5. Defining $V := (H_0^1(\Omega))^n$, $Q := L^2(\Omega)$ and

$$a(\underline{u}, \underline{v}) := 2\mu \int_\Omega \underline{\underline{\varepsilon}}(\underline{u}) : \underline{\underline{\varepsilon}}(\underline{v})\, dx \tag{8.2.1}$$

$$b(\underline{v}, q) := -\int_\Omega q \operatorname{div} \underline{v}\, dx, \tag{8.2.2}$$

problem (8.1.1) can clearly be written in the form: *find* $\underline{u} \in V$ *and* $p \in Q$ *such that*

$$\begin{cases} a(\underline{u}, \underline{v}) + b(\underline{v}, p) = (\underline{f}, \underline{v}) \quad \forall\, \underline{v} \in V, \\ b(\underline{u}, q) = (g, q) \quad \forall\, q \in Q, \end{cases} \tag{8.2.3}$$

which is a saddle point problem in the sense of Chap. 4. Indeed, we have already seen that p is the Lagrange multiplier associated with the incompressibility constraint.

Remark 8.2.1. It is apparent, from the definition (8.2.2) of $b(\cdot, \cdot)$ and from the boundary conditions of the functions in V, that p, if exists, is defined up to a constant. Therefore, we change the definition of the space Q into

$$Q := L_0^2(\Omega) = L^2(\Omega)/\mathbb{R}, \tag{8.2.4}$$

where two elements $q_1, q_2 \in L^2(\Omega)$ are identified if their difference is constant. It is not difficult to show that Q is isomorphic to the subspace of $L^2(\Omega)$ consisting of functions with zero mean value on Ω. □

With this choice, our problem reads: *find* $\underline{u} \in V$ *and* $p \in Q$ *such that*

$$\begin{cases} a(\underline{u}, \underline{v}) + b(\underline{v}, p) = (\underline{f}, \underline{v}) \quad \forall\, \underline{v} \in V, \\ b(\underline{u}, q) = (g, q) \quad \forall\, q \in Q. \end{cases} \tag{8.2.5}$$

Let us check the hypotheses of Theorem 4.2.2 to ensure that our problem is well-posed. Using the notation of Chap. 4, we can write

$$B = -\operatorname{div} : (H_0^1(\Omega))^n \to L^2(\Omega)/\mathbb{R} \tag{8.2.6}$$

and

$$B^t = \underline{\operatorname{grad}} : L^2(\Omega)/\mathbb{R} \to (H^{-1}(\Omega))^n. \tag{8.2.7}$$

It can be shown (see, e.g., [362]) that

$$\mathrm{Im}B = Q \cong \left\{ q \,|\, q \in L^2(\Omega), \int_\Omega q \, dx = 0 \right\}, \tag{8.2.8}$$

hence the operator B has a continuous lifting and the continuous *inf-sup* condition (4.2.26) holds. We also notice that, with our definition of the space Q, the kernel $\mathrm{Ker}B^t$ reduces to zero.

The bilinear form $a(\cdot,\cdot)$ is coercive on V: there exists α such that

$$a(\underline{v}, \underline{v}) \geq \alpha \|\underline{v}\|_V^2. \tag{8.2.9}$$

This is the well known Korn inequality (see [183, 362]), whence (4.2.12) also will follow (i.e., A is invertible on $\mathrm{Ker}B$).

We state the well-posedness of problem (8.2.5) in the following theorem. The proof follows from Theorem 4.2.1.

Theorem 8.2.1. *Let $\underline{f}$ be given in $(H^{-1}(\Omega))^n$ and g in $Q = L_0^2(\Omega)$. Then, there exists a unique $(\underline{u}, p) \in V \times Q$, solution to problem (8.2.5), which satisfies*

$$||\underline{u}||_V + ||p||_Q \leq C(||\underline{f}||_{H^{-1}} + \|g\|_Q). \tag{8.2.10}$$

Now, choosing an approximation $V_h \subset V$ and $Q_h \subset Q$ yields the discrete problem

$$\begin{cases} 2\mu \displaystyle\int_\Omega \underline{\underline{\varepsilon}}(\underline{u}_h) : \underline{\underline{\varepsilon}}(\underline{v}_h)\, dx - \int_\Omega p_h \ \mathrm{div}\, \underline{v}_h \, dx = \int_\Omega \underline{f} \cdot \underline{v}_h \, dx \quad \forall\, \underline{v}_h \in V, \\ \displaystyle\int_\Omega q_h \ \mathrm{div}\, \underline{u}_h \, dx = (g, q_h) \quad \forall\, q_h \in Q_h. \end{cases} \tag{8.2.11}$$

The bilinear form $a(\cdot,\cdot)$ is coercive on V; hence, according to the theory developed in Chaps. 3 and 4, there is no problem for the *existence* of a solution $\{\underline{u}_h, p_h\}$ to problem (8.2.11), at least with $g = 0$. Indeed, we have a finite-dimensional problem where $\mathrm{Im}B$ is closed and the right-hand side of the second equation of (8.2.11) is zero. It should be noted, however, that we might have trouble with the *uniqueness* of p_h and that there might be compatibility conditions on g for some approximations.

We thus try to obtain estimates of the errors $||\underline{u} - \underline{u}_h||_V$ and $||p - p_h||_Q$.

First, we observe that, even for $g = 0$, the discrete solution $\underline{u}_h$ *needs not be divergence-free*. Indeed, the bilinear form $b(\cdot,\cdot)$ defines a discrete divergence operator

$$B_h = -\,\mathrm{div}_h : V_h \to Q_h \tag{8.2.12}$$

(it is convenient here to identify $Q = L^2(\Omega)/\mathbb{R}$ and $Q_h \subset Q$ with their dual spaces). In fact, we have

$$(\mathrm{div}_h\, \underline{u}_h, q_h)_Q = \int_\Omega q_h \,\mathrm{div}\, \underline{u}_h \, dx \tag{8.2.13}$$

and thus $\mathrm{div}_h\, \underline{u}_h$ turns out to be the L^2-projection of $\mathrm{div}\, \underline{u}$ onto Q_h.

The discrete divergence operator coincides with the standard divergence operator if $\mathrm{div}\, V_h \subset Q_h$. Referring to Chap. 5, we see that obtaining error estimates requires a careful study of the properties of the operator $B_h = -\mathrm{div}_h$ and of its transpose that we denote by $\underline{\mathrm{grad}}_h$.

The first issue is to characterise the kernel $\mathrm{Ker}B_h^t = \mathrm{Ker}(\underline{\mathrm{grad}}_h)$. It might happen that $\mathrm{Ker}B_h^t$ contains non-trivial functions. In these cases, $\mathrm{Im}B_h = \mathrm{Im}(\mathrm{div}_h)$ will be *strictly smaller* than $Q_h = P_{Q_h}(\mathrm{Im}B)$; this may lead to pathologies. In particular, if we consider a modified problem, like the one that usually originates when dealing with Dirichlet boundary conditions, the strict inclusion $\mathrm{Im}B_h \subset Q_h$ may even imply trouble with the existence of the solution. This situation is made clearer with the following example.

Remark 8.2.2. Let us consider problem (8.1.4) with *non-homogeneous boundary conditions*, that is, let $\underline{r}$ be such that

$$\underline{u}|_\Gamma = \underline{r}, \quad \int_\Gamma \underline{r} \cdot \underline{n}\, ds = 0. \tag{8.2.14}$$

It is classical to reduce this case to a problem with homogeneous boundary conditions by first introducing a function $\underline{\tilde{u}} \in (H^1(\Omega))^2$ such that $\underline{\tilde{u}}|_\Gamma = \underline{r}$. Setting $\underline{u} = \underline{u}_0 + \underline{\tilde{u}}$ with $\underline{u}_0 \in (H_0^1(\Omega))^2$, we have to solve

$$\begin{cases} -2\mu A\underline{u}_0 + \underline{\mathrm{grad}}\, p = \underline{f} + 2\mu A\underline{\tilde{u}} = \underline{\tilde{f}}, \\ \mathrm{div}\, \underline{u}_0 = -\,\mathrm{div}\, \underline{\tilde{u}} = g, \quad \underline{u}_0|_\Gamma = 0, \end{cases} \tag{8.2.15}$$

with A defined in (8.1.3). We thus find a problem with a constraint $B\underline{u}_0 = g$ where $g \neq 0$. We have seen in Chap. 5 that the associated discrete problem may fail to have a solution because $g_h = P_{Q_h} g$ does not necessarily belong to $\mathrm{Im}B_h$, whenever $\mathrm{Ker}B_h^t \not\subset \mathrm{Ker}B^t$. Discretisations where $\mathrm{Ker}(\underline{\mathrm{grad}}_h)$ is non-trivial *can therefore lead to ill-posed problems* in particular for some non-homogeneous boundary conditions. Examples of such conditions can be found in [340,341]. In general, any method that relies on extra compatibility conditions is a source of trouble when applied to more complicated (non-linear, time-dependent, etc.) problems. □

For a first attempt to error estimates, we shall use Theorem 5.2.2. Since the bilinear form $a(\cdot,\cdot)$ is coercive on V, we only have to worry about the *inf-sup* condition. The following proposition will be the starting point for the analysis of any finite element approximation of (8.2.5).

Proposition 8.2.1. *Let* $(\underline{u}, p) \in V \times Q$ *be the solution of* (8.2.5) *and suppose the following inf-sup condition holds true*

$$\inf_{q_h \in Q_h} \sup_{\underline{v}_h \in V_h} \frac{\int_\Omega q_h \operatorname{div} \underline{v}_h \, dx}{||q_h||_Q ||\underline{v}_h||_V} \geq k_h. \tag{8.2.16}$$

Then, there exists a unique $(\underline{u}_h, p_h) \in V_h \times Q_h$, *solution to* (8.2.11), *and the following estimate holds*

$$\|u_h - u\|_V \leq \left(\frac{2\|a\|}{\alpha} + \frac{2\|a\|^{1/2}\|b\|}{(\alpha)^{1/2} k_h} \right) E_u + \frac{\|b\|}{\alpha} E_p, \tag{8.2.17}$$

$$\|p_h - p\|_Q \leq \left(\frac{2\|a\|^{3/2}}{(\alpha)^{1/2} k_h} + \frac{\|a\| \, \|b\|}{k_h^2} \right) E_u + \frac{3\|a\|^{1/2}\|b\|}{(\alpha)^{1/2} k_h} E_p \tag{8.2.18}$$

with α *given by* (8.2.9). □

Remark 8.2.3. Actually, as it has been already observed, the existence of the discrete solution $(\underline{u}_h, p_h)$ (when the right-hand side in the second equation of (8.2.5) is zero) is not a consequence of the *inf-sup* condition (8.2.16). However, we should not forget about the possible situation presented in Remark 8.2.2. □

Of course, we shall be looking for cases where

$$k_h \geq k_0 > 0. \tag{8.2.19}$$

In this case, it may be useful to summarise the estimates (8.2.17) and (8.2.18) in the following result.

Proposition 8.2.2. *With the same hypotheses as in Proposition 8.2.1, let us suppose that* (8.2.19) *holds. Then, there exists* C, *independent of* h, *such that*

$$\|u_h - u\|_V + \|p_h - p\|_Q \leq C(E_u + E_p). \tag{8.2.20}$$

□

Remark 8.2.4. We shall also meet cases in which the constant k_h is not bounded below by k_0. We shall then try to know precisely how it depends on h and to see whether a lower-order convergence can be achieved. When $\operatorname{Ker}(\underline{\operatorname{grad}}_h)$ is non-trivial, we are interested in a weaker form of (8.2.16)

$$\sup_{\underline{v}_h \in V_h} \frac{\int_\Omega q_h \operatorname{div} \underline{v}_h \, dx}{||\underline{v}_h||_V} \geq k_h \inf_{q \in \operatorname{Ker}(\underline{\operatorname{grad}}_h)} ||q_h - q||_{L^2(\Omega)}, \tag{8.2.21}$$

and in the dependence of k_h in terms of h. From (8.2.17) and (8.2.18), one sees that the effect will be stronger on the error $\|p - p_h\|_Q$. □

8.3 Some Examples of Failure and Empirical Cures

This section will present some classical troubles associated to the approximation of incompressible materials. We shall thus recall the difficulties associated with some 'obvious' approximations. We shall consider some examples of possible choices for the spaces V_h and Q_h, namely the $\underline{P}_1 - P_1$ element, a case of continuous pressure, and the $\underline{P}_1 - P_0$ element, a case of discontinuous pressure. These elements do not satisfy the *inf-sup* condition (8.2.16) and are not applicable in practice. We shall introduce some cures which will be developed and eventually justified later in this chapter.

8.3.1 Continuous Pressure: The $\underline{P}_1 - P_1$ Element

As we stated in the introduction, the development of finite element methods for incompressible problems was done, at least in the beginning, independently of the theory of mixed methods. The natural idea when attempting to solve a problem involving incompressibility would be to employ the same approximation for both velocity and pressure, in the simplest case a P_1 continuous interpolation

$$V_h := (\mathcal{L}_1^1)^n \cap V, \quad Q_h := \mathcal{L}_1^1 \cap Q. \tag{8.3.1}$$

In the two-dimensional case, it is easy to check that if the number of triangles is large enough, then there exist non-trivial functions satisfying the *discrete* divergence-free condition. Thus, no locking will occur and a solution can be computed. Indeed, this method would not provide an optimal approximation of the pressures by virtue of the unbalanced approximation properties of the discrete spaces (while Q_h achieves second order in L^2, V_h gives only first order in H^1). On the other hand, users of such methods (you can think of using also, for instance, $(\underline{P}_2 - P_2)$, $(\underline{Q}_1 - Q_1)$, etc.) soon became aware that their results were strongly mesh dependent. In particular, the computed pressures exhibited a very strange instability. This comes from the fact that for some meshes, the kernel of the discrete gradient operator, $\mathrm{Ker}(\underline{\mathrm{grad}}_h)$, is not the subspace of constant functions, as one would expect from the continuous problem, but is a larger subspace. This means that the solution obtained is determined only up to a given number of *spurious pressure modes* [340, 341] and that, at best, some filtering will have to be done before accurate results are available. We shall come back later on to this phenomenon also named chequerboarding in Sect. 8.10. We have already stated in Remark 8.2.2 that such spurious modes can impose non physical conditions on the data. To better understand the nature of spurious pressure modes, the reader may check the results of Fig. 8.1 in which different symbols denote points where functions in $\mathrm{Ker}(\underline{\mathrm{grad}}_h)$ must have equal values for a $(\underline{P}_1 - P_1)$ approximation.

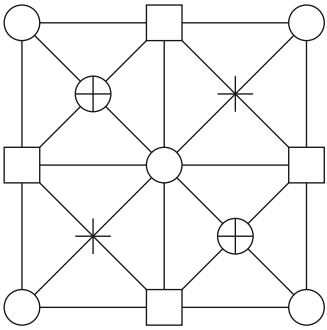

Fig. 8.1 Spurious modes for the $\underline{P}_1 - P_1$ case

In this case, we have *three* spurious pressure modes. This also shows that there exists on this mesh one non-trivial discrete divergence-free function whereas a direct count would predict locking.

Remark 8.3.1 (Possible cures). A cure for this problem was found empirically [249]: good results can be obtained using a $\underline{P}_2$ approximation for velocity but a P_1 approximation for pressure. It is also clear that this does not impair the order of accuracy. This will be analysed in Sect. 8.8.

Another possibility to obtain stable elements is to add some internal degrees of freedom. The simplest case is the MINI element of [25] which we present in Sect. 8.4.2 and in a more general form in Sect. 8.5.5. □

8.3.2 Discontinuous Pressure: The $\underline{P}_1 - P_0$ Approximation

A second natural approach would be to try imposing directly the divergence-free condition. The simplest element one can imagine for the approximation of an incompressible flow would use a standard $\underline{P}_1$ approximation for the velocities and a piecewise constant approximation for the pressures. With the notation of Chap. 2, this would read, again in the two-dimensional case,

$$V_h := (\mathcal{L}^1_1)^2 \cap V, \quad Q_h := \mathcal{L}^0_0 \cap Q. \tag{8.3.2}$$

As the divergence of a $\underline{P}_1$ velocity field is piecewise constant, this would lead to a truly divergence-free approximation. Moreover, this would give a well-balanced $O(h)$ approximation in estimates (8.2.17) and (8.2.18).

However, it is easy to see that such an element will not work for a general mesh. Indeed, consider a triangulation of a (simply connected) domain Ω and let us denote by

- t the number of triangles,
- v_I the number of internal vertices,
- v_B the number of boundary vertices.

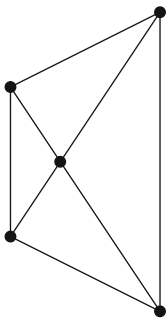

Fig. 8.2 The cross-grid element

We shall thus have $2v_I$ degrees of freedom (d.o.f.) for the space V_h (since the velocities vanish on the boundary) and $(t-1)$ d.o.f. for Q_h (because of the zero mean value of the pressures) leading to $(t-1)$ independent divergence-free constraints. By Euler's relations, we have

$$t = 2v_I + v_B - 2 \tag{8.3.3}$$

and thus

$$(t-1) \geq 2(v_I - 1). \tag{8.3.4}$$

A function $\underline{u}_h \in V_h$ is thus over-constrained and a *locking phenomenon* is likely to occur: in general, the only divergence-free discrete function is $\underline{u}_h \equiv 0$.

When the mesh is built under certain restrictions, it is however possible that some linear constraints become dependent: this will be the case for the cross-grid macro-element (Fig. 8.2) which will be analysed in Example 8.10.3.

As we shall see in Sect. 8.8.1, in general, obtaining truly divergence-free elements requires high degree approximations and some conditions on the mesh. We shall give, in the next section, the simplest example of a stable discontinuous pressure element, the $\underline{P}_2 - P_0$ element.

8.4 Building a B-Compatible Operator: The Simplest Stable Elements

We shall first recall here some of the results of Sect. 5.4.4 as applied to our incompressible problems. Then, we present a complete analysis of the MINI and $\underline{P}_2 - P_0$ elements and of the nonconforming $\underline{P}_1 - P_0$ elements. We shall obtain in Sect. 8.5.5 a more general proof for the MINI element.

It is not recommended to use the element $\underline{P}_2 - P_0$ because of its "unbalanced" approximation properties ($O(h^2)$ for V_h in the V-norm and only $O(h)$ for Q_h in the norm of Q), so that estimate (8.2.20) turns out to be suboptimal. However, the analysis of this element contains basic issues for getting familiar with the

approximation of the Stokes problem. Moreover, the stability properties of this element will often be used as an intermediate step for the analysis of other, more efficient, elements. It must also be said that this element is not directly generalisable to the three-dimensional case.

8.4.1 Building a B-Compatible Operator

An efficient way (sometimes known as Fortin's trick) of proving the *inf-sup* condition (8.2.16) consists in building a B-compatible interpolation operator Π_h like in Sect. 5.4 (see [201]). We write down, here, how the hypotheses of Proposition 5.4.3 read in this particular situation.

Proposition 8.4.1. *If there exists a linear operator $\Pi_h : V \to V_h$ such that*

$$\int_\Omega \mathrm{div}(\underline{u} - \Pi_h \underline{u}) q_h \, dx = 0 \quad \forall\, \underline{v} \in V,\ q_h \in Q_h, \tag{8.4.1}$$

$$||\Pi_h \underline{u}||_V \leq c ||\underline{u}||_V, \tag{8.4.2}$$

then the inf-sup condition (8.2.16) holds true. □

Remark 8.4.1. As it is shown in Chap. 5, condition (8.4.1) is equivalent to $\mathrm{Ker}(\underline{\mathrm{grad}}_h) \subset \mathrm{Ker}(\underline{\mathrm{grad}})$. An element with this property will present no spurious pressure modes. □

In several cases, the operator Π_h can be constructed in two steps as in Proposition 5.4.4. This was the case, for instance, in the proof of Proposition 8.4.3. In general, it will be enough to build two operators $\Pi_1, \Pi_2 \in \mathcal{L}(V, V_h)$ such that

$$||\Pi_1 \underline{v}||_V \leq c_1 ||\underline{v}||_V \qquad \forall\, \underline{v} \in V, \tag{8.4.3}$$

$$||\Pi_2 (I - \Pi_1) \underline{v}||_V \leq c_2 ||\underline{v}||_V \quad \forall\, \underline{v} \in V, \tag{8.4.4}$$

$$\int_\Omega \mathrm{div}(\underline{v} - \Pi_2 \underline{v}) q_h = 0 \qquad \forall\, \underline{v} \in V,\ \forall\, q_h \in Q_h, \tag{8.4.5}$$

where the constants c_1 and c_2 are independent of h. Then, the operator Π_h satisfying (8.4.1) and (8.4.2) will be found as

$$\Pi_h \underline{u} = \Pi_1 \underline{u} + \Pi_2 (\underline{u} - \Pi_1 \underline{u}). \tag{8.4.6}$$

In many cases, Π_1 will be the interpolation operator of [154] (cf. Chap. 2) defined in $H^1(\Omega)$.

On the contrary, the choice of Π_2 will vary from one case to the other, according to the choice of V_h and Q_h. However, the common feature of the various choices for

Π_2 will be the following one: the operator Π_2 is constructed on each element K in order to satisfy (8.4.5). In many cases, it will be such that

$$||\Pi_2 \underline{v}||_{1,K} \leq c(h_K^{-1}||\underline{v}||_{0,K} + |\underline{v}|_{1,K}). \tag{8.4.7}$$

We can summarise this result in the following proposition.

Proposition 8.4.2. *Let V_h be such that a "Clément's operator": $\Pi_1 : V \to V_h$ exists and satisfies (8.4.24). If there exists an operator $\Pi_2 : V \to V_h$ such that (8.4.5) and (8.4.7) hold, then the operator Π_h defined by (8.4.6) satisfies (8.4.1) and (8.4.2) and therefore the discrete inf-sup condition (8.2.16) holds.* □

We now consider some simple examples where this construction can be used.

8.4.2 A Stable Case: The MINI Element

We now show how we can enrich the space V_h of Example 8.3.1 so that, in the end, the new choice will yield a stable and convergent approximation to the Stokes problem (8.2.3). We set, as in (2.2.28),

$$B_3 := \{b(\underline{x}) \,|\, b(\underline{x})|_T \in P_3(T) \cap H_0^1(T), \ \forall\, T \in \mathcal{T}_h\}. \tag{8.4.8}$$

Hence, each $b(\underline{x})$ of B_3, on each triangle T, has the form $\alpha(T)\ \lambda_1(\underline{x})\ \lambda_2(\underline{x})\ \lambda_3(\underline{x})$ with $\alpha(T)$ constant in T. Following [25], we set

$$V_h := \{\mathcal{L}_1^1(\mathcal{T}_h) \oplus B_3\}^2 \cap V \quad Q_h := \mathcal{L}_1^1(\mathcal{T}_h) \cap Q \tag{8.4.9}$$

and we want to show that (8.4.9) leads to a stable and convergent approximation of the Stokes problem. For this, we are going to apply Proposition 8.4.2. We therefore have to construct an operator Π_h such that

$$\int_\Omega \operatorname{div}(\underline{v} - \Pi_h \underline{v})\, q_h\, dx = 0 \ \forall\, q_h \in Q_h \ \forall\, \underline{v} \in V, \tag{8.4.10}$$

$$\|\Pi_h \underline{v}\|_V \leq c\, \|\underline{v}\|_V \ \forall\, \underline{v} \in V. \tag{8.4.11}$$

Following Proposition 8.4.2, we first take for Π_1 the operator r_h of Proposition 2.2.1 and Corollary 2.2.1. We set

$$\Pi_1 \underline{v}|_K = r_h \underline{v}|_K \tag{8.4.12}$$

which, from (2.2.20), yields

$$|\underline{v} - \Pi_1 \underline{v}|_{m,K} \leq c \Big(\sum_{\vec{K}' \cap \vec{K} \neq \emptyset} h_{K'}^{1-m} |\underline{v}|_{1,K'} \Big). \tag{8.4.13}$$

In particular, (8.4.13) implies the first condition of (5.4.12)

$$\|\Pi_1 \underline{v}\|_V \leq c \, \|\underline{v}\|_V . \tag{8.4.14}$$

We now define the operator $\Pi_2 : V \to (B_3)^2$ by means of

$$\int_\Omega \operatorname{div}(\Pi_2 \underline{v} - \underline{v}) q_h \, dx = \int_\Omega (\underline{v} - \Pi_2 \underline{v}) \cdot \underline{\operatorname{grad}}\, q_h \, dx = 0 \ \forall \, q_h \in Q_h . \tag{8.4.15}$$

Since $\underline{\operatorname{grad}}\, q_h$ is piecewise constant, (8.4.15) is easily satisfied by choosing, in each K, bubbles with the same mean value as $\underline{v}$. It is easy to check that (under a minimum angle condition)

$$\|\Pi_2 \underline{v}\|_{r,K} \leq c h_K^{-r} \, \|\underline{v}\|_{0,K} \ \forall \, \underline{v} \in V, \ r = 0, 1. \tag{8.4.16}$$

Indeed, for $r = 1$, this is the inverse inequality of Sect. 2.2.7.

From (8.4.15), it is then immediate to check that the second condition of (5.4.12) is fulfilled and, from (8.4.16) and (8.4.13), we easily have the third condition.

We can thus apply Proposition 8.4.2 and the *inf-sup* condition holds. Now, we apply Proposition 8.2.2 (or the more complete result of Proposition 8.2.1) and we obtain

$$\|\underline{u} - \underline{u}_h\|_V + \|p - p_h\|_Q \leq c h \, (\|\underline{u}\|_{2,\Omega} + \|p\|_1), \tag{8.4.17}$$

that is, an optimal error estimate for $\underline{u}$.

8.4.3 *Another Stable Approximation: The Bi-dimensional $\underline{P}_2 - P_0$ Element*

Let us now move, in the two-dimensional case, to the *stable* $\underline{P}_2 - P_0$ element. Precisely, we use continuous piecewise quadratic vectors for the approximation of the velocities and piecewise constants for the pressures.

The discrete divergence-free condition can then be written as

$$\int_K \operatorname{div} \underline{u}_h \, dx = \int_{\partial K} \underline{u}_h \cdot \underline{n} \, ds = 0, \quad \forall \, K \in \mathcal{T}_h , \tag{8.4.18}$$

that is, as a conservation of mass on every element. This is intuitively an approximation of $\operatorname{div} \underline{u}_h = 0$, directly related to the physical meaning of this condition. It is clear from error estimates (8.2.17), (8.2.18) and standard approximation results (cf. Chap. 2) that such an approximation will lead to the loss of one order of accuracy due to the poor approximation of the pressures. However, an augmented Lagrangian technique can be used in order to recover a part of the accuracy loss (see Remark 8.4.4).

Fig. 8.3 The $\underline{P}_2$ element

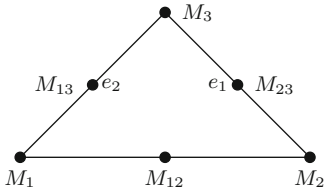

Proposition 8.4.3. *The choice*

$$V_h := (\mathcal{L}_2^1)^2 \cap V, \quad Q_h := \mathcal{L}_0^0 \cap Q \tag{8.4.19}$$

fulfils the inf-sup condition (8.2.16).

Proof. Before giving the rigorous proof of Proposition 8.4.3, we are going to sketch the main argument.

If we try to check the *inf-sup* condition by building an operator Π_h satisfying (5.4.10), then, given $\underline{u}$, we have to build $\underline{u}_h = \Pi_h \underline{u}$ such that

$$\int_\Omega \operatorname{div}(\underline{u} - \underline{u}_h) q_h \, dx = 0 \quad \forall\, q_h \in Q_h. \tag{8.4.20}$$

Since q_h is constant on every element $K \in \mathcal{T}_h$, this is equivalent to

$$\int_K \operatorname{div}(\underline{u} - \underline{u}_h) \, dx = \int_{\partial K} (\underline{u} - \underline{u}_h) \cdot \underline{n} \, ds = 0. \tag{8.4.21}$$

This last condition would be satisfied if $\underline{u}_h$ could be built in the following way. Let us denote by M_i and e_i, $i = 1, 2, 3$, the vertices and the sides of the triangular element K (Fig. 8.3); the mid-side nodes are denoted by M_{ij}.

We then define

$$\underline{u}_h(M_i) = \underline{u}(M_i), \quad i = 1, 2, 3 \tag{8.4.22}$$

$$\int_{e_i} \underline{u}_h \, ds = \int_{e_i} \underline{u} \, ds. \tag{8.4.23}$$

Condition (8.4.23) can be fulfilled by a correct choice of $\underline{u}_h(M_{ij})$. Moreover, this construction can be done at element level as the choice of $\underline{u}_h(M_{ij})$ is compatible on adjacent elements (that is, with this definition, $\underline{u}_h$ turns out to be continuous).

Although this is the basic idea, some technicalities must be introduced before a real construction is obtained. Indeed, for $\underline{u} \in (H_0^1(\Omega))^2$, condition (8.4.22) does not make sense.

Let us then give a rigorous proof of Proposition 8.4.3. We shall rely again on Proposition 8.4.2. Denoting by $\Pi_1 : V \to V_h$ the Clément interpolant [154] described in Proposition 2.2.1, we then have

$$\sum_K h_K^{2r-2}|\underline{v} - \Pi_1\underline{v}|_{r,K}^2 \leq c||\underline{v}||_{1,\Omega}^2, \quad r = 0, 1. \tag{8.4.24}$$

Setting $r = 1$ and using the triangular inequality $||\Pi_1\underline{v}|| \leq ||\underline{v} - \Pi_1\underline{v}|| + ||\underline{v}||$ gives

$$||\Pi_1\underline{v}||_V \leq c_1||\underline{v}||_V \quad \forall\, \underline{v} \in V. \tag{8.4.25}$$

We now modify Π_1 in a suitable way. Let us define $\Pi_2 : V \to V_h$ in the following way:

$$\Pi_2\underline{v}|_K(M) = 0 \quad \forall\, M \text{ vertex of } K, \tag{8.4.26}$$

$$\int_e \Pi_2\underline{u}\, ds = \int_e \underline{u}\, ds \quad \forall\, e \text{ edge of } K. \tag{8.4.27}$$

By construction, Π_2 satisfies

$$\int_\Omega \operatorname{div}(\underline{v} - \Pi_2\underline{v}) q_h\, dx = 0 \quad \forall\, \underline{v}_h \in V_h,\ q_h \in Q_h \tag{8.4.28}$$

and a scaling argument (see Sect. 2.2.7) gives

$$|\Pi_2\underline{v}|_{1,K} = |\widehat{\Pi_2\underline{v}}|_{1,\hat{K}} < c(K, \theta_0)||\hat{\underline{v}}||_{1,\hat{K}} \leq c(K, \theta_0)(h_K^{-1}|\underline{v}|_{0,K} + |\underline{v}|_{1,K}). \tag{8.4.29}$$

We can now define, as in Proposition 5.4.4,

$$\Pi_h\underline{u} = \Pi_1\underline{u} + \Pi_2(\underline{u} - \Pi_1\underline{u}) \tag{8.4.30}$$

and observe that (8.4.29) and (8.4.24) imply

$$||\Pi_2(I - \Pi_1)\underline{u}||_V \leq c_2||\underline{u}||_V \quad \forall\, \underline{v} \in V, \tag{8.4.31}$$

since

$$\begin{aligned} ||\Pi_2(I - \Pi_1)\underline{v}||_{1,\Omega}^2 &= \sum_K ||\Pi_2(I - \Pi_1)\underline{v}||_{1,K}^2 \\ &\leq c \sum_K \left\{h_K^{-2}||(I - \Pi_1)\underline{v}||_{0,K}^2 + |(I - \Pi_1)\underline{v}|_{1,K}^2\right\} \leq c||\underline{v}||_{1,\Omega}^2. \end{aligned} \tag{8.4.32}$$

Hence, Proposition 5.4.4 applies and the proof is concluded. □

The above proof can easily be extended to more general cases. It applies to the $(Q_2)^2 - P_0$ quadrilateral element, provided that the usual regularity assumptions on quadrilateral meshes are made.

Remark 8.4.2 (The 2D SMALL element). The proof will hold for elements in which only the normal component of velocity is used as a d.o.f. at the mid-side nodes

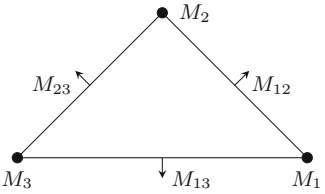

Fig. 8.4 The 2d SMALL element

[70, 198, 202]. Indeed, if only the normal component of $\underline{u}_h$ is used as a degree of freedom, the $(P_2)^2 - P_0$ element becomes the element of Fig. 8.4 in which, on each side, the normal component of $\underline{u}_h$ is quadratic, whereas the tangential component is only linear.

In this case, we can define $\Pi_2 \underline{v}$ by setting

$$\int_e (\Pi_2 \underline{v} \cdot \underline{n})\, ds = \int_e \underline{v} \cdot \underline{n}\, ds. \tag{8.4.33}$$

The same remark is valid for the $(Q_2)^2 - P_0$ quadrilateral element. □

Remark 8.4.3. The philosophical idea behind the $(P_2)^2 - P_0$ element is that we need one degree of freedom per each interface (actually, the normal component of the velocity) in order to control the jump of the pressures. This is basically the meaning of Green's formula (8.4.21). For three-dimensional elements, however, we would need a **mid-face** node instead of a mid-side node in order to control the normal flux from one element to the other.

In particular, we point out that adding *internal degrees of freedom* to the velocity space *cannot stabilise* elements with *piecewise constant pressures* which do not satisfy the *inf-sup* condition. □

Remark 8.4.4. To reduce the loss of accuracy due to the unbalanced approximation properties of the spaces V_h and Q_h, we can employ the augmented Lagrangian technique of Sect. 5.6.3. The discrete scheme reads: *find* $(\underline{u}_h, p_h) \in V_h \times Q_h$ *such that*

$$\begin{aligned} &\int_\Omega \underline{\underline{\varepsilon}}(\underline{u}_h) : \underline{\underline{\varepsilon}}(\underline{v}_h)\, dx + h^{-1/2} \int_\Omega \operatorname{div} \underline{u}_h \ \operatorname{div} \underline{v}_h\, dx \\ &\qquad - \int_\Omega p_h \ \operatorname{div} \underline{v}_h\, dx = \int_\Omega \underline{f} \cdot \underline{v}_h\, dx, \quad \forall\, \underline{v}_h \in V_h, \\ &\int_\Omega q_h \operatorname{div} \underline{u}_h\, dx = 0, \quad \forall\, q_h \in Q_h. \end{aligned} \tag{8.4.34}$$

Following [95], we have the following error estimate

$$||\underline{u} - \underline{u}_h||_V + ||p - p_h||_Q \le c h^{3/2} \inf_{\underline{v} \in V_h,\ q \in Q_h} \left(||\underline{u} - \underline{v}||_V + ||p - q||_Q \right). \tag{8.4.35}$$

□

Fig. 8.5 $\underline{P}_1^{NC} - P_0$ element

8.4.4 The Nonconforming $\underline{P}_1 - P_0$ Approximation

Finally, to conclude this section about simple examples, we consider the classical (almost) stable nonconforming triangular element introduced in [165], in which mid-side nodes are used as degrees of freedom for the velocities. This generates a piecewise linear nonconforming approximation; pressures are taken constant on each element as illustrated in Fig. 8.5. It is also possible to build a three-dimensional version of this element, using mid-face nodes as degrees of freedom. We thus choose again $Q_h := \mathcal{L}_0^0 \cap Q$ and

$$V_h := \{v_h \mid v_h \in \mathcal{L}^{1,NC}(P_1, \mathcal{T}_h)^2 \text{ vanishing at the boundary midpoints.}\} \quad (8.4.36)$$

We remark that this method is attractive for several reasons. In particular, the restriction to an element K of the solution $\underline{u}_h \in V_h$ is exactly divergence-free, since $\operatorname{div} V_h \subset Q_h$.

As we have a nonconforming element, we must define discrete bilinear forms,

$$a_h(\underline{u}_h, \underline{v}_h) := \sum_K \int_K \underline{\underline{\operatorname{grad}}}\, \underline{u}_h : \underline{\underline{\operatorname{grad}}}\, \underline{v}_h \, dx, \quad (8.4.37)$$

$$b_h(\underline{v}_h, q_h) := \sum_K \int_K \operatorname{div} \underline{v}_h q_h \, dx \quad (8.4.38)$$

and consider the problem

$$a_h(\underline{u}_h, \underline{v}_h) + b_h(\underline{v}_h, p_h) = (\underline{f}, \underline{v}_h) \ \forall\, \underline{v}_h \in V_h, \quad (8.4.39)$$

$$b_h(\underline{u}_h, q_h) = 0 \qquad \forall\, q_h \in \mathcal{L}_0^0. \quad (8.4.40)$$

Remark 8.4.5 (Problem with coercivity). It must also be recalled that coercivity is a problem for the $\underline{P}_1^{NC} - P_0$ element. The trouble is that the bilinear form (8.2.1) is not coercive on the nonconforming space V_h and we do not have the discrete version of Korn's inequality. This issue has been deeply investigated and clearly illustrated in [16]. It is important to note that (8.4.37) is not the same as in (8.2.1). As we stated earlier, the modified problem is valid only for Dirichlet boundary conditions. Even for the Stokes problem, the *inf-sup* condition is not always the only relevant one.

□

Nevertheless, let us see how we can show the *inf-sup* condition. We may now construct $\Pi_h : V \to V_h$ by

$$\int_{\partial K} (\Pi_h \underline{v} - \underline{v}) \cdot \underline{\phi}\, ds = 0 \ \forall\, \underline{\phi} \in R_0(\partial K) \tag{8.4.41}$$

and, again, it is easy to see that

$$|\Pi_h \underline{v}|_{1,h} \leq c\, \|\underline{v}\|_{1,h} \tag{8.4.42}$$

(where as usual $|v_h|^2_{1,h} = \sum_K |v_h|^2_{1,K}$) and

$$b_h(\underline{v} - \Pi_h \underline{v}, q_h) = 0 \ \forall\, q_h \in \mathcal{L}^0_0, \tag{8.4.43}$$

which implies, by Proposition 5.4.2,

$$\inf_{q \in Q_h/\mathbb{R}} \sup_{\underline{v} \in V_h} \frac{b_h(\underline{v}, q)}{|\underline{v}|_{1,h} \|q\|_{0/\mathbb{R}}} \geq c > 0. \tag{8.4.44}$$

On the other hand, we also have

$$a_h(\underline{v}_h, \underline{v}_h) \geq \alpha\, \|\underline{v}_h\|^2_{1,h} \ \forall\, v_h \in V_h. \tag{8.4.45}$$

We may now apply Proposition 5.5.6 and get

$$|\underline{u} - \underline{u}_h|_{1,h} + \|p - p_h\|_{0,\mathbb{R}} \leq ch + E_h(\underline{u}, p), \tag{8.4.46}$$

where

$$\begin{aligned} E_h(\underline{u}, p) &= \sup_{\underline{v}_h \in V_h} |\underline{v}_h|^{-1}_{1,h} \{a_h(\underline{u}, \underline{v}_h) + b_h(\underline{v}_h, p) - (\underline{f}, \underline{v}_h)\} \\ &= \sup_{\underline{v}_h \in V_h} |\underline{v}_h|^{-1}_{1,h} \sum_K \int_{\partial K} [(\underline{\operatorname{grad}}\, \underline{u}) \cdot \underline{n}] \cdot \underline{v}_h\, ds \\ &\leq ch\, \|\underline{u}\|_{2,\Omega}, \end{aligned} \tag{8.4.47}$$

so that, in the end, we have the optimal estimate

$$|\underline{u} - \underline{u}_h|_{1,h} + \|p - p_h\|_{0/\mathbb{R}} \leq ch\, \|\underline{u}\|_{2,\Omega}. \tag{8.4.48}$$

The present element has been generalised to second order in [209]. In this case, there is no problem with coercivity.

Remark 8.4.6. The generalisation of nonconforming finite elements to quadrilaterals is not straightforward. In particular, approximation properties of the involved spaces are not obvious. More details can be found in [330]. □

8.5 Other Techniques for Checking the *inf-sup* Condition

Having presented a few simple examples, we now consider, in a more systematic way, standard techniques for the proof of the *inf-sup* stability condition (8.2.16) that can be applied to a large class of elements. For ease of presentation, in this section, we develop the theory and postpone the examples to Sects. 8.6 and 8.7, for two- and three-dimensional schemes, respectively. However, after the description of each technique, we list some schemes to which that technique can be applied.

8.5.1 Projection onto Constants

Following [116], we now consider a modified *inf-sup* condition

$$\inf_{q_h \in Q_h} \sup_{\underline{v}_h \in V_h} \frac{\int_\Omega q_h \ \mathrm{div}\, \underline{v}_h \, dx}{||\underline{v}_h||_V ||q_h - \bar{q}_h||_Q} \geq k_0 > 0, \tag{8.5.1}$$

where $\bar{q}_h$ is the L^2-projection of q_h onto $\mathcal{L}_0^0$ (that is, piecewise constant functions).

Proposition 8.5.1. *Let us suppose that the modified inf-sup condition* (8.5.1) *holds with k_0 independent of h. Assume moreover that V_h is such that, for any $q_h \in \mathcal{L}_0^0 \cap Q$,*

$$\sup_{\underline{v}_h \in V_h} \frac{\int_\Omega q_h \, \mathrm{div}\, \underline{v}_h \, dx}{||\underline{v}_h||_V} \geq \gamma_0 ||q_h||_Q, \tag{8.5.2}$$

with γ_0 independent of h. Then, the inf-sup condition (8.2.16) *holds true.*

Proof. For any $q_h \in Q_h$, one has

$$\begin{aligned} \sup_{\underline{v}_h \in V_h} \frac{b(\underline{v}_h, q_h)}{||\underline{v}_h||_V} &= \sup_{\underline{v}_h \in V_h} \left\{ \frac{b(\underline{v}_h, q_h - \bar{q}_h)}{||\underline{v}_h||_V} + \frac{b(\underline{v}_h, \bar{q}_h)}{||\underline{v}_h||_V} \right\} \\ &\geq \sup_{\underline{v}_h \in V_h} \frac{b(\underline{v}_h, \bar{q}_h)}{||\underline{v}_h||_V} - \sup_{\underline{v}_h \in V_h} \frac{b(\underline{v}_h, q_h - \bar{q}_h)}{||\underline{v}_h||_V} \\ &\geq \gamma_0 ||\bar{q}_h||_Q - ||q_h - \bar{q}_h||_0, \end{aligned} \tag{8.5.3}$$

which implies

$$\sup_{\underline{v}_h \in V_h} \frac{b(\underline{v}_h, q_h)}{||\underline{v}_h||_V} \geq \frac{k_0 \gamma_0}{1 + k_0} ||\bar{q}_h||_Q. \tag{8.5.4}$$

Putting together (8.5.1) and (8.5.4) proves the proposition. □

Remark 8.5.1. In the case of *continuous pressures* schemes, hypothesis (8.5.2) can be replaced with the following approximation assumption: for any $\underline{v} \in V$ there exists $\underline{v}^I \in V_h$ such that

$$||\underline{v} - \underline{v}^I||_{L^2(\Omega)} \leq c_1 h ||\underline{v}||_V, \quad ||\underline{v}^I||_V \leq c_2 ||\underline{v}||_V. \tag{8.5.5}$$

The details of the proof can be found in [116] when the mesh is quasi-uniform. The quasi-uniformity assumption is actually not needed, as it can be shown with an argument similar to the one which will be presented in the next subsection (see, in particular, Remark 8.5.2). □

Example 8.5.1. The technique presented in this section will be used, for instance, for the stability proof of the generalised two-dimensional Hood–Taylor element (see Sect. 8.8.2 and Theorem 8.8.1). □

8.5.2 Verfürth's Trick

Verfürth's trick [375], already presented in Sect. 5.4.5, applies to *continuous pressure* approximations and is essentially based on two steps. The first step is quite general and can be summarised in the following Lemma.

Lemma 8.5.1. *Let Ω be a bounded domain in $\mathbb{R}^n$ with Lipschitz continuous boundary. Let $V_h \subset (H_0^1(\Omega))^n =: V$ and $Q_h \subset H^1(\Omega) \cap Q$ be closed subspaces. Assume that there exists a linear operator Π_h^0 from V into V_h and a constant c (independent of h) such that*

$$||\underline{v}_h - \Pi_h^0 \underline{v}||_r \leq c \sum_{K \in \mathcal{T}_h} \left(h_K^{2-2r} ||\underline{v}||_{1,K}^2 \right)^{1/2} \quad \forall\, \underline{v} \in V,\ r = 0, 1. \tag{8.5.6}$$

Then, there exist two positive constants c_1 and c_2 such that, for every $q_h \in Q_h$,

$$\sup_{\underline{v} \in V_h} \frac{\int_\Omega q_h \operatorname{div} \underline{v}_h \, dx}{||\underline{v}_h||_V} \geq c_1 ||q_h||_Q - c_2 \left(\sum_{K \in \mathcal{T}_h} h_K^2 ||\operatorname{\underline{grad}} q_h||_{0,K}^2 \right)^{1/2}. \tag{8.5.7}$$

Proof. Given $q_h \in Q_h$, let $\underline{\bar{v}} \in V$ be such that

$$\frac{\int_\Omega q_h \ \mathrm{div}\, \underline{\bar{v}}\, dx}{||\underline{\bar{v}}||_V ||q_h||_Q} \geq \beta > 0, \tag{8.5.8}$$

where β is the continuous *inf-sup* constant. Then,

$$\begin{aligned}
\sup_{\underline{v}_h \in V_h} \frac{\int_\Omega q_h \ \mathrm{div}\, \underline{v}_h\, dx}{||\underline{v}_h||_V} &\geq \frac{\int_\Omega q_h \ \mathrm{div}\, \Pi_h^0 \underline{\bar{v}}\, dx}{||\Pi_h^0 \underline{\bar{v}}||_V} \geq \frac{1}{2c} \frac{\int_\Omega q_h \ \mathrm{div}\, \Pi_h^0 \underline{\bar{v}}\, dx}{||\underline{\bar{v}}||_V} \\
&= \frac{1}{2c} \frac{\int_\Omega q_h \ \mathrm{div}\, \underline{\bar{v}}\, dx}{||\underline{\bar{v}}||_V} + \frac{1}{2c} \frac{\int_\Omega q_h \ \mathrm{div}(\Pi_h^0 \underline{\bar{v}} - \underline{\bar{v}})\, dx}{||\underline{\bar{v}}||_V} \\
&\geq \beta/4c ||q_h||_Q + \frac{1}{2c} \frac{\int_\Omega \underline{\mathrm{grad}}\, q_h \cdot (\Pi_h^0 \underline{\bar{v}} - \underline{\bar{v}})\, dx}{||\underline{\bar{v}}||_V} \\
&\geq \beta/4c ||q_h||_Q - \left(\frac{1}{2} \sum_{K \in \mathcal{T}_h} h_K^2 ||\, \underline{\mathrm{grad}}\, q_h||_{0,K}^2 \right)^{1/2}.
\end{aligned} \tag{8.5.9}$$

□

Remark 8.5.2. Indeed, via a scaling argument, it can be shown that the last term in the right-hand side of equation (8.5.7) is equivalent to $||q_h - \bar{q}_h||_0$, where $\bar{q}_h$ denotes, as in the previous subsection, the L^2-projection onto the piecewise constants. □

We are now in the position of stating the main result of this subsection. Note that Verfürth's trick consists in proving a kind of *inf-sup* condition where the zero norm of q_h is substituted by $h|q_h|_1$.

Proposition 8.5.2. *Suppose that the hypotheses of Lemma 8.5.1 hold true. Assume, moreover, that there exists a constant c_3 such that, for every $q_h \in Q_h$,*

$$\sup_{\underline{v}_h \in V_h} \frac{\int_\Omega q_h \, \mathrm{div}\, \underline{v}_h}{||\underline{v}_h||_V} \geq c_3 \left(\sum_{K \in \mathcal{T}_h} h_K^2 |q_h|_{1,K}^2 \right)^{1/2}. \tag{8.5.10}$$

Then, the standard inf-sup condition (8.2.16) holds true.

Proof. Let us multiply (8.5.7) by c_3 and (8.5.10) by c_2 and sum up the two equations. We have

$$(c_3 + c_2) \sup_{\underline{v}_h \in V_h} \frac{\int_\Omega q_h \ \mathrm{div}\, \underline{v}_h\, dx}{||\underline{v}_h||_V} \geq c_1 c_3 ||q_h||_Q, \tag{8.5.11}$$

that is, the *inf-sup* condition (8.2.16). □

Example 8.5.2. The Verfürth trick has been designed for the stability analysis of the Hood–Taylor method. It will be used for this purpose in Sect. 8.8.2 (see Theorem 8.8.1). □

8.5.3 Space and Domain Decomposition Techniques

Sometimes, the spaces V_h and Q_h decompose into the sum (direct or not) of subspaces for which it might be easier to prove an *inf-sup* condition. This is the case, for instance, when a *domain decomposition* technique is employed. Some of the results we are going to present can be viewed as a particular case of the macro-element technique which will be introduced in Sect. 8.5.4.

The next result has been presented and proved in [223].

Proposition 8.5.3. *Suppose Ω can be decomposed as the union of disjoint subdomains with Lipschitz continuous boundaries*

$$\Omega := \bigcup_{r=1}^{R} \Omega_r. \tag{8.5.12}$$

We make use of the following notation:

$$\begin{aligned} V_{0,r} &:= \{\underline{v} \,|\, \underline{v} \in V_h, \underline{v} = 0 \text{ in } \Omega \setminus \Omega_r\}, \\ Q_{0,r} &:= \{q \,|\, q \in Q_h, \int_{\Omega_r} q \, dx = 0\}, \\ K &:= \{q \,|\, q \in Q, q|_{\Omega_r} \text{ is constant}, \ r = 1, \ldots, R\}. \end{aligned} \tag{8.5.13}$$

Suppose, moreover, that the spaces $V_{0,r}$ and $Q_{0,r}$ satisfy the following inf-sup condition

$$\inf_{q_h \in Q_{0.r}} \sup_{\underline{v}_h \in V_{0,r}} \frac{\int_{\Omega_r} q_h \operatorname{div} \underline{v}_h \, dx}{||q_h||_Q ||\underline{v}_h||_V} \geq k_r > 0, \tag{8.5.14}$$

with k_r independent of h ($r = 1, \ldots, R$) and that the following inf-sup condition between V_h and K holds true

$$\inf_{q_h \in K} \sup_{\underline{v}_h \in V_h} \frac{\int_{\Omega} q_h \operatorname{div} \underline{v}_h \, dx}{||q_h||_Q ||\underline{v}_h||_V} \geq k_K > 0, \tag{8.5.15}$$

with k_K independent of h. Then, the spaces V_h and Q_h satisfy the inf-sup condition (8.2.16). □

Sometimes, it is not possible (or it is not the best choice) to partition Ω into *disjoint* sub-domains. Let us describe the case of two overlapping sub-domains. The following proposition can be checked by a direct computation.

Proposition 8.5.4. *Let Ω be the union of two sub-domains Ω_1 and Ω_2 with Lipschitz continuous boundaries. With the notation of the previous proposition, suppose that the spaces $V_{0,r}$ and $Q_{0,r}$ satisfy the inf-sup conditions*

$$\inf_{q_h \in Q_{0,r}} \sup_{\underline{v}_h \in V_{0,r}} \frac{\int_{\Omega_r} q_h \operatorname{div} \underline{v}_h \, dx}{||q_h||_Q ||\underline{v}_h||_V} \geq k_r > 0, \tag{8.5.16}$$

for $r = 1, 2$. Then, the spaces V_h and Q_h satisfy the condition

$$\inf_{q_h \in Q_h} \sup_{\underline{v}_h \in V_h} \frac{\int_{\Omega} q_h \operatorname{div} \underline{v}_h \, dx}{||q_h - \overline{q}_h||_Q ||\underline{v}_h||_V} \geq \frac{1}{\sqrt{2}} \min(k_1, k_2), \tag{8.5.17}$$

where, as in Sect. 8.5.1, we have denoted by $\overline{q}_h$ the L^2 projection of q_h onto the space $\mathcal{L}^0_0$. □

Another useful technique for proving the *inf-sup* condition can be found in [328]. This result is quite general; in particular, the decomposition of the spaces V_h and Q_h does not rely on a decomposition of the domain Ω. In [328], the following proposition is stated for a two-subspaces decomposition, but it obviously extends to more general situations.

Proposition 8.5.5. *Let Q_1 and Q_2 be subspaces of Q_h such that*

$$Q_h := Q_1 + Q_2. \tag{8.5.18}$$

If V_1, V_2 are subspaces of V_h and α_1, α_2 positive constants such that

$$\inf_{q_h \in Q_i} \sup_{\underline{v}_h \in V_i} \frac{\int_{\Omega} q_h \operatorname{div} \underline{v}_h \, dx}{||q_h||_Q ||\underline{v}_h||_V} \geq \alpha_i, \quad i = 1, 2 \tag{8.5.19}$$

and β_1, β_2 are non-negative constants such that

$$\begin{aligned} \left| \int_{\Omega} q_1 \operatorname{div} \underline{v}_2 \, dx \right| &\leq \beta_1 ||q_1||_Q ||\underline{v}_2||_V \quad \forall q_1 \in Q_1, \ \forall \underline{v}_2 \in V_2, \\ \left| \int_{\Omega} q_2 \operatorname{div} \underline{v}_1 \, dx \right| &\leq \beta_2 ||q_2||_Q ||\underline{v}_1||_V \quad \forall q_2 \in Q_2, \ \forall \underline{v}_1 \in V_1, \end{aligned} \tag{8.5.20}$$

with

$$\beta_1 \beta_2 < \alpha_1 \alpha_2, \tag{8.5.21}$$

then the inf-sup condition (8.2.16) *holds true with* k_0 *depending only on* α_i, β_i, $i = 1, 2$. □

Remark 8.5.3. Condition (8.5.21) is trivially true, for instance, when $\beta_1\beta_2 = 0$ and $\alpha_1\alpha_2 > 0$. □

Example 8.5.3. Most of the techniques presented in this section can be seen as a particular case of the macro-element technique (see Sect. 8.5.4). Proposition 8.5.4 will be used in Theorem 8.8.1 for the stability proof of the Hood–Taylor scheme. □

8.5.4 Macro-element Technique

In this section we present a technique introduced by Stenberg (see [351–355]) which, under suitable hypotheses, reduces the matter of checking the *inf-sup* condition (8.2.16) to an algebraic problem. We also refer to [98] for related results in a somewhat different setting.

The present technique is based on a decomposition of the triangulation $\mathcal{T}_h$ into disjoint macro-elements, where we refer to a *macro-element* as an open polygon (resp., polyhedron in $\mathbb{R}^3$) which is the union of adjacent elements.

Let us introduce some notation.

A macro-element M is said to be *equivalent* to a reference macro-element $\hat{M}$ if there exists a mapping $F_M : \hat{M} \to M$ such that

1. F_M is continuous and invertible;
2. $F_M(\hat{M}) = M$;
3. If $\hat{M} = \cup \hat{K}_j$, where K_j, $j = 1, \dots m$, are the elements defining $\hat{M}$, then $K_j = F_M(\hat{K}_j)$, $j = 1, \dots m$, are the elements of M;
4. $F_M|_{\hat{K}_j} = F_{K_j} \circ F_{\hat{K}_j}^{-1}$, $j = 1, \dots m$, where F_K denotes the affine mapping from the reference element to a generic element K.

We denote by $\mathcal{E}_{\hat{M}}$ the equivalence class of $\hat{M}$. We now introduce the discrete spaces associated with V_h and Q_h on the generic macro-element M (N is the dimension of Ω):

$$\begin{aligned} V_{0,M} &:= \left\{ \underline{v} \,|\, \underline{v} \in (H_0^1(M))^N, \underline{v} = \underline{w}|_M \text{ with } \underline{w} \in V_h \right\}, \\ Q_{0,M} &:= \left\{ p \,|\, p \in L^2(\Omega), \int_M p \, dx = 0, \ p = q|_M \text{ with } q \in Q_h \right\}. \end{aligned} \tag{8.5.22}$$

We finally introduce a space which corresponds to the kernel of B_h^t on the macro-element M:

$$K_M := \left\{ p \,|\, p \in Q_{0,M}, \int_M p \ \operatorname{div} \underline{v} \, dx = 0, \ \forall \, \underline{v} \in V_{0,m} \right\}. \tag{8.5.23}$$

The *macro-elements condition* reads

$$K_M = \{0\}, \tag{8.5.24}$$

that is, the analogous (at a macro-element level) of the necessary condition for the discrete Stokes problem to be well-posed that the kernel of B_h^t reduces to the zero function.

Proposition 8.5.6. *Suppose that each triangulation $\mathcal{T}_h$ can be decomposed into disjoint macro-elements belonging to a* fixed *number (independent of h) of equivalence classes $\mathcal{E}_{\hat{M}_i}$, $i = 1, \ldots n$. Suppose, moreover, that the pair $V_h - \mathcal{L}_0^0/\mathbb{R}$ is a stable Stokes element, that is,*

$$\inf_{q_h \in \mathcal{L}_0^0/\mathbb{R}} \sup_{\underline{v}_h \in V_h} \frac{\int_\Omega q_h \operatorname{div} \underline{v}_h \, dx}{||q_h||_Q ||\underline{v}_h||_V} \geq \beta > 0, \tag{8.5.25}$$

with β independent of h. Then, the macro-element condition (8.5.24) *(for every $M \in \mathcal{E}_{\hat{M}_i}$, $i = 1, \ldots n$) implies the inf-sup condition* (8.2.16)*.*

Proof. We do not give the technical details of the proof, for which we refer to [351]. The basic arguments of the proof are sketched in Remark 8.5.4. □

Remark 8.5.4. The macro-element condition (8.5.24) is strictly related to the *patch test* used by engineers (cf., e.g., [388]). However, the count of the degrees of freedom is clearly insufficient by itself. Hence, let us point out how the hypotheses of Proposition 8.5.6 are important.

Hypothesis (8.5.24) (the macro-element condition) implies, via a compactness argument, that a discrete *inf-sup* condition holds true between the spaces $V_{0,M}$ and $Q_{0,M}$. The *finite* number of equivalent macro-elements classes is sufficient to conclude that the corresponding *inf-sup* constants are uniformly bounded below by a positive number.

Then, we are basically in the situation of the domain decomposition technique of Sect. 8.5.3. We now use hypothesis (8.5.25) to control the constant functions on each macro-element and to conclude the proof. □

Remark 8.5.5. Hypothesis (8.5.25) is satisfied in the two-dimensional case whenever V_h contains piecewise quadratic functions (see Sect. 8.3). In the three-dimensional case, things are not so easy: to control the constants, we need extra degrees of freedom on the faces, as observed in Remark 8.4.3. For this reason, let us state the following proposition which can be proved with the technique of Sect. 8.5.1 (see Remark 8.5.1) and which applies to the case of *continuous pressures* approximations. □

Proposition 8.5.7. *Let us make the same assumptions as in Proposition 8.5.6 with* (8.5.25) *replaced by the condition of Remark 8.5.1 (see* (8.5.5)*). Then, provided $Q_h \subset C^0(\Omega)$, the inf-sup condition* (8.2.16) *holds true.* □

Remark 8.5.6. The hypothesis that the macro-element partition of $\mathcal{T}_h$ is *disjoint* can be weakened, in the spirit of Proposition 8.5.4, by requiring that each element K of $\mathcal{T}_h$ belongs at most to a finite number N of macro-elements with N independent of h. □

Example 8.5.4. The macro-element technique can be used in order to prove the stability of several schemes. Among those, we recall the $\underline{Q}_2 - P_1$ element (see Sect. 8.6.3) and the three-dimensional generalised Hood-Taylor scheme (see Theorem 8.8.2). □

8.5.5 *Making Use of the Internal Degrees of Freedom*

This subsection presents a general framework providing a general tool for the analysis of finite element approximations to problems of incompressible materials.

The basic idea has been used several times on particular cases, starting from [165] for discontinuous pressures and from [24] and [25] for continuous pressures. We are going to present it in its final general form given by Brezzi and Pitkiäranta [131]. It consists essentially in stabilising an element by adding suitable bubble functions to the velocity field.

In order to do that, following the notation of Remark 2.2.4, we first associate to every finite element discretisation $Q_h \subset Q$ the space

$$B(b_K \ \underline{\text{grad}}\ Q_h) := \left\{ \underline{\beta} \mid \underline{\beta} \in V, \underline{\beta}|_K = b_K \ \underline{\text{grad}}(q_h|_K) \text{ for some } q_h \in Q_h \right\}, \tag{8.5.26}$$

where b_K is a bubble function defined in K. In particular, we can take $b_K = b_{3,K}$ as the standard cubic bubble if K is a triangle, or a bi-quadratic bubble if K is a square or other obvious generalisations in 3D. In other words, the restriction of a $\underline{\beta} \in B(b_K \ \underline{\text{grad}}\ Q_h)$ to an element K is the product of the bubble functions b_K times the gradient of a function of $Q_h|_K$.

Remark 8.5.7. In (8.5.26), we take the gradient on K so that $B(b_K \ \underline{\text{grad}}\ Q_h)$ is well defined even if Q_h is a space of discontinuous pressures. □

Remark 8.5.8. Notice that the space $B(b_k \ \underline{\text{grad}}\ Q_h)$ is not defined through a basic space $\hat{B}$ on the reference element. This could be easily done in the case of *affine* elements, for all the reasonable choices of Q_h. However, this is clearly *unnecessary*: if we know how to compute q_h on K, we also know how to compute $\underline{\text{grad}}\, q_h$ and there is no need for a reference element. □

We can now prove our basic results, concerning the two cases of continuous or discontinuous pressures.

Proposition 8.5.8 (Stability of continuous pressure elements). *Assume that there exists an operator $\Pi_1 \in \mathcal{L}(V, V_h)$ satisfying the property of the Clément interpolant (8.4.24). If $Q_h \subset C^0(\Omega)$ and V_h contains the space $B(b_k \ \underline{\text{grad}}\ Q_h)$, then*

the pair (V_h, Q_h) *is a stable element, in the sense that it satisfies the inf-sup condition* (8.2.16).

Proof. We shall build a B-compatible operator, like in Proposition 8.4.2. We only need to construct the operator Π_2. We define $\Pi_2 : V \to B(b_k \underline{\text{grad}}\, Q_h)$, on each element, by requiring

$$\begin{aligned} &\Pi_2 \underline{v}|_K \in B(b_K \underline{\text{grad}}\, Q_h)|_K, \\ &\int_K (\Pi_2 \underline{v} - \underline{v}) \cdot \underline{\text{grad}}\, q_h \, dx = 0, \quad \forall\, q_h \in Q_h. \end{aligned} \tag{8.5.27}$$

Problem (8.5.27) has obviously a unique solution and Π_2 satisfies (8.4.5). Finally, (8.4.7) follows by a scaling argument. Hence, Proposition 8.4.2 gives the desired result. □

Corollary 8.5.1. *Assume that* $Q_h \subset Q$ *is a space of continuous piecewise smooth functions. If* V_h *contains* $(\mathcal{L}^1_1)^2 \oplus B(b_K \underline{\text{grad}}\, Q_h)$, *then the pair* (V_h, Q_h) *satisfies the inf-sup condition* (8.2.16).

Proof. Since V_h contains piecewise linear functions, there exists a Clément interpolant Π_1 satisfying (8.4.24). Hence, we can apply Proposition (8.5.8). □

We now consider the case of discontinuous pressure elements.

Proposition 8.5.9 (Stability of discontinuous pressure elements). *Assume that there exists an operator* $\tilde{\Pi}_1 \in \mathcal{L}(V, V_h)$ *satisfying*

$$\begin{aligned} &||\tilde{\Pi}_1 \underline{v}||_V \le c||\underline{v}||_V \quad \forall\, \underline{v} \in V, \\ &\int_K \text{div}(\underline{v} - \tilde{\Pi}_1 \underline{v})\, dx = 0 \quad \forall\, \underline{v} \in V \ \forall\, K \in \mathcal{T}_h. \end{aligned} \tag{8.5.28}$$

If V_h *contains* $B(b_K \underline{\text{grad}}\, Q_h)$, *then the pair* (V_h, Q_h) *is a stable element, in the sense that it satisfies the inf-sup condition* (8.2.16).

Proof. We are going to use Proposition 8.5.8. We take $\tilde{\Pi}_1$ as operator Π_1. We are not defining Π_2 on the whole V, but only in the subspace

$$V^0 := \left\{ \underline{v} \,|\, \underline{v} \in V, \int_K \text{div}\, \underline{v}\, dx = 0 \quad \forall\, K \in \mathcal{T}_h \right\}. \tag{8.5.29}$$

This will be enough, since we need to apply Π_2 to the difference $\underline{v} - \tilde{\Pi}_1 \underline{v}$ which is in V^0 by (8.5.28).

For every $\underline{v} \in V^0$, we define $\Pi_2 \underline{v} \in B(b_K \underline{\text{grad}}\, Q_h)$ by requiring that, in each element K,

$$\begin{aligned} &\Pi_2 \underline{v}|_K \in B(b_K \, \underline{\mathrm{grad}} \, Q_h)|_K, \\ &\int_K \mathrm{div}(\Pi_2 \underline{v} - \underline{v}) q_h \, dx = 0 \quad \forall \, q_h \in Q_h|_K. \end{aligned} \tag{8.5.30}$$

Note that (8.5.30) is uniquely solvable, if $\underline{v} \in V^0$, since the divergence of a bubble function has always zero mean value (hence, the number of non-trivial equations is equal to $\dim(Q_h|_K) - 1$, which is equal to the number of unknowns; the non-singularity then follows easily). It is obvious that Π_2, as given by (8.5.30), will satisfy (8.4.5) for all $\underline{v} \in V^0$. We have to check that

$$\|\Pi_2 \underline{v}\|_1 \leq c \|\underline{v}\|_V, \tag{8.5.31}$$

which actually follows by a scaling argument making use of the following bound

$$|\widehat{\Pi_2 \underline{v}}|_{0,\hat{K}} \leq c(\theta_0) |\hat{\underline{v}}|_{1,\hat{K}}. \tag{8.5.32}$$

□

Corollary 8.5.2 (Two-dimensional case). *Assume that $Q_h \subset Q$ is a space of piecewise smooth functions. If V_h contains $(\mathcal{L}^1_2)^2 \oplus B(b_K \, \underline{\mathrm{grad}} \, Q_h)$, then the pair (V_h, Q_h) satisfies the inf-sup condition* (8.2.16).

Proof. The stability of the $(P_2)^2 - P_0$ element (see Sect. 8.3) implies the existence of $\tilde{\Pi}_1$ as in Proposition 8.5.9. □

Propositions 8.5.8 and 8.5.9 are worth a few comments. They show that almost any element can be stabilised by using bubble functions. For continuous pressure elements, this procedure is mainly useful in the case of affine elements. For discontinuous pressure elements, it is possible to stabilise elements which are already stable for a piecewise constant pressure field. Examples of such a procedure can be found in [199]. Stability with respect to piecewise constant pressure implies that at least one degree of freedom on each side or face of the element is linked to the normal component of velocity (see [202] and Remark 8.4.3).

Example 8.5.5. Internal degrees of freedom can be used in the stability analysis of several methods. For instance, we use it for the analysis of the MINI element (see Sects. 8.6.1 and 8.7.1) in the case of continuous pressures and of the Crouzeix-Raviart element (see Proposition 8.6.2 and Sect. 8.7.2) in the case of discontinuous pressures. □

8.6 Two-Dimensional Stable Elements

In this section, we shall make use of the techniques presented in Sect. 8.5 to prove the stability for some of the most popular two-dimensional Stokes elements. The degrees of freedom corresponding to some of those are collected in Fig. 8.6.

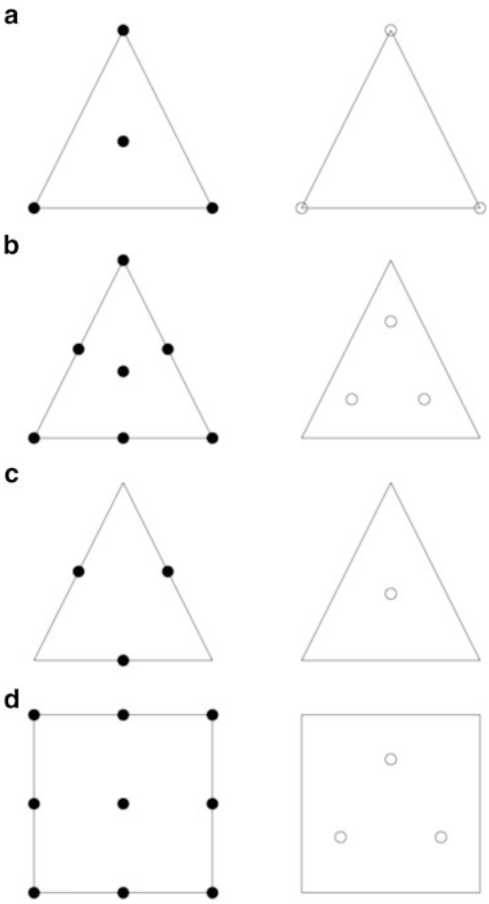

Fig. 8.6 Some stable two-dimensional Stokes elements: (**a**) the MINI element, (**b**) the Crouzeix–Raviart element, (**c**) the $\underline{P}_1^{NC} - P_0$ element, (**d**) the $\underline{Q}_2 - P_1$ element

We start with triangular elements and then we present schemes based on quadrilaterals.

The Hood–Taylor element (two- and three-dimensional) and its generalisation will be presented in Sect. 8.8. Figure 8.6 presents the most simple cases of the elements that we shall discuss.

8.6.1 Continuous Pressure Elements

We have already presented in Sect. 8.4.2 the MINI element. This element, which is probably the simplest one for the approximation of the Stokes equation, has been introduced in [25]. Using the results of Sect. 8.5.5, in particular Corollary 8.5.1, we easily deduce the following result.

Proposition 8.6.1. *The following pair of spaces are stable for any* $k \geq 1$

$$V_h := (\mathcal{L}_1^k \oplus B(b_{3,K}\ \underline{\text{grad}}\ Q_h))^2 \cap V, \qquad Q_h := \mathcal{L}_1^k \cap Q, \tag{8.6.1}$$

$$V_h := (\mathcal{L}_1^{k+1} \oplus B(b_{3,K}\ \underline{\text{grad}}\ Q_h))^2 \cap V, \qquad Q_h := \mathcal{L}_1^k \cap Q. \tag{8.6.2}$$

□

For $k = 1$, (8.6.1) is the MINI element while (8.6.2) defines a variant of the Hood-Taylor element, which we shall consider in Sect. 8.8, enriched by bubbles. This produces an element with a slightly better k_h in the *inf-sup* condition.

8.6.2 Discontinuous Pressure Elements

We have already considered in Sect. 8.4.3 the element $\underline{P}_2 - P_0$. Using a P_0 pressure ensures an element-wise conservation of mass which is an advantage in some situations. We now rely on Proposition 8.5.9 and more precisely on Corollary 8.5.2.

Example 8.6.1 (The Crouzeix-Raviart element). This element, presented in [165], is an enrichment to the $\underline{P}_2 - P_0$ scheme which provides well-balanced approximation properties. Given a mesh of triangles, the approximating spaces are

$$V_h := (\mathcal{L}_2^1 \oplus B_3)^2 \cap V, \qquad Q_h := \mathcal{L}_1^0 \cap Q. \tag{8.6.3}$$

The proof of the stability for this element is a direct consequence of Proposition 8.5.8. □

The Crouzeix-Raviart element is the simplest one of a general family. Indeed, the construction of the Crouzeix-Raviart element relies on the fact that, as we have seen in Proposition 8.5.9 and Corollary 8.5.2, adding enough bubbles (that is, internal degrees of freedom) to an element which is stable for pressures in $\mathcal{L}_0^0$ can make it stable for pressures in $\mathcal{L}_k^0$. We can thus state the following proposition.

Proposition 8.6.2. *For* $k \geq 2$, *let*

$$V_h := (\mathcal{L}_k^1 \oplus B_{k+1})^2 \cap V, \quad Q_h = \mathcal{L}_{k-1}^0 \cap Q. \tag{8.6.4}$$

Then, the couple $V_h \times Q_h$ *is stable.* □

Remark 8.6.1 (A nonconforming version). It can easily be checked [209] that one obtains a stable element of second order accuracy by replacing the standard bubble by the nonconforming bubble of (2.2.39), that is, taking

$$V_h := (\mathcal{L}_2^1 \oplus B_{NC})^2 \cap V, \quad Q_h = \mathcal{L}_1^0 \cap Q. \tag{8.6.5}$$

Besides some nice continuity properties of the stress at mid-side nodes, the fact that second order polynomials are employed simplifies things for the numerical integration when building the discrete problem. □

Remark 8.6.2. Instead of enriching V_h, stability can be obtained by taking a smaller Q_h, in general to the expense of accuracy. It can easily be checked that if we take, for $k \geq 2$, $V_h = (\mathcal{L}^1_k)^2$ and $Q_h = \mathcal{L}^0_{k-2}$, we have enough internal degrees of freedom in V_h to ensure stability. This is not true in the three-dimensional case where one would need $Q_h = \mathcal{L}^0_{k-3}$ and, evidently, $k \geq 3$. This choice of elements would have a severe impact on accuracy. □

8.6.3 Quadrilateral Elements, $\underline{Q}_k - P_{k-1}$ Elements

We now discuss the stability and convergence of a family of quadrilateral elements. The lowest order of this family, the $\underline{Q}_2 - P_1$ element, is one of the most popular Stokes elements. These elements are *discontinuous pressure* elements and they originate from attempts to use the reduced integration technique which will be analysed in Sect. 8.12. Let us first consider what would appear to be a natural construction. Given $k \geq 1$, the discrete spaces are defined as follows:

$$V_h := (\mathcal{L}^1_{[k]})^2 \cap V, \qquad Q_h := \mathcal{L}^0_{[k-1]} \cap Q. \tag{8.6.6}$$

For $k = 1$, this yields the unstable $\underline{Q}_1 - P_0$ which will be considered in detail in Sect. 8.10. For $k = 2$, we have the $\underline{Q}_2 - Q_1$ element which appears quite naturally in the use of reduced integration penalty methods (see [60]). This element is not stable and suffers from the same problems as the $\underline{Q}_1 - P_0$ element.

Let us now consider, instead of (8.6.6),

$$V_h := (\mathcal{L}^1_{[k]})^2 \cap V, \qquad Q_h := \mathcal{L}^0_{k-1} \cap Q. \tag{8.6.7}$$

Using P_k pressure instead of Q_k is not a natural choice, although it is the good one. If the mesh is built of *rectangles*, the stability proof is an immediate consequence of Proposition 8.5.9, since (8.5.28) is satisfied for V_h (indeed, the $\underline{Q}_2 - P_0$ is a stable Stokes element, see Remark 8.4.3). In the case of a general *quadrilateral* mesh, things are not so easy; even the definition of the space Q_h is not so obvious and there have been different opinions, during the years, about two possible natural definitions. Following [90], we discuss in detail the case $k = 2$. We shall see that in this case there are important issues related to the approximation properties of finite elements on non-affine meshes.

8.6.3.1 The $\underline{Q}_2 - P_1$ Element

This element was apparently discovered around a blackboard at the Banff Conference on Finite Elements in Flow Problems (1979). Two different proofs of stability

can be found in [223] and [351] for the rectangular case. This element is a relatively late comer in the field; the reason for this is that, as we stated earlier, using a P_1 pressure on a quadrilateral is not a standard procedure. It appeared as a cure for the instability of the $\underline{Q}_2 - Q_1$ element which appears quite naturally in the use of reduced integration penalty methods (see [60]). Another cure can be obtained by adding internal nodes (see [199]).

On a general quadrilateral mesh, the space Q_h can be defined in two different ways: either Q_h consists of (discontinuous) piecewise linear functions, or it is built by considering three linear shape functions on the reference unit square and mapping them to the general elements like it is usually done for continuous finite elements (see (2.1.59)). We point out that since the mapping F_K from the reference element $\hat{K}$ to the general element K in this case is bilinear but not affine, the two constructions are not equivalent. We shall refer to the first possibility as the **unmapped** pressure approach and to the second one as the **mapped** pressure approach.

In order to analyse the stability of either scheme, we use the macro-element technique presented in Sect. 8.5.4 with macro-elements consisting of one single element.

The **unmapped** pressure approach yields the original proof presented in [351]. Let M be a macro-element and $q_h = a_0 + a_x x + a_y y \in Q_{0,M}$ an arbitrary function in K_M. If $b(x, y)$ denotes the bi-quadratic bubble function on K, then $\underline{v}_h = (a_x b(x, y), 0)$ is an element of $V_{0,M}$ and

$$0 = \int_M q_h \operatorname{div} \underline{v}_h \, dx\, dy = -\int_M \underline{\operatorname{grad}}\, q_h \cdot \underline{v}_h \, dx\, dy = -a_x \int_M b(x, y)\, dx\, dy$$

implies $a_x = 0$. In a similar way, we get $a_y = 0$ and, since the average of q_h on M vanishes, we have the macro-element condition $q_h = 0$.

We now consider the **mapped** pressure approach, following the proof presented in [90]. There, it is recalled that the macro-element condition (8.5.24) can be related to an algebraic problem in which we are led to prove that a two-by-two matrix is non-singular. Actually, it turns out that the determinant of such a matrix is a multiple of the Jacobian determinant of the function mapping the reference square $\hat{K}$ onto M, evaluated at the barycentre of $\hat{K}$. Since this number must be non-zero for any element of a well-defined mesh, we can deduce that the macro-element condition is also satisfied in this case, and we can then conclude that the stability holds thanks to Proposition 8.5.6.

So far, we have shown that both the **unmapped** and the **mapped** pressure approach give rise to a stable $Q_2 - P_1$ scheme. However, as a consequence of the results proved in [20], we have that the mapped pressure approach *cannot achieve optimal approximation order*. Namely, the unmapped pressure space provides a second order convergence in L^2, while the mapped one achieves only $O(h)$ in the same norm. In [90], several numerical experiments have been reported, showing that on general quadrilateral meshes (with constant distortion), the unmapped pressure approach provides a second order convergence (for both velocity in H^1 and pressure in L^2), while the mapped approach is only sub-optimally first order convergent.

It is interesting to remark that, in this case also, the convergence of the velocities is suboptimal, according to the error estimate (8.2.17).

8.7 Three-Dimensional Stable Elements

Many elements presented in Sect. 8.6 have a three-dimensional extension. Some of them are schematically plotted in Fig. 8.7. However, there are important differences between the two and three-dimensional cases. One is that *bubbles* are at least of fourth degree in the three-dimensional case. Another difference is that the $\underline{P}_2 - P_0$ element is not stable: to control piecewise constant pressure, we need some degrees of freedom on the faces. It would indeed be possible to prove that the $\underline{P}_3 - P_0$ is stable but this yields a highly unbalanced approximation.

8.7.1 Continuous Pressure 3-D Elements

The most important continuous pressure element is the Hood-Taylor element, and its generalisations, which will be presented in the next section.

The families associated with the MINI element introduced in (8.6.1) and (8.6.2) can be generalised to the three-dimensional with an appropriate choice of bubbles. Consider a regular sequence of decompositions of Ω into tetrahedra.

Proposition 8.7.1. *The following pair of spaces are stable for any* $k \geq 1$

$$V_h := (\mathcal{L}_1^k \oplus B(b_{4,K}\ \underline{\text{grad}}\ Q_h))^3 \cap V, \qquad Q_h := \mathcal{L}_1^k \cap Q, \tag{8.7.1}$$

$$V_h := (\mathcal{L}_1^{k+1} \oplus B(b_{4,K}\ \underline{\text{grad}}\ Q_h))^3 \cap V, \qquad Q_h := \mathcal{L}_1^k \cap Q. \tag{8.7.2}$$

The proof follows easily, like in the 2D case, from Corollary 8.5.1. □

The first member of the first family is the MINI element and the first member of the second family is a version of the Hood-Taylor element where the velocities are enriched by quartic bubbles. Paradoxically, this may increase the precision on pressure through a better *inf-sup* constant.

8.7.2 Discontinuous Pressure 3-D Elements

As we stated earlier, the situation for discontinuous pressure elements is less favourable than in the two-dimensional case. We first consider an example.

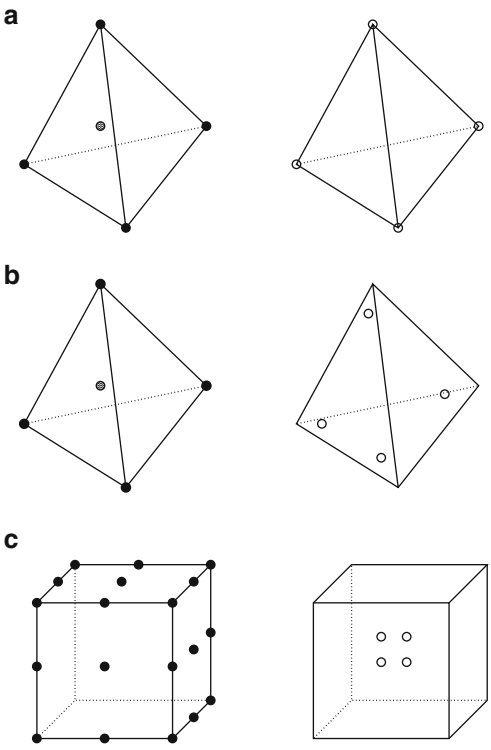

Fig. 8.7 Some stable three-dimensional Stokes elements: (**a**) the MINI element, (**b**) the Crouzeix–Raviart element, (**c**) the $\underline{Q}_2 - P_1$ element

Example 8.7.1. The SMALL element is the smallest three-dimensional one if one wants to use piecewise constant pressure. It is the analogue of the two-dimensional construction of Remark 8.4.2, but we now have to work on the faces and not on the edges. Let us thus consider, on a tetrahedral element, the cubic bubble $\underline{b}_{3,F}$ associated to the face $F = (i, j, k)$ and defined, using barycentric coordinates, by

$$b_{3,F} := \lambda_i \, \lambda_j \, \lambda_k. \tag{8.7.3}$$

We define our new space by adding on each face of a standard piecewise linear element such a cubic bubble. We shall denote this extra space on an element K by

$$BF_3 := \left\{ v_h \,|\, v_h \in P_3(K), v_h = \sum_F \alpha_F b_{3,F} \right\}. \tag{8.7.4}$$

The final space is thus

$$V_h := (\mathcal{L}^1_1 + BF_3)^3 \cap V, \qquad Q_h := \mathcal{L}^0_0 \cap Q.$$

This provides the control of the flux on the face and one can easily check that we have stability for piecewise constant pressure.

Remark 8.7.1. In fact, the bubble on the face is needed only for the normal component of the velocity. This implies some complexity for the implementation but greatly reduces the global number of degrees of freedom. We could thus use, instead of (8.7.4), denoting $\underline{n}_F$ the normal to the face,

$$BF_3^n := \left\{ v_h \mid v_h \in P_3(K), v_h = \sum_F \alpha_F b_{3,F} \underline{n}_F \right\} \tag{8.7.5}$$

and $V_h := ((\mathcal{L}_1^1)^3 + BF_3^n) \cap V$. □

We must retain that discontinuous pressure elements in 3D require third degree polynomials. □

Example 8.7.2 (3D analogues of the Crouzeix–Raviart element). In order to generalise the Crouzeix-Raviart element, we must first get a stable element for constant pressure. The previously defined SMALL element provides only first order accuracy. We therefore start from a quadratic approximation and enrich it by face bubbles to control the fluxes on the faces and by internal bubbles to control linear pressure. This yields

$$V_h := (\mathcal{L}_2^1 + BF_3 + B_4)^3 \cap V, \qquad Q_h := \mathcal{L}_1^0 \cap Q.$$

The stability is an easy consequence of Proposition 8.5.9.

The face bubbles do not increase the order of accuracy and we could employ the normal bubbles of (8.7.5) However, if one wants to stick to more standard elements, the natural thing would be to start from the stable $\underline{P}_3 - P_0$ element. To get a balanced precision, we define

$$V_h := (\mathcal{L}_3^1 + B_5)^3 \cap V, \qquad Q_h := \mathcal{L}_2^0 \cap Q. \tag{8.7.6}$$

We would then have third order accuracy but to the price of a quite large number of degrees of freedom. This can obviously be extended to higher degrees. □

Example 8.7.3 (Nonconforming elements). A possibility to reduce the order of polynomials needed to obtain stable elements is to use nonconforming elements. The triangular $P_1^{NC} - P_0$ easily generalises to tetrahedra in 3D. Also in this case, since div $V_h \subset Q_h$, the restriction of the discrete solution to every element is truly divergence-free. The problems of coercivity are still there.

However, it is also possible to obtain second order without this problem. We have already seen in Remark 8.6.1 that one could get a variant of the Crouzeix-Raviart element using nonconforming bubbles. The construction can be extended to the three-dimensional case. Indeed, one can replace the face-bubble of (8.7.3) by its nonconforming version of (2.2.39), that is,

$$b_{NC,F} = (\lambda_i^2 + \lambda_j^2 + \lambda_k^2) - 1. \tag{8.7.7}$$

The internal bubble is also replaced by $(\lambda_i^2 + \lambda_j^2 + \lambda_k^2 + \lambda_l^2) - 1$ and we now manipulate only second degree polynomials, which is definitely an advantage. However, things are a little more complicated: we have too many degrees of freedom and one must remove the vertices. We refer to [203] for details. □

Example 8.7.4 (Quadrilateral $\underline{Q}_k - P_{k-1}$ elements). Given a mesh of hexahedra, we define

$$V_h := (\mathcal{L}_k^1)^3 \cap V, \qquad Q_h := \mathcal{L}_{k-1}^0 \cap Q, \tag{8.7.8}$$

for $k \geq 2$. We refer to the two-dimensional case (see Sect. 8.6.3) for the definition of the pressure space. In particular, we recall that Q_h on each element consists of true polynomials and is not defined via the reference element. With the correct definition of the pressure space, the proof of stability for this element is a simple generalisation of the corresponding two-dimensional version. □

8.8 $\underline{P}_k - P_{k-1}$ Schemes and Generalised Hood–Taylor Elements

The main result of this section (see Theorems 8.8.1 and 8.8.2) consists in showing that a family of popular Stokes elements satisfies the *inf-sup* condition (8.2.16). The first element of this family has been introduced in [249] and for this reason, the members of the whole family are usually referred to as *generalised* Hood–Taylor elements.

This section is organised in two subsections. In the first one, we discuss discontinuous pressure approximations for the $\underline{P}_k - P_{k-1}$ element in the two-dimensional triangular case; it turns out that this choice is not stable in the lower order cases and requires suitable conditions on the mesh sequences for the stability of the higher order elements.

The last subsection deals with the generalised Hood–Taylor elements, which provide a continuous pressure approximation in the plane (triangles and quadrilaterals) and in the three-dimensional space (tetrahedra and hexahedra).

8.8.1 Discontinuous Pressure $\underline{P}_k - P_{k-1}$ Elements

In this subsection, we shall recall the statement of a basic result by Scott and Vogelius (see [347]) which, roughly speaking, says: *under suitable assumptions on the decomposition $\mathcal{T}_h$ (in triangles), the pair $V_h := (\mathcal{L}_k^1)^2 \cap V$, $Q_h := \mathcal{L}_{k-1}^0 \cap Q$ satisfies the inf-sup condition for $k \geq 4$.*

On the other hand, the problem of finding stable lower order approximations has been studied by Q in [328], where interesting remarks are made on this scheme and where the possibility of filtering out the spurious pressure modes is considered.

In order to state in a precise way the restrictions that have to be made on the triangulation for higher order approximations, we assume that Ω is a polygon, and that its boundary $\partial\Omega$ has no double points. In other words, there exist two continuous piecewise linear maps $x(t)$, $y(t)$ from $[0, 1[$ into $\mathbb{R}$ such that

$$\begin{cases} (x(t_1) = x(t_2) \text{ and } y(t_1) = y(t_2)) \text{ implies } t_1 = t_2, \\ \partial\Omega = \{(x, y) \,|\, x = x(t),\ y = y(t) \text{ for some } t \in [0, 1[\}. \end{cases} \tag{8.8.1}$$

Clearly, we will have $\lim_{t\to 1} x(t) = x(0)$ and $\lim_{t\to 1} y(t) = y(0)$. We remark that we are considering a less general case than the one treated by Scott and Vogelius [347]. We shall make further restrictions in what follows, so that we are actually going to present a particular case of their results.

Now let V be a vertex of a triangulation $\mathcal{T}_h$ of Ω and let $\theta_1, \ldots, \theta_n$, be the angles, at V, of all the triangles meeting at V, ordered, for instance, in the anticlockwise sense. If V is an internal vertex, we also set $\theta_{n+1} := \theta_1$. Now we define $S(V)$ according to the following rules.

$$n = 1 \quad \Rightarrow \quad S(V) = 0 \tag{8.8.2}$$

$$n > 1,\ V \in \partial\Omega \quad \Rightarrow \quad S(V) = \max_{i=1,n-1} (\pi - \theta_1 - \theta_{i+1}) \tag{8.8.3}$$

$$V \notin \partial\Omega \quad \Rightarrow \quad S(V) = \max_{i=1,n} (\pi - \theta_i - \theta_{i+1}). \tag{8.8.4}$$

It is easy to check that $S(V) = 0$ if and only if all the edges of $\mathcal{T}_h$ meeting at V fall on two straight lines. In this case, V is said to be singular [347]. If $S(V)$ is positive but very small, then V will be "almost singular". Thus, $S(V)$ measures how close V is to be singular.

We are now able to state the following result.

Proposition 8.8.1 ([347]). *Assume that there exist two positive constants c and δ such that*

$$ch \le h_K \ \forall\, K \in \mathcal{T}_h \tag{8.8.5}$$

and

$$S(V) \ge \delta \text{ for all } V \text{ vertex of } \mathcal{T}_h. \tag{8.8.6}$$

Then, the choice $V_h = (\mathcal{L}^1_k)^2 \cap V$, $Q_h = \mathcal{L}^0_{k-1} \cap Q$, $k \ge 4$, satisfies the inf-sup condition with a constant depending on c and δ but not on h. □

Remark 8.8.1. Condition (8.8.6) is worth a few comments. The trouble is that $S(V) = 0$ makes the linear constraints on $\underline{u}_h$, arising from the divergence-free condition, linearly dependent (see, also, Examples 8.10.2 and 8.10.3). When this linear dependence appears, some part of the pressure becomes unstable. However,

we have met this situation in Example 8.10.3 and this was in fact the key to convergence, provided a condition on data was fulfilled. The same analysis would hold here and the unstable part of pressure could be filtered out. □

Remark 8.8.2. The $\underline{P}_k - P_{k-1}$ element can obviously be stabilised by adding bubbles to the velocity space in the spirit of Sect. 8.5.5 (see Proposition 8.5.9). For a less expensive stabilisation, consisting in adding bubbles only in few elements, see [72]. □

8.8.2 Generalised Hood–Taylor Elements

In this subsection, we recall the results proved in [71, 73] concerning the stability of the generalised Hood–Taylor schemes. On triangles or tetrahedra, velocities are approximated by a standard $\underline{P}_k$ element and pressures by a standard *continuous* P_{k-1}, that is, $\underline{v}_h \in (\mathcal{L}^1_k)^n \cap V$ $(n = 2, 3)$, $p \in \mathcal{L}^1_{k-1} \cap Q$. This choice has an analogue on rectangles or cubes using a $\underline{Q}_k$ element for velocities and a Q_{k-1} element for pressures. The lowest order triangular element (i.e., $k = 2$) has been introduced by Hood and Taylor in [249]. Several papers are devoted to the analysis of this popular element.

The degrees of freedom of some elements belonging to this family are reported in Fig. 8.8.

Remark 8.8.3. Another element that has been used because of the simplicity of its shape functions is the so-called $(\underline{P}_1 - iso - \underline{P}_2) - P_1$ element, It is sketched in Fig. 8.9. It is a composite element assembled from four piece-wise linear elements for velocity while pressure remains linear on the macro-element. The same technique of proof that yields stabiliy of the classical Hood-Taylor element could be used to show the inf-sup condition for this composite element. □

The first proof of convergence was given for the two-dimensional case in [61] where a weaker form of the *inf-sup* condition was used. The analysis was subsequently improved in [375], who showed that the classical *inf-sup* condition is indeed satisfied (see Verfürth's trick in Sect. 8.5.2). The macro-element technique can easily be used for the stability proof of the rectangular and cubic element (of any order) as well as for the tetrahedral case when $k = 2$ (see [351]). In [122], an alternative technique of proof has been presented for the triangular and tetrahedral cases when $k = 2$. This proof generalises to the triangular case when $k = 3$ (see [121]). Finally, a general proof of convergence can be found in [71] and [73] for the triangular and tetrahedral case, respectively.

We now state and prove the theorem concerning the two-dimensional triangular case (see [71]).

Theorem 8.8.1. *Let Ω be a polygonal domain and $\mathcal{T}_h$ a regular sequence of triangular decompositions of it. Then, the choice $V_h := (\mathcal{L}^1_k \cap H^1_0(\Omega))^2$ and*

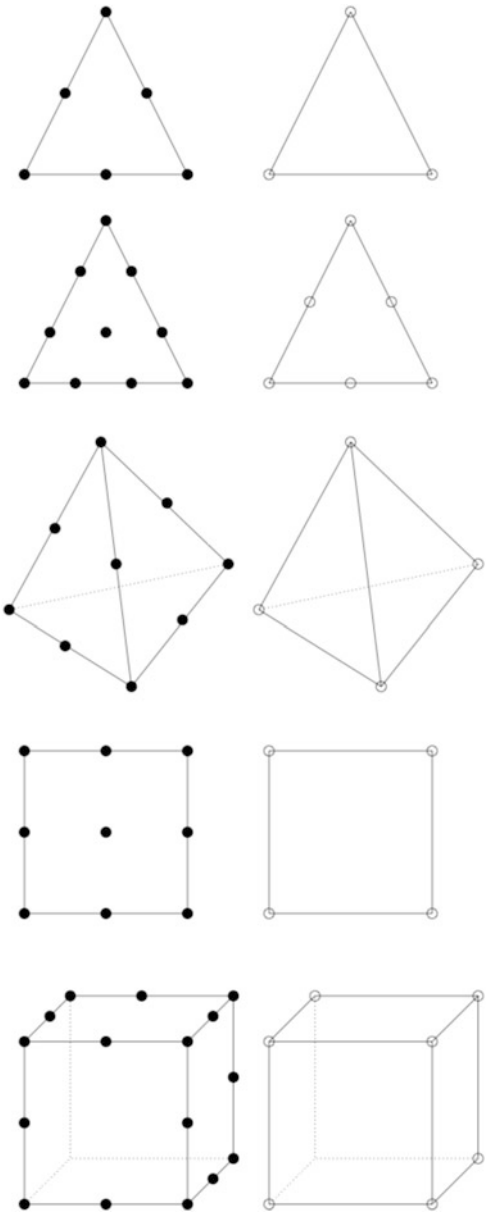

Fig. 8.8 Some stable elements belonging to the Hood–Taylor family

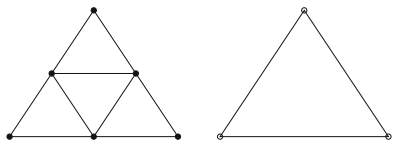

Fig. 8.9 The $(\underline{P}_1 iso \underline{P}_2) - P_1$ element

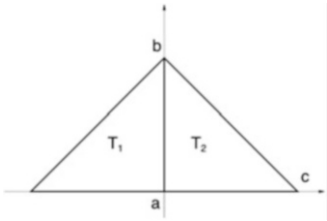

Fig. 8.10 The reference triangle and its symmetric

$Q_h := \mathcal{L}^1_{k-1} \cap L^2_0(\Omega)$ *satisfies the inf-sup condition* (8.2.16) *for any* $k \geq 2$ *if and only if each triangulation contains at least three triangles.*

Proof (Step 1: necessary part). Let us show first that the hypothesis on the mesh is necessary. If $\mathcal{T}_h$ only contains one element, then it is easy to see that the *inf-sup* constant is zero (otherwise, it should be $\operatorname{div} V_h \subset Q_h$, which is not the case since the functions in Q_h are not zero at the vertices). We shall show that if $\mathcal{T}_h$ contains only two triangles T_1 and T_2, then there exists one spurious pressure mode. This implies that, also in this case, the *inf-sup* constant vanishes. We choose the coordinate system (x, y) in such a way that the common edge of T_1 and T_2 lies on the y-axis. Moreover, we suppose that T_2 is the reference triangle and T_1 the symmetric one with respect to the x-axis (see Fig. 8.10). The general case can then be handled by means of suitable affine mappings.

We denote by $\lambda_{i,a}$ and $\lambda_{i,b}$ the barycentric coordinates relative to the vertices a and b, respectively, belonging to the element T_i, $i = 1, 2$. It is easy to check that it holds: $\lambda_{1,a} = 1 + x - y$, $\lambda_{1,b} = y$, $\lambda_{2,a} = 1 - x - y$, and $\lambda_{2,b} = y$. We shall also make use of the function $\lambda_{2,c} = x$. Let $L(x)$ be the Legendre polynomial of degree $k-2$ on the unit interval with respect to the weight $w(x) = x(1-x)^3$ and consider the function $p(x) \in Q_h$ defined as follows:

$$p'(x) = \begin{cases} -L(-x) & \text{for } x < 0, \\ L(x) & \text{for } x > 0. \end{cases} \tag{8.8.7}$$

We shall show that $\underline{\operatorname{grad}}\, p$ is orthogonal to any velocity $\underline{v} \in V_h$. Since p does not depend on y, we can consider the first component v_1 of $\underline{v}$ only, which, by virtue of the continuity at $x = 0$ and of the boundary conditions, has the following general form:

$$v_1 = \begin{cases} \lambda_{1,a}\lambda_{1,b}(C_{k-2}(y) + xA_{k-3}(x, y)) & \text{in } T_1, \\ \lambda_{2,a}\lambda_{2,b}(C_{k-2}(y) + xB_{k-3}(x, y)) & \text{in } T_2, \end{cases} \tag{8.8.8}$$

where the subscripts denote the degrees of the polynomials A, B and C. We then have

$$\begin{aligned}\int_{T_1\cup T_2} \underline{v}\cdot \underline{\mathrm{grad}}\, p\, dx\, dy &= \int_{T_1} v_1\, p'\, dx\, dy + \int_{T_2} v_1\, p'\, dx\, dy \\ &= \int_{T_2} \lambda_{2,a}\lambda_{2,b} L(x) x (B_{k-3}(x,y) - A_{k-3}(-x,y))\, dx\, dy \\ &= \int_{T_2} \lambda_{2,a}\lambda_{2,b}\lambda_{2,c} L(x) q(x,y)\, dx\, dy,\end{aligned} \tag{8.8.9}$$

where $q(x, y)$ is a polynomial of degree $k - 3$ and where the term involving C disappears by virtue of the symmetries. The last integral reads

$$\int_{T_2} xy(1-x-y)L(x)q(x)\, dx\, dy = \int_0^1 xL(x)Q(x)\, dx \tag{8.8.10}$$

and an explicit calculation shows that $Q(x)$ is of the form

$$Q(x) = (1-x)^3 p_{k-3}(x), \tag{8.8.11}$$

where p_{k-3} is a polynomial of degree $k - 3$. We can now conclude with the final computation

$$\int_{T_1\cup T_2} \underline{v}\cdot \underline{\mathrm{grad}}\, p\, dx\, dy = \int_0^1 x(1-x)^3 L(x) p_{k-3}(x)\, dx = 0. \tag{8.8.12}$$

Step 2: sufficient part. The idea of the proof consists in considering, for each h, a partition of the domain Ω in sub-domains containing exactly three adjacent triangles. By making use of Proposition 8.5.4 and the technique presented in Sect. 8.5.1, it will be enough to prove the *inf-sup* condition for a single macro-element, provided we are able to bound the number of intersections between different sub-domains (basically, every time two sub-domains intersect each other, a factor $1/\sqrt{2}$ shows up in front of the final *inf-sup* constant). Indeed, it is possible to prove that, given a generic triangulation of a polygon, it can be presented as the disjoint union of triplets of triangles and of polygons that can be obtained as unions of triplets with at most three intersections.

Given a generic macro-element $a' \cup b' \cup c'$, consider the (x, y) coordinate system shown in Fig. 8.11, so that the vertices are $B' = (0, 0)$, $D' = (1, 0)$, $E' = (\alpha, \beta)$. By means of the affine mapping $x' = x + \alpha y$, $y' = \beta y$, the Jacobian of which is β, we can consider the macro-element $a \cup b \cup c$ shown in Fig. 8.12, so that b is the unit triangle. Since $\beta \neq 0$, the considered affine mapping is invertible. With an abuse of notation, we shall now denote by Ω the triplet $a \cup b \cup c$ and by V_h and Q_h the finite element spaces built on it.

We denote by λ^a_{AB} the barycentric coordinate of the triangle a vanishing on the edge AB (analogous notation holds for the other cases). Moreover, we denote by

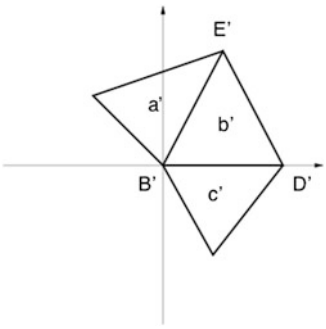

Fig. 8.11 A generic triplet of triangles

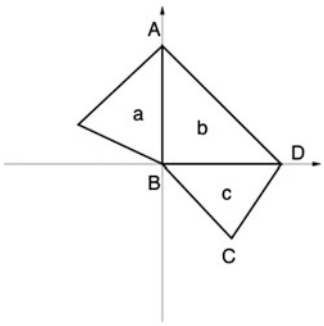

Fig. 8.12 A macro-element where b is the reference triangle

$L^a_{i,x}(x)$ the i-th Legendre polynomial in $[x_A, 0]$, with respect to the measure $\mu_{a,x}$ defined by

$$\int_{x_A}^{0} f(x)\, d\mu_{a,x} = \int_a \lambda^a_{AB}\lambda^a_{AE} f(x)\, dx\, dy \qquad \forall\, f(x) : [x_A, 0] \to \mathbb{R}, \tag{8.8.13}$$

where x_A is the x-coordinate of the vertex A. We shall make use of the following Legendre polynomials, which are defined in a similar way: $L^b_{i,x}$ (its definition involves λ^b_{ED} and λ^b_{BD}), $L^b_{i,y}$ (using λ^b_{BE} and λ^b_{BD}), and $L^c_{i,y}$ (using λ^c_{BC} and λ^c_{CD}).

Standard properties of the Legendre polynomials ensure that we can normalise them, for instance, by requiring that they assume the same value (say 1) at the origin. We now prove by induction with respect to the degree k that a modified *inf-sup* condition holds true (see Verfürth's trick in Sect. 8.5.2). Namely, for any $q_h \in Q_h$, we shall construct $\underline{v}_h \in V_h$ such that

$$-\int_{a\cup b\cup c} \underline{v}_h \cdot \underline{\mathrm{grad}}\, q_h\, dx\, dy \geq c_1 ||\, \underline{\mathrm{grad}}\, q_h||^2_0,$$
$$||\, \underline{v}_h||_0 \leq c_2 ||\, \underline{\mathrm{grad}}\, q_h||_0. \tag{8.8.14}$$

The case k=2. This is the original Hood–Taylor method. Given $p \in Q_h$, we define $\underline{v}_h = (v_1(x,y), v_2(x,y))$, triangle by triangle, as follows:

$$v_1(x,y)|_a = -\lambda^a_{AB}\lambda^a_{AE}||\,\underline{\text{grad}}\; p||_0\sigma, \tag{8.8.15}$$

$$v_2(x,y)|_a = -\lambda^a_{AB}\lambda^a_{AE}\frac{\partial p}{\partial y}, \tag{8.8.16}$$

$$v_1(x,y)|_b = -\lambda^b_{ED}\lambda^b_{BD}||\,\underline{\text{grad}}\; p||_0\sigma - \lambda^b_{ED}\lambda^b_{EB}\frac{\partial p}{\partial x}, \tag{8.8.17}$$

$$v_2(x,y)|_b = -\lambda^b_{ED}\lambda^b_{BD}\frac{\partial p}{\partial y} - \lambda^b_{ED}\lambda^b_{EB}||\,\underline{\text{grad}}\; p||_0\tau, \tag{8.8.18}$$

$$v_1(x,y)|_c = -\lambda^c_{BC}\lambda^c_{CD}\frac{\partial p}{\partial x}, \tag{8.8.19}$$

$$v_2(x,y)|_c = -\lambda^c_{BC}\lambda^c_{CD}||\,\underline{\text{grad}}\; p||_0\tau, \tag{8.8.20}$$

where the quantities σ and τ are equal to ± 1 so that the expressions

$$H = \sigma||\,\underline{\text{grad}}\; p||_0\left(\int_a \lambda^a_{AB}\lambda^a_{AE}\frac{\partial p}{\partial x} + \int_b \lambda^b_{ED}\lambda^b_{BD}\frac{\partial p}{\partial x}\right), \tag{8.8.21}$$

$$K = \tau||\,\underline{\text{grad}}\; p||_0\left(\int_b \lambda^b_{EB}\lambda^b_{ED}\frac{\partial p}{\partial y} + \int_c \lambda^c_{BC}\lambda^c_{CD}\frac{\partial p}{\partial y}\right) \tag{8.8.22}$$

are non-negative. First of all, we observe that $\underline{v}_h$ is an element of V_h: its degree is at most two in each triangle, it vanishes on the boundary and it is continuous across the internal edges because so is the tangential derivative of p.

It is easy to check that $||\underline{v}_h||_0 \le c_1||\;\underline{\text{grad}}\; p||_0$. In order to prove the first equation in (8.8.14), we shall show that the quantity
$|||\,\underline{\text{grad}}\; p||| = -\int_\Omega \underline{v}_h \cdot \underline{\text{grad}}\; p$ vanishes only when $\underline{\text{grad}}\; p$ is zero. From the equality

$$\begin{aligned} 0 = |||\,\underline{\text{grad}}\; p||| = &\int_a \lambda^a_{AB}\lambda^a_{AE}\left(\frac{\partial p}{\partial y}\right)^2 + H \\ &+ \int_b \left(\lambda^b_{ED}\lambda^b_{EB}\left(\frac{\partial p}{\partial x}\right)^2 + \lambda^b_{ED}\lambda^b_{BD}\left(\frac{\partial p}{\partial y}\right)^2\right) \\ &+ K + \int_c \lambda^c_{BC}\lambda^c_{CD}\left(\frac{\partial p}{\partial x}\right)^2, \end{aligned} \tag{8.8.23}$$

it follows that

$$\frac{\partial p}{\partial y} = 0 \quad \text{in } a, \tag{8.8.24}$$

$$\frac{\partial p}{\partial x} = \frac{\partial p}{\partial y} = 0 \quad \text{in } b, \tag{8.8.25}$$

$$\frac{\partial p}{\partial x} = 0 \quad \text{in } c, \tag{8.8.26}$$

$$H = K = 0. \tag{8.8.27}$$

These last equations, together with the fact that each component of $\underline{\text{grad}}\, p$ is constant if $p \in Q_h$, easily imply that

$$\underline{\text{grad}}\, p = (0,0) \quad \text{in } \Omega. \tag{8.8.28}$$

The case $k > 2$. Given p in Q_h, if p is locally of degree $k-2$, then the result follows from the induction hypothesis. Otherwise, there exists at least one triangle of Ω in which p is exactly of degree $k-1$. Like in the previous case, we define $\underline{v}_h = (v_1(x,y), v_2(x,y))$ as follows:

$$v_1(x,y)|_a = -\lambda^a_{AB}\lambda^a_{AE} || \underline{\text{grad}}\, p||_0 L^a_{k-2,x}\sigma, \tag{8.8.29}$$

$$v_2(x,y)|_a = -\lambda^a_{AB}\lambda^a_{AE}\frac{\partial p}{\partial y}, \tag{8.8.30}$$

$$v_1(x,y)|_b = -\lambda^b_{ED}\lambda^b_{BD} || \underline{\text{grad}}\, p||_0 L^b_{k-2,x}\sigma - \lambda^b_{ED}\lambda^b_{EB}\frac{\partial p}{\partial x}, \tag{8.8.31}$$

$$v_2(x,y)|_b = -\lambda^b_{ED}\lambda^b_{BD}\frac{\partial p}{\partial y} - \lambda^b_{ED}\lambda^b_{EB} || \underline{\text{grad}}\, p||_0 L^b_{k-2,y}\tau, \tag{8.8.32}$$

$$v_1(x,y)|_c = -\lambda^c_{BC}\lambda^c_{CD}\frac{\partial p}{\partial x}, \tag{8.8.33}$$

$$v_2(x,y)|_c = -\lambda^c_{BC}\lambda^c_{CD} || \underline{\text{grad}}\, p||_0 L^c_{k-2,y}\tau, \tag{8.8.34}$$

with the same assumption on σ and τ, so that the terms

$$H = \sigma || \underline{\text{grad}}\, p||_0 \left(\int_a \lambda^a_{AB}\lambda^a_{AE} L^a_{k-2,x}\frac{\partial p}{\partial x} + \int_b \lambda^b_{ED}\lambda^b_{BD} L^b_{k-2,x}\frac{\partial p}{\partial x} \right), \tag{8.8.35}$$

$$K = \tau || \underline{\text{grad}}\, p||_0 \left(\int_b \lambda^b_{EB}\lambda^b_{ED} L^b_{k-2,y}\frac{\partial p}{\partial y} + \int_c \lambda^c_{BC}\lambda^c_{CD} L^c_{k-2,y}\frac{\partial p}{\partial y} \right) \tag{8.8.36}$$

are non-negative. The same arguments as for $k = 2$, together with the described normalisation of the Legendre polynomials, show that $\underline{v}_h$ belongs to V_h.

In order to conclude the proof, we need to show that if $||| \underline{\text{grad}}\, p||| = -\int_\Omega \underline{v}_h \cdot \underline{\text{grad}}\, p = 0$, then the degree of $\underline{\text{grad}}\, p$ is strictly less than $k-2$. As before, $||| \underline{\text{grad}}\, p||| = 0$ implies

$$\frac{\partial p}{\partial y} = 0 \quad \text{in } a, \tag{8.8.37}$$

$$\underline{\text{grad}}\, p = 0 \quad \text{in } b, \tag{8.8.38}$$

$$\frac{\partial p}{\partial x} = 0 \quad \text{in } c, \tag{8.8.39}$$

$$H = K = 0. \tag{8.8.40}$$

The last equalities imply

$$\int_a \lambda^a_{AB} \lambda^a_{AE} L^a_{k-2,x} \cdot \frac{\partial p}{\partial x} = 0 \tag{8.8.41}$$

and

$$\int_c \lambda^c_{BC} \lambda^c_{CD} L^c_{k-2,y} \cdot \frac{\partial p}{\partial y} = 0. \tag{8.8.42}$$

It follows that the degree of $\underline{\text{grad}}\, p$ is strictly less than $k-2$ in contrast to our assumption. □

Remark 8.8.4. The proof of the theorem shows that the continuity hypothesis on the pressure space Q_h can be weakened up to require that q_h is only continuous on triplets of elements. □

We conclude this subsection by stating the three-dimensional analogue to the previous theorem and by recalling the main argument of the proof presented in [73].

Theorem 8.8.2. *Let Ω be a polyhedral domain and $\mathcal{T}_h$ a regular sequence of decompositions of it into tetrahedra. Assume that every tetrahedron has at least one internal vertex. Then, the choice $V_h := (\mathcal{L}^1_k \cap H^1_0(\Omega))^3$ and $Q_h := \mathcal{L}^1_{k-1} \cap Q$ satisfies the inf-sup condition (8.2.16) for any $k \geq 2$.*

Proof. We shall make use of the macro-element technique presented in Sect. 8.5.4. In particular, we shall use Proposition 8.5.7 and the comments included in Remark 8.5.6.

We consider an overlapping macro-element partition of $\mathcal{T}_h$ as follows: for each internal vertex x_0, we define a corresponding macro-element M_{x_0} by collecting all elements which touch x_0. Thanks to the regularity assumptions on the mesh, we only have to show that the macro-element condition (8.5.24) holds true (see, in particular, Remark 8.5.6).

Let us consider an element $K \in M = M_{x_0}$ and an edge e of K which touches x_0. With a suitable choice of the coordinate system, we can suppose that the direction of e coincides with that of the x axis. With the notation of Sect. 8.5.4, we shall show that a function in K_M cannot contain functions which depend on x in K.

Namely, given a function $p \in Q_{0,M}$, we can define a function $\underline{v} \in V_{0,M}$ as follows:

$$\underline{v} := \left(-\lambda_{1,i}\lambda_{2,i}\frac{\partial p}{\partial x}, 0, 0 \right) \qquad \text{in } K_i,$$

where K_i is a generic element of M sharing the edge e with K and $\lambda_{j,i}$, $j = 1, 2$, are the barycentric coordinates of K_i associated with the two faces of K_i which do not touch e. On the remaining elements, each component of $\underline{v}$ is set equal to zero. It is clear that $\underline{v}$ is a k-th order polynomial in K_i and, since p is continuous in M, $\partial p/\partial x$ is continuous across the faces which meet at e and the function $\underline{v}$ is continuous as well. Hence, $\underline{v}$ belongs to $V_{0,M}$.

From the definition of $Q_{0,M}$, it turns out that

$$0 = \int_M p \,\mathrm{div}\,\underline{u} = -\int_M \underline{\mathrm{grad}}\, p \cdot \underline{v} = \sum_i \int_{K_i} \lambda_{1,i}\lambda_{2,i} \left| \frac{\partial p}{\partial x} \right|^2 .$$

The last relation implies that p does not depend on x in K_i for any i and, in particular, in K. On the other hand, we can repeat the same argument using as e the other two edges of K meeting at x_0 and, since the directions of the three used edges are independent, we obtain that p is constant in K. □

Remark 8.8.5. From the previous proof, we can deduce that the hypotheses on the triangulation can be weakened, by assuming that each tetrahedron has at least three edges which do not lie on the boundary of Ω and which are not in the same plane. On the other hand, given a generic mesh of tetrahedra, it is not difficult to add suitable elements in order to meet the requirements of the previous theorem. □

Remark 8.8.6. The main argument in the proof of the previous theorem is the straightforward generalisation of the two-dimensional case. Indeed, the proof of Theorem 8.8.1 could be carried out using the macro-element technique as well. □

8.9 Other Developments for Divergence-Free Stokes Approximation and Mass Conservation

From the discussion presented so far, it is clear that, in general, the incompressibility constraint $\mathrm{div}\underline{u} = 0$ is not satisfied exactly at the discrete level. More precisely, the discrete velocity field $\underline{u}_h$ fulfills the following equation

$$\int_\Omega \mathrm{div}\underline{u}_h \, q_h \, dx = 0 \quad \forall q_h \in Q_h,$$

so that the equality $\mathrm{div}\underline{u}_h = 0$ holds in general only if

$$\mathrm{div}(V_h) \subset Q_h. \tag{8.9.1}$$

Almost all stable elements that we have presented up to now do not satisfy (8.9.1), the only exception being the two dimensional Scott–Vogelius scheme $\underline{P}_k - P_{k-1}$, which however requires severe mesh restrictions (see Sect. 8.8.1). Another example is presented in Example 8.10.3, On the other hand, discrete schemes that fail to satisfy the divergence-free condition (at least locally) can lead to undesired instabilities when used for the resolution of more complex problems. This is the case, for instance, when a Stokes solver is used for the approximation of non linear problems (see [39]), or when the incompressibility condition is related to a physical mass conservation property, like in fluid-structure interaction problems (see [78, 280]).

For this reason, a very active research area concerns investigations trying to develop divergence-free Stokes elements, at least in a local sense.

8.9.1 Exactly Divergence-Free Stokes Elements, Discontinuous Galerkin Methods

The simplest idea in order to satisfy (8.9.1) is to use a C^1 approximation of the velocity field and to take as space of pressures exactly $Q_h = \mathrm{div}(V_h)$. Here we do not follow this approach, but we focus on suitably chosen mixed approximations of the Stokes problem.

Early attempts to develop divergence-free finite elements for the approximation of the Stokes problem made use of particular mesh sequences. Besides the already mentioned Scott–Vogelius family (see Sect. 8.8.1), a two dimensional approximation involving a mesh of *rectangles* has been introduced in [253, 385]. The lowest element of the family is constructed as follows: $V_h = \mathcal{L}^1(P_{2,1} \times P_{1,2}, \mathcal{T}_h)$, $Q_h = \mathrm{div}(V_h) \subset \mathcal{L}^1_{[1]}$. It is clear that the use of rectangular elements imposes limitations to the geometry of the domain Ω, which make the scheme unappealing for practical applications.

8.9.1.1 Discontinuous Galerkin Approximations

A more interesting approach arises from the use of *discontinuous Galerkin approximations*. A first possibility is to use a completely discontinuous finite element space for the approximation of the velocity together with a postprocessing procedure (see [156]), or $H(\mathrm{div})$ conforming elements in order to avoid the postprocessing (see [157]).

A more recent approach is based on the idea of using $H(\mathrm{div})$ conforming elements for the approximation of the velocities and to enrich them in order to obtain the stability (see [238]); the enrichment is performed locally by means of divergence-free polynomials (defined as the curl of suitably chosen bubble functions), so that the scheme remains conservative. The construction holds on

simplicial meshes in two and three dimensions and is based on $\mathcal{BDM}$ and $\mathcal{RT}$ spaces. This research is further improved in [237], where a conforming divergence-free element, which can be implemented on two dimensional triangular meshes, is presented. In this case the enrichment is based on *rational* functions which ensure stability and modify the tangential components of the basis functions across the interelements in order to guarantee their continuity. Some a posteriori error estimators (Sect. 7.11) for these methods have been considered in [251].

8.9.2 Stokes Elements Allowing for Element-Wise Mass Conservation

From what we have seen, it is not so easy to obtain a discrete velocity with vanishing divergence *pointwise*. On the other hand, in several applications it might be desirable to have a local (element-wise) conservation of mass. From (8.9.1) it is clear that *discontinuous pressure* schemes enjoy automatically a local conservation property. In particular, if Q_h contains piecewise constants, then $\mathrm{div}\underline{u}_h$ has zero mean value on each element. In this respect, we believe that the $\underline{Q}_2 - P_1$ scheme (see Sect. 8.6.3.1) is one of the best performing method for quadrilateral meshes. For simplicial meshes, the SMALL element of Example 8.7.1 provides what seems to be the simplest element ensuring local mass conservation.

Non conforming schemes can also achieve this goal. In particular the use of non conforming piecewise linear element for the velocity and piecewise constants for the pressures yields a simple locally divergence-free scheme. (see [165] and Sect. 8.4.4 for a discussion about this method). The extension to quadrilateral meshes requires a careful choice of the non conforming space (see [330]).

For *continuous pressure* schemes, however, the situation is more complicate. Relation (8.9.1), in particular, shows that the discrete divergence-free condition has to be considered in a non local sense. For this reason, there have been studies trying to modify standard spaces in order to achieve a more local conservation of mass. The main idea behind this technique consists in adding piecewise constants to the pressure space. It is clear that this modification allows for a local mass conservation (actually, the method is transformed into a scheme with discontinuous pressures), but can work only if it does not affect the validity of the inf-sup condition: a larger pressure space is indeed a potential source of trouble for the stability.

Indeed, it can be shown that generalised Hood–Taylor (see Sect. 8.8) can be modified by adding piecewise constants to the pressure space and preserving the inf-sup condition ($k \geq 2$ in two dimensions and $k \geq 3$ in three dimensions). The same procedure can be applied to the $\underline{P}_1\mathrm{iso}\underline{P}_2 - P_1$ element. For the Hood–Taylor scheme, the idea was suggested in [231, 232, 369], where numerical evidence of the improvement was given (see also [144]). The proof of the stability of the enhanced lowest order Hood–Taylor scheme for triangular and rectangular meshes, can be found in [322, 329, 364]. A more comprehensive discussion, including a general proof of stability, can be found in [83].

8.10 Spurious Pressure Modes

As we stated in the introduction to this chapter, the approximation of the Stokes problem has been developed mostly independently of the theory of mixed methods. This led to the use of some approximations which did not satisfy the *inf-sup* conditions and which generated strange results, specially for the pressure components. This generated the concept of spurious pressure modes.

For the Stokes problem with Dirichlet boundary conditions, pressure is defined up to a constant which is the kernel of the gradient operator. This is a natural pressure mode. However, this mode may not be the only one in discrete problems. For a given choice of V_h and Q_h, we define the space S_h of spurious pressure modes as follows:

$$S_h := \mathrm{Ker} B_h^t \setminus \mathrm{Ker} B^t. \tag{8.10.1}$$

It is clear that a necessary condition for the validity of the *inf-sup* condition (8.2.16) is the absence of spurious modes, that is,

$$S_h = \{0\}. \tag{8.10.2}$$

In particular, if S_h is non-trivial, then the solution p_h to the discrete Stokes problem (8.2.11) can be changed to $p_h + s_h$, which is still a solution when $s_h \in S_h$. Spurious modes correspond to null singular values as discussed in Sect. 5.6.2. The existence of spurious modes is in many cases strongly mesh dependent. They will appear on special regular meshes but will remain if such meshes are slightly distorted.

We shall illustrate how this situation may occur with the following example.

Example 8.10.1 (The $Q_1 - P_0$ element). Among quadrilateral elements, the $\underline{Q}_1 - P_0$ element is the first that comes to mind. It is defined as (see Fig. 8.13):

$$V_h := (\mathcal{L}^1_{[1]})^2 \cap V, \qquad Q_h := \mathcal{L}^0_0 \cap Q. \tag{8.10.3}$$

This element is strongly related, for rectangular meshes, to some finite difference methods [206]. Its first appearance in a finite element context seems to be in [255].

However simple it may look, the $\underline{Q}_1 - P_0$ element is one of the hardest elements to analyse and many questions are still open about its properties. This element does not satisfy the *inf-sup* condition: it strongly depends on the mesh. For a regular mesh, the space of spurious modes is one-dimensional. More precisely, $\underline{\mathrm{grad}}_h\, q_h = 0$ implies that q_h is constant on the red and black cells if the mesh is viewed as a *chequerboard* (Fig. 8.14).

This means that one singular value (cf. Chap. 3.4.3) of the operator $B_h = \mathrm{div}_h$ is zero. Moreover, it has been checked by computation [286] that a large number of positive singular values converge to zero when h becomes small. In [263], it has indeed been proved that the second singular value is $O(h)$ and is not bounded below

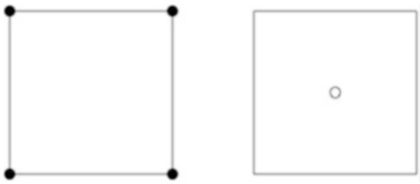

Fig. 8.13 The $\underline{Q}_1 - P_0$ element

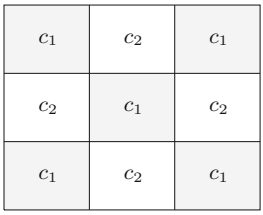

Fig. 8.14 The chequerboard mode

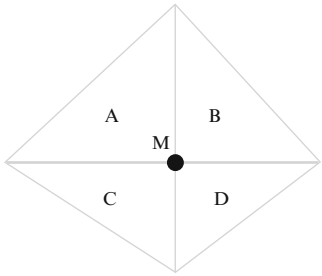

Fig. 8.15 The reference criss-cross

(see also [314]). The $\underline{Q}_1 - P_0$ element has been the subject of a vast literature. We shall come back to it in Sect. 8.10.2. □

We shall now present a few more examples and distinguish between local and global spurious pressure modes.

Example 8.10.2 (The criss-cross $\underline{P}_1 - P_0$ element). Let us consider a mesh of quadrilaterals divided into four triangles by their diagonals (Fig. 8.2). We observed, in Example 8.3.2, that the $\underline{P}_1 - P_0$ element, on *general meshes*, is affected by locking, that is, the computed velocity vanishes. On the mesh introduced above, however, it is easy to see that non-zero divergence-free functions can be obtained. The divergence is constant on each triangle. This means that there are four linear relations between the values of the partial derivatives. It is easily seen that one of them can be expressed as a combination of the others, this fact being caused by equality of tangential derivatives along the diagonals. To make things simpler, we consider the case where the diagonals are orthogonal (Fig. 8.15) and we label by A, B, C, D the four triangles. We then have, by taking locally the coordinate axes along the diagonals and by denoting by $\underline{u}^K$ the restriction of a function of V_h to the element K,

$$\frac{\partial u_1^K}{\partial x_1} + \frac{\partial u_2^K}{\partial x_2} = 0, \quad K = A, B, C, D. \tag{8.10.4}$$

On the other hand, one has at the point M

$$\frac{\partial u_1^A}{\partial x_2} = \frac{\partial u_2^B}{\partial x_2}, \quad \frac{\partial u_1^A}{\partial x_1} = \frac{\partial u_1^C}{\partial x_1}, \quad \frac{\partial u_2^C}{\partial x_2} = \frac{\partial u_2^D}{\partial x_2}, \quad \frac{\partial u_1^B}{\partial x_1} = \frac{\partial u_1^D}{\partial x_1}. \tag{8.10.5}$$

It is easy to check that this makes one of the four conditions (8.10.4) redundant. The reader may check the general case by writing the divergence operator in a non orthogonal coordinate system.

The consequence of the above discussion is that on each composite quadrilateral, one of the four constant pressure values will be undetermined. The dimension of $\mathrm{Ker} B_h^t$ will be *at least* as large as the number of quadrilaterals minus one. This is what we shall call *local modes*.

Thus, three constraints remain on each composite quadrilateral element. If we admit that two of them can be controlled, using the methods of Sect. 8.5.5, by the "internal" node M, we obtain an element that is very similar to the $\underline{Q}_1 - P_0$ element with respect to the degrees of freedom. Indeed, it can be checked that on a regular mesh, an additional, *global* chequerboard mode occurs and that the behaviour of this approximation is essentially the same as that of the $\underline{Q}_1 - P_0$ element that will be discussed in details in Sect. 8.10.2. These analogies have been pointed out, for instance, in [82]. □

The above example has shown the existence of two kinds of spurious pressure modes. In the case of the criss-cross $\underline{P}_1 - P_0$ element presented in the previous example, $\dim S_h$ grows as h goes to 0 and there exists a basis of S_h with local support (that is, the support of each basis function can be restricted to one macro-element). We shall refer to these modes as *local spurious modes*. Such pressure modes can be eliminated by considering a composite mesh (in the previous example a mesh of quadrilaterals instead of triangles) and using a smaller space for the pressures by deleting some degrees of freedom from the composite elements. If the original space is to be employed, one must check the extra compatibility conditions. This can often be done by a small change in the data. This will be the case in Example 8.10.3.

If we now consider the $\underline{Q}_1 - P_0$ example (see Example 8.10.1), the dimension of S_h does not grow when h goes to 0 and no basis can be found with a local support. We then have a *global spurious mode* which cannot be eliminated as easily as the local ones. Global modes usually appear on special (regular) meshes and are symptoms that the behaviour of the element at hand is strongly mesh dependent and requires a special care. Some elements may generate both local and global modes as we have seen in the criss-cross $\underline{P}_1 - P_0$ method (see Example 8.10.2).

Example 8.10.3 (The criss-cross $\underline{P}_2 - P_1$ element). Another simple example where a local mode occurs is the straightforward extension of the previous example to the case of a $\underline{P}_2 - P_1$ approximation. This element has an interest because it is the simplest really divergence-free element, that is, $\mathrm{Ker} B_h \subset \mathrm{Ker} B$. Unfortunately, its

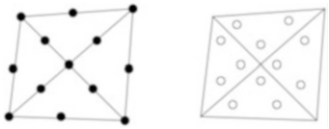

Fig. 8.16 The criss-cross $\underline{P_2} - P_1$ element

three-dimensional counterpart does not seem to exist. We consider, as in Fig. 8.16, a mesh of quadrilaterals divided into triangles by its diagonal. This means that on each quadrilateral, we have 12 discrete divergence-free constraints, and it is easily seen by the argument of Example 8.10.2, written at the point M, that one of them is redundant. Thus, one spurious mode will appear for each composite quadrilateral. However, in this case, no global mode will appear. The analysis of this element is also related to the work of [153] by considering the stream function associated with a divergence-free function. Considering the space of discrete pressures where the spurious modes are removed, a standard proof using internal degrees of freedom shows that one has a stable approximation. □

8.10.1 Living with Spurious Pressure Modes: Partial Convergence

The presence of spurious modes can be interpreted as a signal that the pressure space used is in some sense too rich. We therefore can hope to find a cure by using a strict subspace $\hat{Q}_h$ of Q_h as the space of the discrete pressures, in order to obtain a stable approximation. The question arises whether or not this stability can be used to prove at least a partial result on the original approximation. One can effectively get some results in this direction as discussed in Sect. 5.6.3. In general, we cannot make a direct use of the singular value decomposition but, in some cases, we can identify a guilty subspace.

We suppose, here, that Q and Q_h can be identified to their dual, as it is indeed the case for the Stokes problem.

Following Sect. 5.3.3, we suppose that we know subspaces $\hat{V}_h$ and $\hat{Q}_h$ of V_h and Q_h such that the couple $\hat{V}_h \times \hat{Q}_h$ is stable. We denote $\tilde{Q}_h$ the orthogonal complement of $\hat{Q}_h$ in Q_h. To apply the result of Sect. 5.3.3, we shall need to obtain the following:

$$b(\hat{v}_h, \tilde{q}_h) = 0 \qquad \forall\, \tilde{q}_h \in \tilde{Q}_h,\ \forall\, \hat{v}_h \in \hat{V}_h. \tag{8.10.6}$$

We emphasise that this will be generally possible only on special meshes. We now make the hypothesis that in (8.1.1), g has no component in $\tilde{Q}_h$, that is,

$$(g, \tilde{q}_h) = 0, \quad \tilde{q}_h \in \tilde{Q}_h. \tag{8.10.7}$$

This condition is a restriction on admissible data. In practice, it will imply an extra regularity condition on g which will in turn enable us to obtain (8.10.7) through a *small* modification of g. We mean by small that this modification should not jeopardise the accuracy of the approximation. If we refer to Sect. 5.6.2, by supposing (8.10.7), we have killed the unstable part of $\underline{u}_h$. On the other hand, p_h will have components in $\tilde{Q}_h$. However, the part of p_h in $\hat{Q}_h$ will be stable and will provide a reasonable approximation of the solution. More precisely, under these hypotheses, Proposition 5.3.1 yields the following results:

$$\|u - u_h\|_V \leq c_1 \Big(\inf_{\hat{v}_h \in \hat{V}_h} \|u - \hat{v}_h\|_V + \inf_{q_h \in Q_h} \|p - q_h\|_Q \Big) \tag{8.10.8}$$

$$\|p - \hat{p}_h\|_Q \leq c_2 \Big(\|u - u_h\|_V + \inf_{q_h \in Q_h} \|p - q_h\|_Q \Big) + \inf_{\hat{q}_h \in \hat{Q}_h} \|p - \hat{p}_h\|_Q . \tag{8.10.9}$$

Example 8.10.4. The simplest example is the case of Example 8.10.3. In this case, we have $\hat{V}_h = V_h$. When the local modes are filtered, pressure will converge, provided g has no component in these modes. This implies a slight restriction of data. □

The most important case is, however, the $\underline{Q}_1 - P_0$ element which we discuss in the next section.

8.10.2 The Bilinear Velocity-Constant Pressure $\underline{Q}_1 - P_0$ Element

We now come back to a rapid analysis of what is probably (and unfortunately!) the most popular of all elements for incompressible materials. This is perhaps also the hardest to analyse and as we shall see, only partial results are known. Origins of this element can be traced back to finite difference methods [206] and its peculiar properties were soon recognised. In particular, the chequerboard pressure mode was already a familiar feature long before the scheme used were written in terms of finite elements.

Let us summarise the basic facts. On a regular mesh, for a problem with Dirichlet boundary conditions, two singular values of the matrix (cf. Sect. 5.6.2) vanish instead of one. We thus have a *pure* spurious pressure mode in the terminology of [340, 341]. This spurious mode implies a compatibility condition on the data, which is, in most cases but not always, easily satisfied. When the mesh is slightly distorted, only one singular value is zero, corresponding to constants, but the second one is very small, as the zero has become some value depending on the mesh distortion, thus implying an ill-conditioning of the problem. In many computations, this ill-conditioning is fortunately almost restricted to pressure: we have what [340, 341] call an *impure* pressure mode which can be eventually filtered but often does not

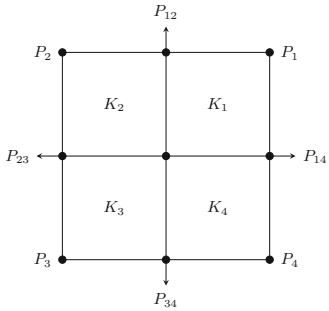

Fig. 8.17 Macro-element and degrees of freedom

seem to affect (at least substantially) the computation of velocity. This is still not, however, the whole story. One could indeed hope from all this that an *inf-sup* stability condition could hold for the third singular value instead of the second and that we could have stability in a simple quotient space. Experimental evidence showed this hope to be false: on a regular mesh, a large number of eigenvalues converge to zero at order h [286]. Johnson and Pitkäranta [263] indeed proved the constant k_h to be $O(h)$ (see also [99, 100, 288, 314]). The standard estimates would then lead to the conclusion that no convergence will occur, in complete contradiction with experience. The paper of Johnson and Pitkäranta provided a first result by showing, on a regular mesh, that under stricter regularity assumptions than usual on the solution, convergence could take place.

Pitkäranta and Stenberg [324] proved a convergence result, without special regularity assumptions for a special type of mesh. We have already discussed, in Sect. 8.10.1, following Sect. 5.6.2, the underlying algebraical issues involved. If there is a "stable part", the data corresponding to the unstable modes should be null or small. In this case, the velocity can indeed be expected to behave well but the pressure part is doomed. We shall now consider these results for our particular case. To make things simpler, we shall first consider the case of a regular rectangular mesh. On such a mesh, we consider a macro-element (Fig. 8.17) M formed of four quadrilaterals.

On this macro-element, a piecewise constant pressure has four degrees of freedom. We introduce a local basis on M, ϕ_1, ϕ_2, ϕ_3, ϕ_4 described symbolically on the Fig. 8.18.

A chequerboard mode will obviously take its roots in ϕ_4. We therefore introduce quite naturally the space

$$\hat{Q}_h := \sum_M \Big(\sum_{i=1}^{3} \alpha_{iM}\ \phi_{i,M} \Big) \tag{8.10.10}$$

which will be the stable part and

$$\tilde{Q}_h := \sum_M \alpha_{4M}\ \phi_{4,M} \tag{8.10.11}$$

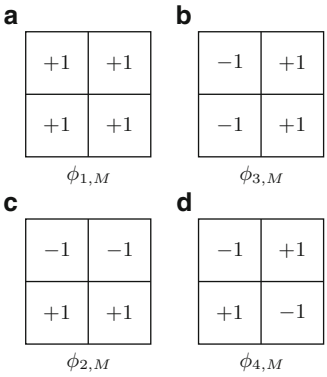

Fig. 8.18 Pressure basis functions on M

the unstable part. Stability of $(V_h,\ \hat{Q}_h)$ is thus immediate from the standard techniques, building a B-compatible operator. In fact, we shall build it for a subspace $\hat{V}_h$ of V_h which will make it, *a fortiori*, valid for V_h. The choice of $\hat{V}_h$ can be inferred from other well-known elements. We now use, as degrees of freedom, the two values of velocity at the vertices of M and at its barycentre and the *normal value* (rather a correction to this value) at mid-side nodes. The tangential component is thus linear on each edge and determined by the values at the vertices (Fig. 8.17). To build a B-compatible operator, we set

$$\underline{\hat{u}}_h(P_i) = \underline{u}(P_i),\ i = 1, 2, 3, 4. \tag{8.10.12}$$

To determine the normal node on the edges of M, we take

$$\int_e (\underline{u} - \underline{\hat{u}}_h) \cdot \underline{n}_e \, ds = 0, \tag{8.10.13}$$

where $\underline{n}_e$ is the normal to e. This is enough to control the flux at interfaces and the part of pressure ($\phi_{1,M}$) which is constant on M is controlled. The $\phi_{2.M}$ and $\phi_{3,M}$ components are controlled by

$$\int_K \operatorname{div}(\underline{u} - \underline{\hat{u}}_h)\phi_{i,M} \, dx = 0,\ i = 2, 3. \tag{8.10.14}$$

It is not difficult to check that $\Pi_h \underline{u} = \underline{\hat{u}}_h$ is a B-compatible operator for $\hat{V}_h \times \hat{Q}_h$.

We would now want to apply Proposition 5.3.1. First, this implies a condition on data.

Remark 8.10.1. Following Sect. 5.3.3, to get reasonable results, the data should satisfy

$$(g, \tilde{q}_h) = \int_\Omega \tilde{q}_h \operatorname{div} \underline{u}_h \, dx = 0 \tag{8.10.15}$$

which means, here,

$$(g, \phi_{4,M}) = \int_{\Omega} \phi_{4,M} \operatorname{div} \underline{u}_h \, dx = 0. \tag{8.10.16}$$

This in fact corresponds to a regularity condition. It is easy to check that on our macro-element, we have

$$\int_M \phi_{4,M} \operatorname{div} \underline{u}_h \, dx = O(h^4) sup|div \frac{\partial^2 \underline{u}}{\partial x \partial y}|. \tag{8.10.17}$$

This is enough to show that this integral can be made null through a small perturbation of data. □

In order to apply Proposition 5.3.1, we now need to check (5.3.19) that is now

$$\int_M \phi_{4M} \ \operatorname{div} \ \underline{\hat{v}}_h \, dx = 0 \ \forall M, \ \forall \underline{\hat{v}}_h. \tag{8.10.18}$$

It should be seen, in order to check this, that the shape function $\underline{w}_1$ associated to vertex P_1, for instance, is a function of $Q_1(M)$ having the whole of M as its support. A straightforward computation then shows that one has

$$\begin{aligned} \int_M \phi_{4M} \ \operatorname{div} \underline{w}_1 \, dx = & \int_{\partial K_1} \underline{w}_1 \cdot \underline{n} \, d\sigma - \int_{\partial K_2} \underline{w}_1 \cdot \underline{n} \, d\sigma \\ & + \int_{\partial K_3} \underline{w}_1 \cdot \underline{n} \, d\sigma - \int_{\partial K_4} \underline{w}_1 \cdot \underline{n} \, d\sigma = 0. \end{aligned} \tag{8.10.19}$$

In the same way, the shape function $\underline{w}_{12}$ associated with node P_{12} satisfies

$$\int_M \phi_{4M} \ \operatorname{div} \underline{w}_{12} \, dx = \int_{\partial K_1} \underline{w}_{12} \cdot \underline{n} \, d\sigma + \int_{\partial K_2} \underline{w}_{12} \cdot \underline{n} \, d\sigma = 0 \tag{8.10.20}$$

and this is also true in the adjacent element because the mesh is aligned. The shape function associated with the barycentre trivially satisfies the condition. Condition (5.3.19) therefore holds and we have, by Proposition 5.3.1,

$$\|\underline{u} - \underline{u}_h\|_V \leq \Big(\inf_{\underline{\hat{v}}_h \in \hat{V}_h} \|\underline{u} - \underline{\hat{v}}_h\|_V + \inf_{q_h \in Q_h} \|q - q_h\|_Q \Big). \tag{8.10.21}$$

In the present case, it is clear that an error estimate in $\hat{V}_h$ has the same order as an estimate in V_h and the result is therefore almost optimal. We also have convergence of (filtered) pressure in $\hat{Q}_h$ by estimate (5.3.25). Following [324], we can now extend this result to the case where the mesh is made from super macro-elements like in Fig. 8.19.

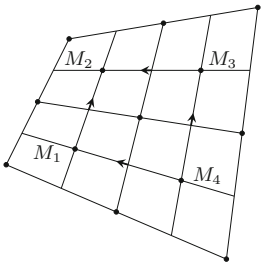

Fig. 8.19 A super-macro $S\,M$ and its sub-macros

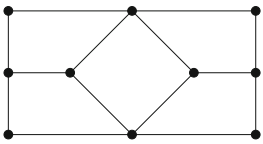

Fig. 8.20 A special macro-element

A general quadrilateral is divided in a regular way into 16 quadrilaterals. It is well-known [202] that on a non rectangular mesh, at least a four by four patch of elements is needed to generate a non-trivial discrete divergence-free function. We thus have four "sub-macros" like in the previous case. The space of filtered pressures $\hat{Q}_h$ is taken exactly as on the regular mesh and is still defined by (8.10.10). The space $\tilde{V}_h$ is defined by the following degrees of freedom: the values of velocity at the vertices of the M_i, the values at the barycentres of the M_i and a correction of the component of velocity parallel to the mesh at the mid-side nodes of the M_i internal to $S\,M$. One can directly build an interpolation operator enabling us to check the *inf-sup* condition. Mid-side nodes of SM control the part of pressure constant on the whole of $S\,M$. Internal mid-side nodes ensure mass-balance on each M_i and the nodes at the barycentres of the M_i end the job. It must be remarked that the alignment of mid-side velocities along the mesh is an essential feature of the construction.

In order to prove condition (5.3.18), the only hard point is to check that (8.10.18) still holds on every M_i. We refer the reader to [324] for this proof. It is then possible to use Proposition 5.3.1 and to get optimal error estimates.

This is still not the whole story about this peculiar element. It is also possible to prove stability [276, 354] on meshes built from macro-elements like in Fig. 8.20 without filtering or using another subterfuge.

This is coherent with the known experimental fact that on a general distorted mesh, pressure modes disappear and the *inf-sup* constant is independent of h. This last fact is still resisting analysis. It is our hope that the above technique could be generalised to yield the complete result.

The above discussion can be extended to the three-dimensional case. Things are made still more complicated by the fact that on a regular mesh (let say a $n \times n \times n$ assembly of elements to fix ideas), we do not have one spurious pressure mode but $3n-2$ of them. This will also mean the same number of compatibility conditions on

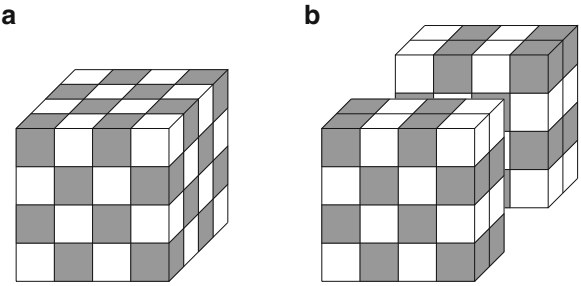

Fig. 8.21 Pressure modes

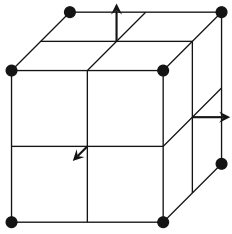

Fig. 8.22 Degrees of freedom for $\hat{V}_h$

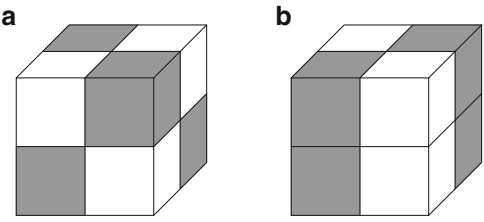

Fig. 8.23 Local spurious modes

data so that trouble should be expected when using apparently reasonable boundary conditions. These spurious modes are depicted in the following Fig. 8.21. One of them is the genuine 3-D chequerboard mode (Fig. 8.21a). The other ones are built from an assembly of 2-D nodes. In Fig. 8.21b, we have sliced the mesh in order to make apparent the internal structure of this mode. There are $3(n-1)$ possible such slices so that we find the number of modes stated above.

We now sketch the extension of the above proof to the 3-D case. We shall only present the rectangular case to avoid lengthening unduly this exposition. We thus suppose that the mesh is built from $2 \times 2 \times 2$ macro-elements (Fig. 8.22).

Our pressure space $\hat{Q}_h$ will be built from Q_h by deleting on each macro-element four $= (3 \times 2 - 2)$ spurious modes sketched in Fig. 8.23.

The mode depicted in Fig. 8.23b has obviously two other symmetrical counterparts. On each macro-element, we thus keep the 3-D analogues of the basis functions $\phi_{1,M}, \phi_{2,M}, \phi_{3,M}$ of Fig. 8.18. We must now introduce $\hat{V}_h$. This is done again by taking off some degrees of freedom from V_h. The remaining ones are sketched in Fig. 8.22 The internal node at the barycentre of the element is also used. It is now clear that $(\hat{V}_h, \hat{Q}_h)$ is a stable pair that provides $O(h)$ convergence. There remains

to check condition (5.3.19) that is that $\hat{V}_h$ is transparent with respect to $\tilde{Q}_h$. This is done exactly as in the 2-D case by a simple check of flow balance at the surface of elements. Proposition 5.3.1 then applies and we get $O(h)$ convergence for velocities and filtered pressures.

It could be hoped that the same kind of analysis could be done for equal interpolation continuous pressure methods such as the $\underline{Q}_1 - Q_1$ approximation. Unfortunately, we know of no way in which condition (5.3.19) could be made to hold and an analysis of the convergence properties of these approximations remains an open question. We can however introduce an alternate way of stabilising such approximations and this is done in the following section.

Remark 8.10.2 (However, this is a dangerous element). As we stated at the beginning of this Section, the $\underline{Q}_1 - P_0$ element is widely employed. We presented the above results to provide the reader with enough information about this unduly popular element. It remains that using an unstable element is a dangerous option and that the price to pay for an apparent simplicity may be inaccurate results. □

Remark 8.10.3 (The worst drawback). An important draw-back for the $\underline{Q}_1 - P_0$ element is that the condition number of the dual problem in p is mesh dependent while it is not for stable Stokes elements. When an iterative solution method is used, this leads to a strong slowdown of the convergence. This is especially disastrous for 3-D problems where iterative methods are likely to be necessary. □

8.11 Eigenvalue Problems

We shall briefly consider, here, the application of the results of Chap. 6 to the approximation of eigenvalues for the Stokes problem. The results will also be applicable to incompressible elasticity. They have some importance in this case because of the popular *modal* method in which a problem is approximated using a few eigenvectors as a basis for a Galerkin's method.

We thus consider the eigenvalue problem introduced in (1.3.84), which we recall for simplicity. We now take $V = (H_0^1(\Omega))^2$ and $Q = L^2(\Omega)/\mathbb{R}$ and we look for $\underline{u} \in V$ and $q \in Q$ satisfying

$$\begin{cases} 2\mu \displaystyle\int_\Omega \underline{\underline{\varepsilon}}(\underline{u}) : \underline{\underline{\varepsilon}}(\underline{v})\, dx + \int_\Omega p \ \operatorname{div} \underline{v}\, dx = \lambda \int_\Omega u \cdot v\, dx \quad \forall \underline{v} \in V, \\ \displaystyle\int_\Omega q \operatorname{div} \underline{u} = 0, \quad \forall q \in L^2(\Omega). \end{cases} \tag{8.11.1}$$

The Lagrange multiplier p ensures the incompressibility of the eigenmodes. This is a problem of the type $(f, 0)$. It is easy to see, in the notation of Sect. 1.2.1, that if Ω is, for instance, a convex polygon, Q_0^H is $H^1(\Omega)/\mathbb{R}$ and V_0^H is the subspace of

$(H^2(\Omega) \cap H_0^1(\Omega))^2$ made of divergence-free functions (see [267]). In particular, we can check that $||\underline{u}||_{V_0^H} = ||\Delta \underline{u}||_0 \sim ||\underline{u}||_2$ and $||p||_{Q_0^H} = ||\underline{\mathrm{grad}}\, p||_0$.

Let V_h and Q_h be finite dimensional subspaces of V and Q respectively. We then consider the discrete version of (8.11.1),

$$\begin{cases} 2\mu \displaystyle\int_\Omega \underline{\underline{\varepsilon}}(\underline{u}_h) : \underline{\underline{\varepsilon}}(\underline{v}_h)\, dx + \int_\Omega p_h \,\mathrm{div}\, \underline{v}_h \, dx = \lambda \int_\Omega u_h \cdot v_h \, dx \quad \forall \underline{v}_h \in V_h, \\ \displaystyle\int_\Omega q_h \,\mathrm{div}\, \underline{u}_h = 0, \quad \forall q_h \in Q_h. \end{cases} \tag{8.11.2}$$

In order to apply the theory of Sect. 1.2.1, we must check a few conditions. With respect to ellipticity, we have no problem with conforming approximations. The weak approximability (6.5.41) of Q_0^H will surely hold if

$$\inf_{q_h \in Q_h} ||p - q_h||_0 \leq \omega_1(h)||p||_1 \quad \text{for all } p \in H^1(\Omega)/\mathbb{R},$$

which is satisfied by all choices of finite element spaces that one may seriously think to use in practice.

The strong approximability (6.5.42) of V_0^H, which now reads

$$||\underline{u} - \underline{u}^I||_1 \leq \omega_2(h)||\underline{u}||_2 \quad \text{for all } \underline{u} \in V_0^H, \tag{8.11.3}$$

is more delicate as $\underline{u}^I$ has to be chosen in $\mathrm{Ker} B_h$. If the pair (V_h, Q_h) satisfies the *inf-sup* condition, then the property trivially holds.

Remark, however, that the typical way of proving the *inf-sup* condition, using a B-compatible operator (Sect. 8.4.1) *for every* $\underline{u}$, is more difficult than proving (8.11.3) directly. Moreover, there are choices of elements that fail to satisfy the *inf-sup* condition, for which (8.11.3) holds true. For instance, we may think of the $\underline{Q}_1 - P_0$ element of Sect. 8.10.2.

Let us assume, for simplicity, that Ω is a square and that the decomposition $\mathcal{T}_h$ is made by $N \times N$ macro-elements M as in Fig. 8.17. We have seen that this choice of elements does not satisfy the *inf-sup* condition: the operator B_h^t has a non-trivial kernel (the chequerboard mode), and by discarding it, we still have at best a discrete *inf-sup* condition with $\beta_h \sim h$ (see [101,264,314]). Nevertheless, for $u \in V_0^H \subset \mathrm{Ker} B$, we can construct $\underline{u}^I$ as in the construction of $\hat{V}_h$ in Sect. 8.10.2: let $\underline{\hat{u}}_h$ be the vector in $\hat{V}_h$ satisfying (8.10.12)–(8.10.14). It is not difficult to check that $\underline{u}^I = \underline{\hat{u}}_h$ satisfies (8.11.3) with $\omega_2(h) = O(h)$. We have here an example where the eigenvalues are approximated correctly even though the global matrix associated to (6.5.8) is singular. The same kind of construction could be extended to a mesh of macro-elements as in Fig. 8.19.

Remark 8.11.1. We have thus another instance in which the $\underline{Q}_1 - P_0$ element, very popular for incompressible elasticity problems, manages to give an impression of rectitude. □

8.12 Nearly Incompressible Elasticity, Reduced Integration Methods and Relation with Penalty Methods

8.12.1 Variational Formulations and Admissible Discretisations

We have already seen in Chap. 1 and in Remark 8.1.2 that there are difficulties associated to approximations of nearly incompressible materials when using the standard variational principle. This section will be devoted to showing how these problems arise and how they can be cured from a proper mixed formulation. Consider, to make things simpler, a problem with homogeneous Dirichlet conditions,

$$\inf_{\underline{v}\in(H_0^1(\Omega))^n} \mu \int_\Omega |\underline{\underline{\varepsilon}}(\underline{v})|^2 \, dx + \frac{\lambda}{2} \int_\Omega |\operatorname{div} \underline{v}|^2 \, dx - \int_\Omega \underline{f} \cdot \underline{v} \, dx. \tag{8.12.1}$$

We already noted in Sect. 8.1 that this problem is closely related to the penalty method used to solve the Stokes problem.

It was soon recognised in practice that a brute force use of (8.12.1) could lead, for large values of λ, to bad results, the limiting case being the locking phenomenon that is an identically zero solution.

Example 8.12.1. The simplest case of such a bad situation would be to employ piecewise linear elements. Then, for λ large, (8.12.1) forces the piecewise constant divergence to be almost null on each element, that is, implicitly using the $\underline{P}_1 - P_0$ element of Example 8.3.2. This led to the still persistent idea that triangular or tetrahedral meshes could not be used for elasticity problems. □

A cure was found in using a reduced (that is, inexact) numerical quadrature when evaluating the term $\lambda \int_\Omega |\operatorname{div} \underline{v}|^2 \, dx$ associated with compressibility effects. We refer the reader to the papers of [287] and [60] for a discussion of the long history of this idea. We shall rather develop in detail in this example the relations of reduced integrations and mixed methods and try to make clear to what extent they may be claimed to be equivalent. For this, we first recall from Chap. 1 that problem (8.12.1) can be transformed by a straightforward application of duality techniques into a saddle point problem

$$\inf_{\underline{v}} \sup_{q} \mu \int_\Omega |\underline{\underline{\varepsilon}}(\underline{v})|^2 \, dx - \frac{2}{2\lambda} \int_\Omega |q|^2 \, dx + \int_\Omega q \, \operatorname{div} \underline{v} \, dx - \int_\Omega \underline{f} \cdot \underline{v} \, dx \tag{8.12.2}$$

for which optimality conditions are, denoting $(\underline{u}, p)$ the saddle point,

$$\mu \int_\Omega \underline{\underline{\varepsilon}}(\underline{u}) : \underline{\underline{\varepsilon}}(\underline{v}) \, dx + \int_\Omega p \, \operatorname{div} \underline{v} \, dx = \int_\Omega \underline{f} \cdot \underline{v} \, dx \quad \forall \, \underline{v} \in (H_0^1(\Omega))^2, \tag{8.12.3}$$

$$\int_\Omega \operatorname{div} \underline{u}\, q\, dx = \frac{1}{\lambda} \int_\Omega pq\, dx \quad \forall\, q \in L^2(\Omega). \tag{8.12.4}$$

This is obviously very close to a Stokes problem and is also an example of the perturbed problem studied in Chap. 4, that is: *find* $u \in V$ *and* $q \in Q$ *such that*

$$a(u, v) + b(v, p) = (f, v), \quad \forall\, v \in V, \tag{8.12.5}$$

$$b(u.q) - c(p, q) = (g, q), \quad \forall\, q \in Q. \tag{8.12.6}$$

We then know from Chap. 5, Sect. 5.5.2, that an approximation of (8.12.3) and (8.12.4) (that is, a choice of an approximation for both $\underline{u}$ and p) which leads to error estimates independent of λ must be a good approximation for the limiting case $\lambda = 0$.

Remark 8.12.1. The preceding sections of this chapter therefore give us a good idea of what should (or should not) be used as an approximation. All stable elements of Sects. 8.6 and 8.7 can be employed and the choice depends on the choice of solver and the mesh generation algorithm. □

What we shall now see is that reduced integration methods correspond to *an implicit choice* of a mixed approximation with a discontinuous pressure approximation. The success of the reduced integration method will thus rely on the qualities of this underlying mixed method. We have seen in Sect. 8.8.1 that discontinuous pressure imposing exactly the divergence-free condition requires high degree polynomials and special meshes. Reduced integration is then a way of reducing the degree of the underlying pressure in order to hopefully obtain a stable approximation.

8.12.2 Reduced Integration Methods

Let us consider a (more or less) standard approximation of the original problem (8.12.1). An exact evaluation of the "penalty term" $\lambda \int_\Omega |\operatorname{div} \underline{v}|^2 dx$ means that for λ large, one tries to get an approximation of $\underline{u}$ which is *exactly* divergence-free. However, as we have already seen, few finite elements can stand such a condition that will in most cases lead to a locking phenomenon due to over-constraining. In a mixed formulation, one relaxes the incompressibility condition by the choice of the approximation for p. Let us now see how this will be translated as a reduced integration method at least in some cases. Let us then consider $V_h \subset V := (H_0^1(\Omega))^n$, $Q_h \subset Q := L_0^2(\Omega)$, these approximation spaces being built from finite elements defined on a partition of Ω. On each element K, let there be given a set of k points x_i and weights ω_i defining a numerical quadrature formula

$$\int_K f(x)\, dx = \sum_{i=1}^{k} \omega_i\ f(x_i). \tag{8.12.7}$$

Remark 8.12.2. It will be convenient to define the numerical quadrature on a reference element K and to evaluate integrals by a change of variables,

$$\int_K f(x)\, dx = \int_{\hat{K}} f(\hat{x})\, J(\hat{x})\, d\hat{x} = \sum_{i=1}^{k} \omega_1\ f(\hat{x}_i)\, J(\hat{x}_i). \tag{8.12.8}$$

The presence of the Jacobian $J(x)$ should be taken into account when discussing the precision of the quadrature rule on K. □

Let us now make the hypothesis that for $\underline{v}_h \in V_h$ and $p_h,\ q_h \in Q_h$, one has exactly

$$\int_K q_h\ \operatorname{div} \underline{v}_h\, dx = \sum_{i=1}^{k} \omega_i\ \hat{q}_h(\hat{x}_i)\widehat{\operatorname{div} \underline{v}_h}(\hat{x}_i)\ J(\hat{x}_i) \tag{8.12.9}$$

and

$$\int_K p_h\, q_h\, dx = \sum_{k=1}^{k} \omega_i\ \hat{p}_h(\hat{x}_i)\ \hat{q}_h(\hat{x}_i)\ J(\hat{x}_i). \tag{8.12.10}$$

Let us now consider the discrete form of (8.12.4),

$$\int_\Omega \operatorname{div} \underline{u}_h\, q_h\, dx = \frac{1}{\lambda} \int_\Omega p_h\, q_h\, dx,\ \forall\, q_h \in Q_h. \tag{8.12.11}$$

When the space Q_h is built from discontinuous functions, this can be read element by element as

$$\int_K q_h\ \operatorname{div} \underline{u}_h\, dx = \frac{1}{\lambda} \int_K p_h\, q_h\, dx\ \forall\, q_h \in Q_h, \tag{8.12.12}$$

so that using (8.12.9) and (8.12.10), one gets

$$\hat{p}_h(\hat{x}_i) = \lambda \widehat{\operatorname{div} \underline{u}_h}(\hat{x}_i) \text{ or } p_h(x_i) = \lambda \operatorname{div} \underline{u}_h(x_i). \tag{8.12.13}$$

Formula (8.12.8) can in turn be used in the discrete form of (8.12.3) which now gives

$$2\mu \int_\Omega \underline{\underline{\varepsilon}}(\underline{u}_h) : \underline{\underline{\varepsilon}}(\underline{v}_h)\, dx + \lambda \sum_K \Big(\sum_{i=1}^{k} \omega_i\ J(\hat{x}_i)(\widehat{\operatorname{div} \underline{u}_h}(\hat{x}_i))(\widehat{\operatorname{div} \underline{v}_h}(\hat{x}_i)) \Big)$$
$$= \int_\Omega \underline{f} \cdot \underline{v}_h\, dx. \tag{8.12.14}$$

In general, the term $\sum_K \left(\sum_{i=1}^{k} \omega_i \; J(\hat{x}_i)(\widehat{\mathrm{div}\underline{u}_h}(\hat{x}_i))(\widehat{\mathrm{div}\underline{v}_h}(\hat{x}_i)) \right)$ *is not* an exact evaluation of $\int_\Omega \mathrm{div}\underline{u}_h \; \mathrm{div} \; \underline{v}_h \; dx$ and reduced integration is effectively introduced. In the case where (8.12.9) and (8.12.10) hold, there is a perfect equivalence between the mixed method and the use of reduced integration. Whatever will come from one can be reduced to the other one. It will however not be possible, in general, to get equalities (8.12.9) and (8.12.10) and therefore, a further analysis will be needed. However, we shall first consider some examples of this complete equivalence case.

Example 8.12.2. Let us consider the $\underline{Q}_1 - P_0$ approximation on a *rectangle* and a one-point quadrature rule. It is clear that $\mathrm{div}\,\underline{u}_h \in P_1(K)$ and is integrated exactly. In the same way, a one-point rule is exact for $\int_\Omega p_h \; q_h \; dx$ whenever $p_h, \; q_h \in P_0(K)$. There is thus a perfect equivalence between reduced integration and the exact penalty method defined by (8.12.11). □

Example 8.12.3. We now consider again the same $\underline{Q}_1 - P_0$ element on a general quadrilateral. To show that we still have equivalence requires a somewhat more delicate analysis. Indeed, at first sight, the quadrature rule is not exact for $\int_{\hat{K}} \widehat{\mathrm{div}\,\underline{u}_h} \; J_K(\hat{x}) \; d\hat{x}$. Let us however consider in detail the term $\widehat{\mathrm{div}\,\underline{u}_h} = \widehat{\frac{\partial u_1}{\partial x_1}} + \widehat{\frac{\partial u_2}{\partial x_2}}$. Let $B = DF$ be the Jacobian matrix of the transformation F from $\hat{K}$ into K. Writing explicitly

$$F = \begin{cases} a_0 + a_1\hat{x} + a_2\hat{y} + a_3\hat{x}\hat{y} \\ b_0 + b_1\hat{x} + b_2\hat{y} + b_3\hat{x}\hat{y}, \end{cases} \tag{8.12.15}$$

one has

$$B = \begin{pmatrix} a_1 + a_3\hat{y} & b_1 + b_3\hat{y} \\ a_2 + a_3\hat{x} & b_2 + b_3\hat{y} \end{pmatrix} \tag{8.12.16}$$

so that we get

$$B^{-1} = \frac{1}{J(\hat{x})} \begin{pmatrix} b_2 + b_3\hat{x} & -b_1 - b_3\hat{y} \\ -a_2 - a_3\hat{x} & a_1 + a_3\hat{y} \end{pmatrix}. \tag{8.12.17}$$

However,

$$\widehat{\frac{\partial u_1}{\partial x_1}} = \left(\frac{\partial \hat{u}_1}{\partial \hat{x}_1}(b_2 + b_3\hat{x}) - \frac{\partial \hat{u}_1}{\partial \hat{x}_2}(b_1 - b_3\hat{y}) \right) \frac{1}{J(\hat{x})}, \tag{8.12.18}$$

$$\widehat{\frac{\partial u_2}{\partial x_2}} = \left(\frac{\partial \hat{u}_2}{\partial \hat{x}_1}(-a_2 - a_3\hat{x}) + \frac{\partial \hat{u}_2}{\partial \hat{x}_2}(a_1 + a_3\hat{y}) \right) \frac{1}{J(\hat{x})}. \tag{8.12.19}$$

When computing $\int_{\hat{K}} \widehat{\mathrm{div}\,\underline{u}_h} \; J(\hat{x}) \; d\hat{x}$, the Jacobians cancel and one is left with the integral of a function which is linear in each variable and which can be computed exactly by a one-point formula. □

Example 8.12.4. Using a 4-point integration formula on a straight-sided quadrilateral can be seen, as in the previous example, to be exactly equivalent to a $\underline{Q}_2 - Q_1$ approximation [59, 60]. □

The above equivalence is, however, not the general rule. Consider the following examples.

Example 8.12.5. We want to use a reduced integration procedure to emulate the Crouzeix-Raviart element (cf. Sect. 8.6.2). To define a P_1 pressure, we need three integration points which can generate a formula that will be exact for second degree polynomials (but not more). The bubble function included in velocity, however, makes that $\operatorname{div} \underline{u}_h \in P_2(K)$ and $\int_K \operatorname{div} \underline{u}_h \; q_h dx$ will not be evaluated exactly. □

Example 8.12.6. A full isoparametric $\underline{Q}_2 - Q_1$ element is not equivalent to its four-point reduced integration analogue. □

Example 8.12.7. A $\underline{Q}_2 - P_0$ approximation is not, even on rectangles, equivalent to a one-point reduced integration method, for $\operatorname{div} \underline{u}_h$ contains second order terms which are not taken into account by a one-point quadrature. □

8.12.3 *Effects of Inexact Integration*

If we now consider into more details the cases where a perfect equivalence does not hold between the mixed method and some reduced integration procedure, we find ourselves in the setting of Sect. 5.5.4. In particular, $b(\underline{v}_h, q_h)$ is replaced by an approximate bilinear form $b_h(\underline{v}_h, q_h)$. We shall suppose, to simplify, that the scalar product on Q_h is exactly evaluated. Two questions must then be answered.

- Does $b_h(.,.)$ satisfy the *inf-sup* condition?
- Do error estimates still hold without loss of accuracy?

We have already introduced in Sect. 5.5.4 a general setting in which this situation can be analysed. We shall first apply Proposition 5.5.8 in order to check the *inf-sup* condition for two examples and we shall give an example where an inexact integral changes the nature of the problem. We shall then consider consistency error for those three examples.

Example 8.12.8. We in fact come back to Example 8.12.7 and study on a rectangular mesh the $\underline{Q}_2 - P_0$ approximation (see Sect. 8.6.3) with a one-point quadrature rule. This is not, as we have said, equivalent to the standard $\underline{Q}_2 - P_0$ approximation. We now want to check, using Proposition 8.4.1, that it satisfies the *inf-sup* condition. We thus have to build a continuous operator (in $H^1(\Omega)$-norm) such that

$$\int_\Omega \operatorname{div} \underline{u}_h \; q_h \; dx = \sum_K [(\operatorname{div} \Pi_h \underline{u}_h)(M_{0,K}) q_K] \; \operatorname{area}(K) \tag{8.12.20}$$

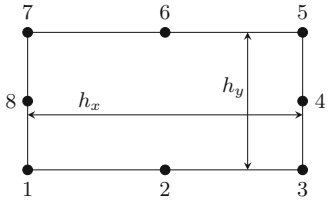

Fig. 8.24 Numbering for the Q_2 element

where $M_{0,K}$ is the barycentre of K and q_K the restriction of q_h to K. As q_h is discontinuous, we can restrict our analysis to one element and we study both sides of equality (8.12.20). We have of course, taking $q_K = 1$,

$$\int_K \operatorname{div} \underline{u}_h \, dx = \int_{\partial K} \underline{u}_h \cdot \underline{n} \, d\sigma. \tag{8.12.21}$$

Using the numbering of Fig. 8.24 and denoting by u_i, v_i the horizontal and vertical components of velocity at node i, we can write (8.12.21) by Simpson's quadrature rule in the form

$$\begin{aligned} \int_K \operatorname{div} \underline{u}_h \, dx = \frac{h_y}{6}[u_5 + 4u_4 + u_3] - \frac{h_y}{6}[u_1 + 4u_8 + u_7] \\ + \frac{h_x}{6}[v_7 + 4v_6 + v_5] - \frac{h_x}{6}[v_1 + 4v_2 + v_3]. \end{aligned} \tag{8.12.22}$$

If we write

$$u_4 = \frac{u_5 + u_3}{2} + \hat{u}_4, \; u_8 = \frac{u_1 + u_7}{2} + \hat{u}_8 \tag{8.12.23}$$

$$v_0 = \frac{v_5 + v_7}{2} + \hat{v}_6, \; v_2 = \frac{v_1 + v_3}{2} + \hat{v}_2, \tag{8.12.24}$$

where $\hat{u}_4, \hat{u}_6, \hat{v}_6$ and $\hat{v}_2$ are corrections with respect to a bilinear interpolation, we may rewrite (8.12.22) as

$$\begin{aligned} \int_K \operatorname{div} \underline{u}_h \, dx = \frac{h_y}{2}[u_5 + u_3 + \frac{4}{3}\hat{u}_4] - \frac{h_y}{2}[u_1 + u_7 + \frac{4}{3}\hat{u}_8] \\ + \frac{h_y}{2}[v_7 + v_5 + \frac{4}{3}\hat{v}_6] - \frac{h_x}{2}[v_1 + v_3 + \frac{4}{3}\hat{v}_2]. \end{aligned} \tag{8.12.25}$$

On the other hand, area (K) $\operatorname{div} \underline{u}_h(M_{0,K})$ can be seen to be equal to

$$\begin{aligned} \frac{h_y}{2}[u_5 + u_3 + 2\hat{u}_4] - \frac{h_y}{2}[u_1 + u_7 + 2\hat{u}_8] \\ - \frac{h_x}{2}[u_7 + v_5 + 2\hat{v}_6] - \frac{h_x}{2}[v_1 + v_3 + 2\hat{u}_2]. \end{aligned} \tag{8.12.26}$$

If we thus split $\underline{u}_h$ into a bilinear part $\underline{u}_h^0$ and a mid-point correction part $\hat{\underline{u}}_h$, one can define $\Pi_h \underline{u}_h$ by setting

$$\begin{cases} (\Pi_h \underline{u}_h)^0 = \underline{u}_h^0, \\ \widehat{(\Pi_h \underline{u}_h)} = \dfrac{2}{3} \hat{\underline{u}}_h. \end{cases} \tag{8.12.27}$$

Equality (8.12.21) will then hold and (8.12.27) is clearly continuous with a continuity constant independent of h. □

Example 8.12.9. We come back to Example 8.12.5 that is a three-point quadrature rule used in conjunction with the Crouzeix-Raviart element. We shall not give the analysis in detail but only sketch the ideas. The problem is again to check that the *inf-sup* condition holds through Proposition 8.4.1. As the quadrature rule *is exact* when q_h is *piecewise constant*, the obvious idea is to build $\Pi_h \underline{u}_h$ by leaving invariant the trace of $\underline{u}_h$ on ∂K and *only modifying the coefficients of the bubble functions*. This can clearly be done. Continuity is now to be checked and the proof is essentially the same as the standard proof of the *inf-sup* condition (Sect. 8.7.2).

□

Example 8.12.10 (A modified $\underline{Q}_1 - P_0$ element). We now present a puzzling example [127] of an element which is stable but for which convergence is tricky due to a consistency error term. We have here a case where using a one-point quadrature rule will change the situation with respect to the *inf-sup* condition. In fact, it will make a stable element from an unstable one but will also introduce an essential change in the problem. The departure point is thus the standard $Q_1 - P_0$ element which was studied in Sect. 8.10.2 and which, as we know, does not satisfy the *inf-sup* condition. We now make it richer by adding to velocity $\underline{u}_h|_K = \{u_1, u_2\}$ what we shall call wave functions. On the reference element $\hat{K} =]-1, 1[\times]-1, 1[$, those functions are defined by

$$\begin{cases} w_1 = \hat{x}\ b_2(\hat{x}, \hat{y}), \\ w_2 = \hat{y}\ b_2(\hat{x}, \hat{y}), \end{cases} \tag{8.12.28}$$

where $b_2(\hat{x}, \hat{y}) = (1 - \hat{x}^2)(1 - \hat{y}^2)$ is the Q_2 bubble function. If we now consider

$$\hat{\underline{u}}_h|_K = \{u_1 + \alpha_K w_1, u_2 + \alpha_K w_2\} = \underline{u}_h|_K + \alpha_k \underline{w}_k, \tag{8.12.29}$$

we obtain a new element with an internal degree of freedom. The wave functions that we added vanish on the boundary and nothing is changed for the stability of the mixed method with exact integration. If we rather use a one-point quadrature rule, things become different. We shall indeed check that the modified bilinear form $b_h(\underline{\hat{v}}_h, q_h)$ satisfies the *inf-sup* condition. We thus have to show that

$$\sup_{\hat{\underline{u}}_h} \frac{\sum_K \operatorname{div} \hat{\underline{u}}_h(M_{0,K})\, p_K\ h_K^2}{\|\hat{\underline{u}}_h\|_1} \geq k_0\ \|p_h\|_0. \tag{8.12.30}$$

This is easily checked by posing on K (we suppose that we have a rectangular mesh to make things simpler)

$$\hat{\underline{u}}_h|_K = h_K \; p_K \underline{w}_K. \tag{8.12.31}$$

We then have $\operatorname{div} \hat{\underline{u}}_h = p_h$ and

$$\|\hat{\underline{u}}_h\|_{1,K} = h \; p_K \; \|\underline{w}_K\|_{1,K}, \tag{8.12.32}$$

which implies

$$\|\underline{u}_h\|_1 \leq c \; \|p_h\|_0, \tag{8.12.33}$$

and (8.12.30) follows. A remarkable point is, now, that even the hydrostatic mode has disappeared. This is an indication that something incorrect has been introduced in the approximation. An analysis of *consistency error* indeed shows that usual error estimates fail and that we are actually approximating a continuous problem in which the incompressibility condition has been replaced by $\operatorname{div} \underline{u} + kp = 0$ where $k = a/b$. We then see that if, in general for the Stokes problem, making the space of velocities richer improves (at least does not reduce) the quality of the method, this fact can become false when numerical integration is used. □

Let us now turn our attention to the problem of error estimation. From Proposition 5.5.6 and Remark 5.5.9, all we have to do is to estimate the consistency terms,

$$\sup_{\underline{v}_h} \frac{|b(\underline{v}_h, p) - b_h(\underline{v}_h, p)|}{\|\underline{v}_h\|_V} \tag{8.12.34}$$

and

$$\sup_{q_h} \frac{|b(\underline{u}, q_h) - b_h(\underline{u}, q_h)|}{\|q_h\|_0}. \tag{8.12.35}$$

We thus have to estimate quadrature errors. It would be out of purpose to enter into details, and we refer the reader to [147, 148] where examples of such analysis are presented exhaustively. The first step is to transform (8.12.34) into a form which is sometimes more tractable. We may indeed write

$$\begin{aligned} b(\underline{v}_h, p) - b_h(\underline{v}_h, p) = (b_h(\underline{v}_h, p - q_h) - b_h(\underline{v}_h, p - q_h)) \\ + (b(\underline{v}_h, q_h) - b_h(\underline{v}_h, q_h)) \end{aligned} \tag{8.12.36}$$

and

$$\begin{aligned} b(\underline{u}, q_h) - b_h(\underline{u}, q_h) = (b(\underline{u} - \underline{v}_h, q_h) - b_h(\underline{u} - \underline{v}_h, q_h)) \\ + (b(\underline{v}_h, q_h) - b_h(\underline{v}_h, q_h)). \end{aligned} \tag{8.12.37}$$

The first parenthesis in the right-hand side of (8.12.36) and (8.12.37) can be reduced to an approximation error. The second parenthesis implies only polynomials.

Let us therefore consider (8.12.37) for the three approximations introduced above. For the Crouzeix-Raviart triangle, taking $\underline{v}_h$ the standard interpolate of $\underline{u}$ makes the second parenthesis vanish while the first yields an $O(h)$ estimate. For the two other approximations, taking $\underline{v}_h$ to be a standard bilinear approximation of $\underline{u}$ makes the second parenthesis vanish while the first yields an $O(h)$ estimate, which is the best that we can hope for anyway. The real trouble is therefore with (8.12.34), with or without (8.12.36). In the case of the Crouzeix-Raviart triangle, we can use directly (8.12.34) and the following result of [147, 148].

Proposition 8.12.1. *Let $f \in W_{k,q}(\Omega)$, $p_k \in P_k(K)$ and denote $E_k(fp_k)$ the quadrature error on element K when numerical integration is applied to fp_k. Let us suppose that $E_K(\hat{\phi}) = 0 \ \forall \hat{\phi} \in P_{2k-2}(K)$. Then, one has*

$$|E_K(fp_k)| \leq ch_K^k \ (meas(K))^{\frac{1}{2}-\frac{1}{9}} |f|_{k,q,K} |p_k|_1. \tag{8.12.38}$$

□

Taking $k = 2$, $q = \infty$ and using the inverse inequality to go from $|p_k|_1$ to $|p_k|_0$, one gets an $O(h^2)$ estimate for (8.12.34).

The two other approximations cannot be reduced to Proposition 8.12.1 and must be studied through (8.12.36). We must study a term like

$$\sup_{\underline{v}_h} \frac{|b(\underline{v}_h, q_h) - b_h(\underline{v}_h, q_h)|}{\|\underline{v}_h\|_1}. \tag{8.12.39}$$

This can at best be *bounded*. For instance in the case of the $\underline{Q}_2 - P_0$ approximation, we can check by hand that the quadrature error on K reduces to $h_K^3 \ |\operatorname{div} \underline{v}_h|_{2,K} \ p_k$.

8.13 Other Stabilisation Procedures

We shall now consider, for the Stokes problem, stabilised formulations presented in Sect. 6.1.1 of Chap. 6. It is clear or should be clear from the results presented in the present chapter that the key of success in stabilising incompressible elements is in weakening the discrete divergence-free condition. This was done, up to now, by reducing the space Q_h of pressures or by enriching the space V_h of velocity field. We now consider the other possibility of a modified variational formulation. In many cases, this will amount to explicitly weaken the condition $\operatorname{div}_h \ \underline{u}_h = 0$ by changing it to

$$\operatorname{div}_h \ \underline{u}_h = g_h, \tag{8.13.1}$$

where g_h is a (well chosen) "small" function. One step in this direction had been done in the work of [131] who considered the relaxed condition

$$\int_\Omega \operatorname{div} \underline{u}_h \; q_h \; dx = \beta \sum_K h_K^2 \int_K \underline{\operatorname{grad}} \; p_h \cdot \underline{\operatorname{grad}} \; q_h \; dx \tag{8.13.2}$$

in the case of a continuous pressure approximation (that is $Q_h \subset H^1(\Omega)$). In (8.13.2), β is any positive real number. On a regular mesh, this is a discrete form of

$$\operatorname{div} \underline{u} = -\beta h^2 \; \triangle p. \tag{8.13.3}$$

It is easy to understand that appearance of oscillations due to spurious pressure modes will make $\triangle_h \; p_h$ large. This will relax the divergence-free condition, thus preventing the growth of such oscillations. The practical use of (8.13.2) indeed requires a delicate balance between two conflicting phenomena. When α is chosen too small, stabilisation is poor and spurious pressure modes persist. On the other hand, taking α too large spoils the value of p_h near the boundary because of the parasitic Neumann condition $\frac{\partial p_h}{\partial n} = 0$ which is implicit in (8.13.2).

This procedure was later generalised by Hughes and Franca [256] and Hughes et al. [257] in order to improve its consistency, in a way that we present below.

We shall first try to give a unified presentation of this kind of methods using the general theory of stabilisation procedures developed in Chap. 5. We shall first consider augmented methods.

8.13.1 Augmented Method for the Stokes Problem

We consider the stabilised formulation (6.1.50) in the special context of the Stokes problem (1.5.23). We now have

$$V := (H_0^1(\Omega))^n, V' := (H^{-1}(\Omega))^n, H := (L^2(\Omega))^n, Q = Q' := L^2(\Omega)$$

and the dense inclusions $V \subset H \subset V'$. We also have, for $\underline{u} \in V$ and $p \in Q$,

$$\begin{aligned} &b(\underline{v}, q) = \textstyle\int_\Omega q \; \operatorname{div} \underline{v} \, dx, \\ &B\underline{u} = -\operatorname{div} \underline{u} \in Q, \;\; B^t p = \underline{\operatorname{grad}} \, p \in V'. \end{aligned} \tag{8.13.4}$$

As to the operator A, it is defined by

$$\langle A\underline{u}, \underline{v} \rangle = a(\underline{u}, \underline{v}) = 2\mu \int_\Omega \underline{\underline{\varepsilon}}(u) : \underline{\underline{\varepsilon}}(v) dx. \tag{8.13.5}$$

The case $t = 1$ of Sect. 6.1.2 (with $\beta_2 = 0$) which corresponds to a stabilisation method introduced by Douglas and Wang [179] now reads as

$$\begin{cases} \langle A\underline{u}_h + \underline{\mathrm{grad}}\, p_h - \underline{f}, \underline{v}_h\rangle_{V'\times V} \\ \qquad + \beta(A\underline{u}_h + \underline{\mathrm{grad}}\, p_h - \underline{f}, A\underline{v}_h)_{V'\times V'} = 0, \quad \forall\, \underline{v}_h \in V_h, \\ \langle \mathrm{div}\, \underline{u}_h + g, q\rangle_{Q'\times Q} \\ \qquad + \beta(A\underline{u}_h + \underline{\mathrm{grad}}\, p_h - \underline{f}, \underline{\mathrm{grad}}\, q_h)_{V'\times V'} = 0, \quad \forall\, q_h \in Q_h, \end{cases} \tag{8.13.6}$$

while in the case $t = 0$, the extra term is only written in the second equation

$$\begin{cases} \langle A\underline{u}_h + \underline{\mathrm{grad}}\, p_h - \underline{f}, \underline{v}_h\rangle_{V'\times V} = 0, \quad \forall\, \underline{v}_h \in V_h, \\ \langle \mathrm{div}\, \underline{u}_h + g, q\rangle_{Q'\times Q} \\ \qquad + \beta(A\underline{u}_h + \underline{\mathrm{grad}}\, p_h - \underline{f}, \underline{\mathrm{grad}}\, q_h)_{V'\times V'} = 0, \quad \forall\, q_h \in Q_h. \end{cases} \tag{8.13.7}$$

We must now build a computable implementation of these formulations. Indeed, the scalar product in V' is not directly handable. In the present case, as the operator A is an isomorphism from V onto V', we can define the scalar product as

$$(\underline{u}', \underline{v}')_{V'\times V'} := \langle A^{-1}\underline{u}', \underline{v}'\rangle_{V\times V'}. \tag{8.13.8}$$

However, this means being able to compute the exact inverse of A. We now have to introduce an approximation and many options are open.

Example 8.13.1 (Defining a scalar product by an approximation of $\mathbf{A^{-1}}$*).* The first idea that comes to mind is to use some approximate operator S_h^{-1} instead of A^{-1}. This could be done by solving an auxiliary problem in a space richer than V_h. Our problem (8.13.7) would now be changed into

$$\begin{cases} \langle A\underline{u}_h + \underline{\mathrm{grad}}\, p_h - \underline{f}, \underline{v}_h\rangle_{V'\times V} = 0, \quad \forall\, \underline{v}_h \in V_h, \\ \langle \mathrm{div}\, \underline{u}_h + g, q\rangle_{Q'\times Q} \\ \qquad + \beta\langle S_h^{-1}(A\underline{u}_h + \underline{\mathrm{grad}}\, p_h - \underline{f}), \underline{\mathrm{grad}}\, q_h\rangle_{V\times V'} = 0, \quad \forall\, q_h \in Q_h, \end{cases} \tag{8.13.9}$$

with a similar expression for (8.13.6). □

Example 8.13.2 (Defining a scalar product by a change of space). Another way of defining a discrete formulation, introduced in [256] and [257], is to replace

$$\beta(A\underline{u}_h + \underline{\mathrm{grad}}\, p_h - \underline{f}, \underline{\mathrm{grad}}\, q_h)_{V'\times V'} \tag{8.13.10}$$

by an expression of the form

$$\beta \sum_K h_K^2 \int_K (A\underline{u}_h|_K + \underline{\mathrm{grad}}\ p_h - \underline{f}) \cdot \underline{\mathrm{grad}}\ q_h\, dx \tag{8.13.11}$$

and by a similar change on the term appearing in the first equation of (8.13.6) if we want to use $t = 1$. This can be seen as another way (through an "inverse inequality")

of defining a discrete scalar product corresponding to the $H^{-1}(\Omega)$ scalar product by using a scalar product in H. If the exact solution $\underline{u}$ is regular enough, this expression written for $\underline{u}$ vanishes and we have what has been termed as "strong consistency". Note that for piecewise linear $\underline{u}_h$, $A\underline{u}_h|_K$ vanishes, leaving only a corrective term of the form

$$\beta \sum_K h_K^2 \int_k (\underline{\text{grad}}\ p_h - \underline{f}) \cdot \underline{\text{grad}}\ q_h\, dx, \tag{8.13.12}$$

which is a variant of (8.13.2). The aim of (8.13.11) is largely to replace the Neumann condition $\frac{\partial p_h}{\partial n} = 0$, which is implicit in (8.13.2), by a more correct one, hopefully making the choice of β easier. □

We now come back to our discrete stabilised problems (8.13.6) or (8.13.9) and we first consider the option of using a discrete operator S_h^{-1}. We shall see that in one important case, both options are equivalent, and that in other cases, we fall back onto known methods.

8.13.2 *Defining an Approximate Inverse* S_h^{-1}

Let V_h be the finite element space in which we compute $\underline{u}_h$. We introduce a space V_h^+ of new degrees of freedom and the space $W_h := V_h \oplus V_h^+$. We can now define $\underline{s}_h^+ := S^{-1}(A\underline{u}_h + \underline{\text{grad}}\ p_h - \underline{f}) \in V_h^+$ by a "hierarchical" computation in V_h^+

$$a(\underline{s}_h^+, \underline{v}_h^+) = \langle A\underline{u}_h + \underline{\text{grad}}\ p_h - \underline{f}, \underline{v}_h^+ \rangle, \quad \forall\, \underline{v}_h^+ \in V_h^+. \tag{8.13.13}$$

In many cases, V_h^+ will be a space of "bubbles" and this problem will be solvable element by element. For the case $t = 0$, our stabilised problem (8.13.7) would now be read, $\underline{s}_h^+$ being defined from (8.13.13), as

$$\begin{cases} \langle (A\underline{u}_h + \underline{\text{grad}}\ p_h - \underline{f}), \underline{v}_h \rangle_{V' \times V} = 0, & \forall\, \underline{v}_h \in V_h, \\ \langle \text{div}\,(\underline{u}_h + \beta \underline{s}_h^+) + g, q \rangle_{Q' \times Q} = 0, & \forall\, q_h \in Q_h, \end{cases} \tag{8.13.14}$$

which indeed contains a weakened condition of the form (8.13.1). The case $t = 1$ of (8.13.6) would yield

$$\begin{cases} \langle A(\underline{u}_h + \beta_1 \underline{s}_h^+) + \underline{\text{grad}}\ p_h - \underline{f}, \underline{v}_h \rangle_{V' \times V} = 0, & \forall\, \underline{v}_h \in V_h, \\ \langle \text{div}\,(\underline{u}_h + \beta_1 \underline{s}_h^+) + g, q \rangle_{Q' \times Q} = 0, & \forall\, q_h \in Q_h. \end{cases} \tag{8.13.15}$$

Taking into account equation (8.13.13), one can see that for $\beta = 1$, this is nothing but the solution of the Stokes problem using $W_h \times Q_h$ as the finite element space. This will obviously work if this choice of spaces is stable and we have rediscovered that enriching the space V_h is a good way of getting a stable method. As for the case (8.13.14), it would be an approximation of this case, which could hardly be

considered as simpler as the matrix of the problem is not symmetric. Proving its stability would require some "quasi-orthogonality" between V_h and V_h^+ of the same type as what is used to study hierarchical error estimators [2, 47]. We shall not try to get much further in this direction. There is however a simple case where both (8.13.14) and (8.13.15) coincide and in fact are equivalent to (8.13.12).

Example 8.13.3 (Defining $\mathbf{S_h^{-1}}$ with bubbles, the MINI element). Let us consider the case of a piecewise linear approximation for both V_h and Q_h, which is well known to be unstable. To fix ideas, we shall use for V_h^+ the space B_3 of conforming cubic bubbles, although we might also use other shapes of bubbles or nonconforming quadratic bubbles. Let then b_K be the bubble associated to element K. We can write any function of V_h^+ in the form

$$\underline{v}_h^+ = \sum_K \underline{\beta}_K b_K.$$

The key of what follows is the fact that we have orthogonality between the space of bubbles and V_h in the sense that

$$a(\underline{s}_h^+, v_h) = a(v_h, \underline{v}_h^+) = 0 \quad \forall\, v_h \in V_h, \forall\, \underline{v}_h^+ \in V_h^+. \tag{8.13.16}$$

As we use bubbles, our Eq. (8.13.13) can be solved element by element and we have on every K

$$\delta_K \underline{\beta}_K = \int_K (\underline{f} - A\underline{u}_h - \underline{\text{grad}}\, p_h) \cdot \underline{b}_K \, dx = \int_K (\underline{f} - \underline{\text{grad}}\, p_h) \cdot \underline{b}_K \, dx \tag{8.13.17}$$

where

$$\delta_K = \mu \int_K |\underline{\underline{\varepsilon}}(\underline{b}_K)|^2 \, dx. \tag{8.13.18}$$

To make things easier, suppose that f is piecewise constant so that we can rewrite (8.13.17) as

$$\delta_K \underline{\beta}_K = \gamma_K (\underline{f} - \underline{\text{grad}}\, p_h) \tag{8.13.19}$$

where we denote

$$\gamma_K = \int_\Omega b_K \, dx. \tag{8.13.20}$$

We thus obtain

$$S^{-1}(A\underline{u}_h + \underline{\text{grad}}\, p_h - \underline{f}) = \sum_K (\gamma_K/\delta_K)(\underline{f} - \underline{\text{grad}}\, p_h) b_K. \tag{8.13.21}$$

Using (8.13.21), (8.13.14) becomes

$$\begin{cases} \langle A\underline{u}_h + \underline{\text{grad}}\, p_h + \underline{f}, \underline{v}_h\rangle_{V'\times V} = 0, \quad \forall\, \underline{v}_h \in V_h, \\ \langle \text{div}\, \underline{u}_h + g, q\rangle_{Q'\times Q} \\ \qquad - \beta \sum_K (\gamma_K^2/\delta_K)(\underline{\text{grad}}\, p_h - \underline{f}, \underline{\text{grad}}\, q_h)_{L^2(K)\times L^2(K)} = 0, \ \forall\, q_h \in Q_h, \end{cases} \tag{8.13.22}$$

and this is nothing but a slight variant of the stabilisation obtained from (8.13.11), as we can check that

$$\gamma_K^2/\delta_K = c_K h_K^2 \tag{8.13.23}$$

with a constant c_K depending on the shape of the element. The same reasoning can be done with other choices for the space of bubbles.

Remark 8.13.1 (The MINI element). Given the orthogonality of (8.13.16), it is easy to see that the formulations of (8.13.6) and (8.13.7) obtained from (8.13.17) coincide and that for $\beta = 1$, they are nothing but the solution of the Stokes problem with the MINI element. □

We thus see that the technique of Example 8.13.2 can be obtained in different ways. We now proceed to develop an error analysis of these methods.

Example 8.13.4 (Error estimates for the Hughes-Franca stabilisation). We place ourselves in the case of "equal interpolation", that is, using polynomials in $\mathcal{L}_k^1$ for V_h and Q_h. Note however that the space V_h will satisfy boundary conditions while Q_h will not. We present the result in the two-dimensional case but it can easily be extended to the three-dimensional case. We have a space of continuous pressures and we have thus $\underline{\text{grad}}\, p_h \in H = (L^2(\Omega))^2$. To simplify the presentation, we define on H

$$\langle \underline{u}, \underline{v}\rangle_H = \sum_K h_K^2 \int_K \underline{u}\cdot\underline{v}\, dx, \quad [\underline{v}]_H^2 = \langle \underline{v}, \underline{v}\rangle_H. \tag{8.13.24}$$

For any $\underline{u}_h \in V_h$, we also define $\underline{Au}_h \in H$ by

$$\underline{Au}_h|_K = A\underline{u}|_K \tag{8.13.25}$$

and we write a stabilised formulation

$$\begin{cases} \langle A\underline{u}_h + \underline{\text{grad}}\, p_h - \underline{f}, \underline{v}_h\rangle_{V'\times V} = 0, \quad \forall\, \underline{v}_h \in V_h, \\ \langle \text{div}\, \underline{u}_h + g, q\rangle_{Q'\times Q} + \langle (\underline{Au}_h|_K + \underline{\text{grad}}\ p_h - \underline{f}), \underline{\text{grad}}\ q_h\rangle_H = 0, \ \forall\, q_h \in Q_h, \end{cases} \tag{8.13.26}$$

which is the method of [256].

Following the procedure of Chap. 5, Sect. 6.1.2, we must obtain a stability result and estimate the consistency term. For stability, we define the bilinear form

$$\begin{aligned}\mathcal{A}\langle(\underline{u}_h, p_h), (\underline{v}_h, q_h)\rangle := a(\underline{u}_h, \underline{v}_h) - b(\underline{v}_h, p_h) + b(\underline{u}_h, q_h) \\ + \beta\langle(\underline{A u}_h + \underline{\text{grad}}\ p_h), \underline{\text{grad}}\ q_h\rangle_H .\end{aligned} \tag{8.13.27}$$

For $\underline{u}_h = \underline{v}_h$ and $p_h = q_h$, we obtain

$$\mathcal{A}\langle(\underline{v}_h, q_h), (\underline{v}_h, q_h)\rangle = \alpha\|\underline{v}_h\|_V^2 + \beta[\underline{\text{grad}}\, q_h]_H^2 + \beta\langle \underline{A u}_h|_K, \underline{\text{grad}}\, q_H\rangle_H . \tag{8.13.28}$$

To prove stability, we recall that from Verfürth's trick (cf. Sect. 8.5.2 and also Chap. 6.3), we have

$$[\underline{\text{grad}}\, q_h]_h \geq k\|q_h\|_Q . \tag{8.13.29}$$

On the other hand, we bound the last term by

$$\beta\langle A\underline{u}_h|_K, \underline{\text{grad}}\, q_H\rangle_H \leq \beta[A\underline{u}_h]_h[\ \underline{\text{grad}}\, q_h]_H \leq \frac{\beta}{2}[A\underline{u}_h]_h^2 + \frac{\beta}{2}[\underline{\text{grad}}\, q_h]_h^2 . \tag{8.13.30}$$

However, using an inverse inequality, we have

$$\int_K |A\underline{u}_h|^2\, dx \leq M\frac{1}{ch_K^2}\|\underline{u}_h\|_{1,K}^2 \tag{8.13.31}$$

and thus

$$\sum_K h_K^2 \int_K |A\underline{u}_h|^2\, dx \leq \frac{M}{c}\|\underline{u}_h\|_V^2 . \tag{8.13.32}$$

Using this last result in (8.13.28), we have

$$\mathcal{A}\langle(\underline{v}_h, q_h), (\underline{v}_h, q_h)\rangle(\alpha - \frac{\beta M}{c})\|\underline{v}_h\|_V^2 + \beta[\ \underline{\text{grad}}\, q_h]_H^2 , \tag{8.13.33}$$

which implies stability for β small enough. It should be remarked that for the degree of the approximation $k = 1$, $A\underline{u}_h|_K = 0$ and that we then have stability for any value of β.

Following Sect. 6.1.1 of Chap. 6, we now have to bound, $(\underline{u}_I, p_I)$ being an interpolate of $(\underline{u}, p)$, a term of the form

$$\beta\sum_K h_K^2 \int_K \left((|(A\underline{u}_I - A\underline{u})|_K|^2) + |p - p_I|^2\right) dx. \tag{8.13.34}$$

The crucial term is the first one. If polynomials of degree k are employed, we have, by classical interpolation results, an estimate on K,

$$\int_K |(A\underline{u}_I - A\underline{u})|_K|^2 \, dx = O(h_K^{2k-2})$$

and the loss of precision is exactly compensated by the choice of the stabilising parameter βh_K^2.

The method does work for any degree of polynomial. However, it should be noted that for $k > 1$, it leads to a non-symmetric system which makes it less appealing.

□

8.13.3 *Minimal Stabilisations for Stokes*

We now consider another class of stabilisations which contains, as a special case, the method of (8.13.2). Although this could be written in general, we shall restrict ourselves to the case of a first order approximation, $V_h \subset (\mathcal{L}_1^1)^n \cap V$, $Q_h \subset \mathcal{L}_k^1 \cap Q$. The method will be a direct adaptation of Sect. 6.3.1 of Chap. 6. We introduce another space $\tilde{V}_h \in (\mathcal{L}_1^1)^2$, denoting $\tilde{P}$ the projection over $\tilde{V}_h$ in the norm of $H := (L^2(\Omega))^n$ and we consider the following problem:

$$\begin{cases} \langle A\underline{u}_h + \underline{\text{grad}}\, p_h - \underline{f}, \underline{v}_h \rangle_{V' \times V} = 0, \quad \forall\, \underline{v}_h \in V_h, \\ \langle \text{div}\, \underline{u}_h + g, q \rangle_{Q' \times Q} \\ \qquad + r(\underline{\text{grad}}\, p_h - \tilde{P}\ \underline{\text{grad}}\, p_h, \underline{\text{grad}}\, q_h)_H = 0, \quad \forall\, q_h \in Q_h. \end{cases} \tag{8.13.35}$$

This fits entirely into the theory of Chap. 6 and we have the error bound

$$\begin{aligned} &\|\underline{u} - \underline{u}_h\|_V^2 + \|p - p_h\|_Q^2 \\ &\qquad \le C\,(\frac{\omega^2(h) + r}{r}) \left(\inf_{\underline{v}_h \in V_H} \|\underline{u} - \underline{v}_h\|_V^2 \right) \\ &\qquad + (1 + \frac{r}{\omega(h)^2}) \inf_{q_h \in Q_h} \|p - q_h\|_Q^2 + r\|(I - \tilde{P})(\underline{\text{grad}}\, p)\|_H^2, \end{aligned} \tag{8.13.36}$$

provided that the following assumption holds:

$$\mathbf{A} \begin{cases} \text{There exists a positive constant } \gamma, \text{ independent of } h \text{ , such that} \\ \|P_{V_h}\, \underline{\text{grad}}\, q_h\|^2 \\ \qquad + \|\,\underline{\text{grad}}\, q_h - \tilde{P}\ \underline{\text{grad}}\, q_h\|^2 \ge \gamma \|\,\underline{\text{grad}}\, q_h\|^2 \quad \forall\, q_h \in Q_h. \end{cases} \tag{8.13.37}$$

Now, as we use an approximation of degree one, we would like all terms on the right-hand side of inequality (8.13.36) to be $O(h^2)$ and we consider three cases.

(i) **The Brezzi-Pitkäranta formulation**. If we take $\tilde{V}_h = \{0\}$ and thus $\tilde{P} = I$, assumption **A** evidently holds. The last term in (8.13.36) reduces to $r\| \underline{\text{grad}}\, p\|_H^2$ and we need to make $r = O(h^2)$ to get the error bound. The drawback of the method is the boundary layer on $\underline{\text{grad}}\, p_h$.

(ii) **Projection on** V_h. Assumption **A** is again immediate. We must again consider the last consistency term. Some trouble arises because V_h satisfies boundary conditions (e.g., $\underline{v}_h = 0$ on the boundary). We can then expect $\|(I - \tilde{P})(\underline{\text{grad}}\, p)\|_H^2$ to be no better than $O(h)$. Taking $r = O(h)$ would restore the optimal order but the problem with the boundary layer is not cured.

(iii) **Optimal projection**. From the previous discussion, one sees that taking $\tilde{V}_h = (\mathcal{L}_1^1)^2$, that is, suppressing boundary conditions, will work with $r = O(1)$ and will eliminate the spurious boundary layer. The trouble is now with assumption **A**. It was proved in [123] that it indeed holds. This method had been used in [51].

In order to prove our assumption **A**, we first consider the following result.

Proposition 8.13.1. *Let Q_h and V_h be the space of piecewise linear pressures and velocities as above, and let $\tilde{V}_h$ be the space of piecewise linear continuous vectors on $\mathcal{T}_h$ (without boundary conditions.) There exists a constant $\beta^* > 0$, independent of h, such that, for every $q_h \in Q_h$ and for every $\underline{w}_h \in \tilde{V}_h$, there exists a $\underline{v}_h^0 \in V_h$ verifying*

$$\|\underline{v}_h^0\|_0 \leq \| \underline{\text{grad}}\, q_h\|_0 \tag{8.13.38}$$

and

$$(\underline{v}_h^0, \underline{\text{grad}}\, q_h)_0 + \| \underline{\text{grad}}\, q_h - \underline{w}_h\|_0^2 \geq \beta^* \| \underline{\text{grad}}\, q_h\|_0^2. \tag{8.13.39}$$

Proof. Let us consider first a macro-element K made by the collection of triangles having one vertex P of $\mathcal{T}_h$ in common. Split $q_h = q_0 + q_\ell$, where q_0 is such that $\underline{\text{grad}}\, q_0$ has zero mean value in K and q_ℓ is linear on K (hence $\underline{\text{grad}}\, q_\ell$ = constant in K.) It is clear that $(\underline{\text{grad}}\, q_0,\ \underline{\text{grad}}\, q_\ell)_K = 0$. We now take $\underline{v}_h^0$, piecewise linear, continuous, vanishing on the boundary of K and having value $\sqrt{6}\, \underline{\text{grad}}\, q_\ell$ at the internal vertex P. An easy computation shows that:

$$\|\underline{v}_h^0\|_{0,K} = \| \underline{\text{grad}}\, q_\ell\|_{0,K} \tag{8.13.40}$$

and

$$(\underline{v}_h^0, \underline{\text{grad}}\, q_\ell)_K = \sqrt{\frac{2}{3}}\, \| \underline{\text{grad}}\, q_\ell\|_{0,K}^2. \tag{8.13.41}$$

On the other hand, $\underline{\mathrm{grad}}\, q_0$ belongs to a space (piecewise constant vectors on K, with continuous tangential components, and zero mean on K) whose intersection with piecewise linear continuous vectors on K is reduced to the zero vector. As we are in finite dimension, there exists a positive constant δ_K such that, for every $\underline{\mathrm{grad}}\, q_0$ and for every $\underline{w}_h$,

$$\| \underline{\mathrm{grad}}\, q_0 - \underline{w}_h \|_0^2 \geq \delta_K \| \underline{\mathrm{grad}}\, q_0 \|_{0,K}^2. \tag{8.13.42}$$

As $\underline{\mathrm{grad}}\, q_\ell$ is clearly continuous and piecewise linear, (8.13.42) easily implies that

$$\begin{aligned} \| \underline{\mathrm{grad}}\, q_h - \underline{w}_h \|_0^2 &= \| \underline{\mathrm{grad}}\, q_0 + \underline{\mathrm{grad}}\, q_\ell - \underline{w}_h \|_0^2 \\ &= \| \underline{\mathrm{grad}}\, q_0 - \tilde{\underline{w}}_h \|_0^2 \geq \delta_K \| \underline{\mathrm{grad}}\, q_0 \|_{0,K}^2, \end{aligned} \tag{8.13.43}$$

and a simple scaling argument shows immediately that δ_K is independent of the *size* of K (notice that (8.13.43) holds *for every* $\underline{w}_h$).

Finally, we explicitly point out that

$$(\underline{v}_h^0, \underline{\mathrm{grad}}\, q_0)_K = \frac{v_h^0(P)}{3} \int_K \underline{\mathrm{grad}}\, q_0 \mathrm{d}x = 0, \tag{8.13.44}$$

where P is the only vertex internal to K. From (8.13.41) to (8.13.44), one then gets that, for every q_h and for every $\underline{w}_h$, there is a $\underline{v}_h^0$, piecewise linear, continuous, and vanishing on the boundary of K, such that (8.13.40) holds and

$$(\underline{v}_h^0, \underline{\mathrm{grad}}\, q_h)_K + \| \underline{\mathrm{grad}}\, q_h - \underline{w}_h \|_{0,K}^2 \geq \beta_K \| \underline{\mathrm{grad}}\, q_h \|_{0,K}^2, \tag{8.13.45}$$

for some positive constant β_K independent of q_h and $\underline{w}_h$. The result (8.13.38) and (8.13.39) then follows easily from (8.13.45) by typical instruments (continuity of β_K, splitting of Ω into macro-elements such that each triangle belongs at most to three different macro-elements, and so on). □

With the aid of Proposition 8.13.1, we can now prove Assumption **A**.

Proposition 8.13.2. *Let Q_h, V_h and $\tilde{V}_h$ be as in Proposition 8.13.1. Then, there exists a constant $\tilde{\beta} > 0$ such that*

$$\| P_{V_h} \underline{\mathrm{grad}}\, q_h \|^2 + \| \underline{\mathrm{grad}}\, q_h - P_{\tilde{V}_h} \underline{\mathrm{grad}}\, q_h \|^2 \geq \tilde{\beta} \| \underline{\mathrm{grad}}\, q_h \|^2 \qquad \forall\, q_h \in Q_h, \tag{8.13.46}$$

where all the norms are in L^2.

Proof. We start by observing that, for every $\underline{v}_h^0$ and q_h, we have

$$\begin{aligned} (\underline{v}_h^0, \underline{\mathrm{grad}}\, q_h) = (\underline{v}_h^0, P_{V_h} \underline{\mathrm{grad}}\, q_h) &\leq \| \underline{v}_h^0 \| \, \| P_{V_h} \underline{\mathrm{grad}}\, q_h \| \\ &\leq \frac{\beta^*}{2} \| \underline{v}_h^0 \|^2 + \frac{1}{2\beta^*} \| P_{V_h} \underline{\mathrm{grad}}\, q_h \|^2, \end{aligned} \tag{8.13.47}$$

where the last inequality clearly holds for every positive β^*, but we shall use it for the value of β^* given in (8.13.39). For every q_h, we now take $\underline{v}_h^0$ as given by Proposition 8.13.1, and using (8.13.38), we have

$$(\underline{v}_h^0, \underline{\mathrm{grad}}\, q_h) \leq \frac{\beta^*}{2} \| \underline{\mathrm{grad}}\, q_h \|^2 + \frac{1}{2\beta^*} \| P_{V_h} \ \underline{\mathrm{grad}}\, q_h \|^2, \tag{8.13.48}$$

which, inserted in (8.13.39) with $\underline{w}_h = P_{\tilde{V}_h} \ \underline{\mathrm{grad}}\, q_h$, gives

$$\frac{\beta^*}{2} \| \underline{\mathrm{grad}}\, q_h \|^2 + \frac{1}{2\beta^*} \| P_{V_h} \ \underline{\mathrm{grad}}\, q_h \|^2 + \| \underline{\mathrm{grad}}\, q_h - P_{\tilde{V}_h} \underline{\mathrm{grad}}\, q_h \|^2 \geq \beta^* \| \underline{\mathrm{grad}}\, q_h \|^2, \tag{8.13.49}$$

and (8.13.46) follows immediately. □

Remark 8.13.2 (Enhanced strain methods). Finally, to conclude this section, we would like to note that another example of stabilisation of the Stokes problem by an enhanced method can be found in the work of [283]. □

8.14 Concluding Remarks: Choice of Elements

We would first like to emphasise that the results of this chapter can be applied as well to flow problems as well as to linear (or linearised) elasticity problems. In this last case, displacement methods also need to be considered from a mixed point of view. Indeed, we have already seen in Sect. 8.12 that there is a close relation between the Stokes problem and linear elasticity problems. However, things are not so simple: fluid people and solid mechanics people form two different communities and information was long to cross the border.

8.14.1 Choice of Elements

We have presented discontinuous pressure and continuous pressure elements. They both have advantages, even though discontinuous pressure is appealing as it enforces an element wise conservation of mass. They can also be implemented by a penalty procedure.

In this respect, the reader should have noticed an important difference between the two-dimensional and the three-dimensional elements presented in this chapter.

- In the 2-D case, we have a choice of discontinuous pressure elements which can be used with a penalty method. Direct solvers are not too sensitive to the ill-conditioning of the resulting system and we thus obtain a good resolution strategy. We can thus recommend the Crouzeix-Raviart element of Example 8.6.1 or its higher order variants.

- In the 3-D case, discontinuous pressure elements satisfying the *inf-sup* condition are expensive as one needs degrees of freedom on the faces. The equivalent of the Crouzeix-Raviart element also uses bubbles of degree four. The ubiquitous $\underline{Q}_1 - P_0$, for which the condition number of the dual problem depends on $\frac{1}{h}$, behaves badly with iterative methods which are essential for large-scale simulations. We therefore recommend the Hood-Taylor continuous pressure element.

Remark 8.14.1 (Solvers). The choice of elements is also dictated by the choice of solvers. In the two-dimensional case, where direct solvers are almost always employed, discontinuous pressure elements are desirable as they are compatible with penalty methods. In the three-dimensional case, where iterative solvers are the rule for large problems, penalty methods are to be avoided as they destroy the condition number of the problem. Recent progress in the construction of solvers for indefinite systems [58, 185, 186] however make the use of a continuous pressure element, such as the Taylor-Hood element, possible and efficient. □

Remark 8.14.2 (Meshes). Another consideration is the choice of affine (triangular or tetrahedral) or quadrilateral hexahedral elements. As we already noted, there was a widespread legend that tetrahedra were not suitable for incompressible solid mechanics problems. This was based on a lack of analysis and we advocate the choice of affine elements for two reasons.

- Mesh generation is much easier with tetrahedra than with hexahedra. Indeed, it can, most of times, be done automatically. This is important in complex engineering problems where the domains may be of a complex shape.
- The second reason is mesh adaptation, which is also much easier for tetrahedra. There exist algorithms which can make a mesh optimal to represent a given solution. □

Finally, let us recall that the approximation of incompressible materials is a central issue in many industrial applications. It has therefore been the subject of a vast literature. We believe to have presented the essential points but we also neglected many aspects. Among those, we did not describe finite volume methods, which are mostly amenable to an analysis by the theory of mixed methods. One can find references in [194] and [195].